

# Agriculture, Trade, and Global Water Use\*

Tamma Carleton<sup>†</sup>  
UC Berkeley and NBER      Levi Crews<sup>‡</sup>  
UCLA      Ishan Nath<sup>§</sup>  
Harvard Kennedy School

26 September 2025

Please [click here](#) for the latest draft.

## Abstract

This paper examines the consequences of international trade for long-run water resources and agricultural productivity. We use a large collection of global spatial data to show that—despite the widespread market failure caused by open access to water as an input with no market price—water-intensive agricultural activity is highly concentrated in water abundant locations, with few exceptions. We use a dynamic spatial equilibrium model of agricultural trade and water resources to quantify the policy consequences of this fact. Model counterfactuals show that international trade in agriculture prevents severe depletion of global water resources and accompanying long-run productivity declines, especially in dry places, by enabling specialization to follow comparative advantage. However, some observed trade liberalization episodes worsen depletion by exacerbating existing inefficiencies.

*JEL codes:* F13, F18, H23, Q15, Q17, Q25, Q27

---

\*We thank Pedro Bento, Tomás Domínguez-Iino, Dave Donaldson, and Louis Preonas for insightful discussions, and Arnaud Costinot, Jonathan Dingel, José-Antonio Espín-Sánchez, Farid Farrokhi, Scott Jasechko, Sam Kortum, Will Rafey, Andrés Rodríguez-Clare, Joe Shapiro, John Sturm Becko, Felix Tintelnot, and seminar participants at CalTech, Exeter, FRB St. Louis, Georgetown, Harvard, Johns Hopkins, Michigan, Minnesota, MIT, NYU, Penn State, Princeton, UBC, UC Berkeley, UC Davis, UCLA, UChicago, USC, UT Austin, the World Bank, Yale, the BFI Coase Project, the Fed Junior Applied Group, the LACEA Annual Meeting, LSE Environment Week, NBER Summer Institute, OSUS, the SED, and the Virtual Workshop on Trade, Spatial Economics, and the Environment for helpful comments. Crews and Nath thank the International Economics Section at Princeton University for their hospitality while working on this project. Zoë Arnaut-Hull, Yang Gao, Ethan Goode, Walker Lewis, and especially Cheikh Fall and Christian Hilgemann provided excellent research assistance. All remaining errors are our own.

<sup>†</sup>[tcarleton@berkeley.edu](mailto:tcarleton@berkeley.edu)

<sup>‡</sup>[lgcrews@econ.ucla.edu](mailto:lgcrews@econ.ucla.edu)

<sup>§</sup>[ishannath@hks.harvard.edu](mailto:ishannath@hks.harvard.edu)

## 1 Introduction

Over 90% of global water consumption occurs in agriculture, which depends critically on the availability of local rainfall, surface water, and groundwater (Mekonnen and Hoekstra, 2011). While water itself is generally prohibitively costly to transport over long distances, the exchange of water's factor services through agricultural trade can alleviate local scarcity by allowing water-intensive production to concentrate in places where the resource is abundant (Allan, 1998). Pervasive distortions, however, affect both input markets for water and output markets for agriculture worldwide. Most farmers extract water as an open-access resource without defined property rights (Libecap, 2008), and agricultural markets face numerous subsidies, taxes, tariffs, and trade restrictions (Anderson, Rausser, and Swinnen, 2013). When input market failures prevent the cost of extracting water from reflecting its scarcity, international trade can worsen resource depletion and reduce long-run welfare (Chichilnisky, 1994). In an environment of second best, output market distortions can correct or compound these effects (Lipsey and Lancaster, 1956).

Several prominent examples suggest global agricultural trade contributes to severe regional water depletion. In California's Central Valley, water tables have declined sharply in recent decades, driven by specialization in highly water-intensive crops grown primarily for export. California alone produces roughly 80% of the world's almonds, the most water-intensive non-fodder crop per planted hectare (Mekonnen and Hoekstra, 2011). Similarly, water depletion in India's northern agricultural regions has outpaced that of nearly any other arable land on earth (Rodell et al., 2018), all while farmers there cultivate water-intensive crops like rice, of which India is now the world's leading exporter. Prior work confirms that policies implemented to promote agricultural exports in India directly accelerated groundwater depletion (Sekhri, 2022).

Beyond these specific examples, no consensus exists regarding the global impact of international trade on long-run water resources and agricultural production. Prominent work by Dalin et al. (2017) finds that most of the world's population lives in countries sourcing nearly all their staple crop imports from partners who deplete groundwater to produce those crops. Earlier work by Allan (1998, 2011) argues instead that trade enhances water security by shifting production to water-abundant regions. Despite the critical role of international markets and agricultural trade in this question, existing research largely lies almost entirely outside of economics, and is held back by both the limited availability of systematic granular data and by the absence of models that capture equilibrium behavior, market adjustments through prices and trade flows, and long-run dynamics.

This paper combines comprehensive global geospatial data with a dynamic spatial equilibrium model to analyze how international trade and agricultural policies affect regional water scarcity and long-run agricultural productivity. We assemble and harmonize a novel collection of 16 globally comprehensive datasets contain-

ing detailed information on water resources, agricultural activity, and agricultural policy. New data from hydrology, agronomy, and remote sensing describe the availability of ground and surface water, trends in water availability in recent decades, and the spatial distribution of agricultural production, irrigation, water consumption, and productivity. Administrative records capture prices, trade patterns, and a wide range of agricultural policy interventions. Altogether, our dataset provides high-resolution information on both water and agriculture for every parcel of land on earth. We plan to make this database publicly available and hope it will serve as a foundation for future research on the economics of water.

Using these data and existing literature, we establish five descriptive facts about water, agriculture, and trade to guide our quantitative analysis. First, water resources differ greatly across regions, with some areas rich in groundwater, surface water, and rainfall, and others experiencing limited and/or declining availability. These differences suggest significant potential gains from spatial reallocation of agricultural production through trade. Second, we show that agriculture dominates global water use and that international trade embeds 21% of water used by crops, motivating our focus on this sector and on trade in particular. Third, over 93% of global agricultural production occurs where farmers extract water without formal property rights, underscoring the importance of analyzing agricultural and trade policies under the presence of this ubiquitous input market failure. Fourth, existing studies show agricultural and trade policies strongly influence water resources.

Fifth, we find that water-intensive agriculture tends to concentrate in areas with abundant water resources. The average water intensity of agricultural land use is two to five times higher in regions in the top quintile of groundwater availability and rainfall than in water-scarce regions in the bottom quintile. Water-rich areas both plant crops on more of their land and choose more water-intensive crops conditional on planting. While a few regions, notably parts of California and Uttarakhand in northern India, rapidly deplete water through intensive farming, these cases stand out as exceptions to the broader pattern. Globally, drier regions conserve scarce water resources by producing less water-intensive crops locally and importing water-intensive goods. This pattern of specialization occurs despite widespread distortions in agricultural markets and water use.

To analyze how trade shapes global water resources and assess policy counterfactuals, we build the first dynamic spatial equilibrium model of agricultural trade explicitly incorporating water resources across multiple crops and countries. In the model, farmers on each parcel of arable land choose between cultivating crops or working outside agriculture. They sell their output in domestic and foreign markets subject to crop-specific subsidies, taxes, and bilateral trade costs. Crop productivity depends on local soil quality, climate, and the cost of extracting crop-specific water needs. Extraction costs rise with local water scarcity. Water tables evolve dynamically based on natural recharge and extraction for agricultural production, capturing the spatial and temporal externalities from open-access water use. As aquifers de-

cline, agricultural productivity falls, food prices rise, and non-agricultural output declines as farming uses more land and labor.

We use our global dataset to calibrate the model for a diverse set of 52 countries that account for 99% of the world's agricultural workers. Farmers in the model operate across more than one million heterogeneous fields, each characterized by local soil and climate conditions, which are grouped into roughly 200 global aquifers that span national boundaries. Our baseline calibration does not impose a steady state; instead, it reproduces current regional levels and trends in water resources. The model simulations include 22 crops, including globally traded staples like wheat, rice, maize, soybeans, and potatoes, as well as specialty cash crops such as coffee, oil palm, and bananas, and regional crops common in dry, low-income areas like cassava, sorghum, millet, barley, and chickpeas. Some parameters, such as crop-specific water intensities, come directly from agronomic literature; others we calibrate to match observed land use, agricultural output, and levels and trends of water availability.

We use the calibrated model to perform three policy counterfactuals. First, we evaluate the fundamental question of how global agricultural trade affects water depletion by considering what the world would like in its absence. To do so, we simulate a scenario of autarky for all crops and countries beginning in our baseline year. Second, we quantify the impact of historical reforms by simulating the effects of the agricultural and trade policy liberalizations resulting from the Uruguay Round of WTO negotiations (1986–1994), which were implemented in the following decades. Third, we consider hypothetical further liberalization by removing all remaining distortionary agricultural policies worldwide.

The paper has three main findings. First, existing global trade dramatically reduces aggregate global land and water use. Without trade, global food prices would rise sharply, and continue growing over time in many places as local water resources diminish. Under autarky, global cropped acreage would double, as countries meet domestic demand without the efficiency gained from trade, which channels farming to the most productive locations. The share of arable land cultivated worldwide rises from about one-third in the baseline (matching observed data) to nearly two-thirds under autarky. Reflecting the allocative efficiency benefits from trade, average global crop yields are 44% lower in autarky than in the baseline. To our knowledge, these estimates are the first to quantify the effect of international trade on global agricultural land use, with potential implications for environmental issues beyond the scope of this paper.

Autarky also raises global agricultural water use by about 60% initially, sharply depleting water resources over time. In the baseline scenario, global average water table depth remains approximately stable, matching observed data. Under autarky, water tables fall about 2.3% annually over the first 30 years, as extraction consistently exceeds recharge. This depletion rate surpasses even the most extreme values in the observational records. The decline in freshwater availability in autarky reduces crop yields, raises food prices, and lowers non-agricultural production as

farming draws more resources. Population-weighted global food prices rise initially by 1,400%, while non-agricultural production falls by 15%. Over 30 years, average water table depths beneath arable land drop from 17 to 28 meters, reducing average crop yields by 2.4% per year beyond the initial drop.

The second key finding is that water-scarce regions would suffer the greatest long-run depletion and productivity losses without global agricultural trade. Under autarky, the 30-year decline in water tables is 2.5 times larger for aquifers initially at the 90<sup>th</sup> percentile of depth than for the global average. These water-scarce areas primarily import food and thus must greatly increase local cropped acreage and water use to meet domestic demand in the absence of trade. In autarky, cropped acreage increases nearly twice as much for the bottom quartile of net water exporters—countries currently importing water-intensive crops—as for the top quartile. Consequently, their increase in water extraction is nearly eight times greater. For regions with limited rainfall and low water tables, global trade is essential to maintaining long-term water availability.

Consistent with previous empirical work ([Sekhri, 2022](#)) and circumstantial evidence, the model simulations show that imposing autarky *slows*, or even reverses, declining trends in water resources in a few rapidly depleting food-exporting regions. In parts of northern India, water resources decline steadily under baseline conditions but stabilize under autarky when farmers no longer export water-intensive crops like rice. In California’s Central Valley, depletion also slows under autarky. Yet, in most regions globally, agricultural trade moves water-intensive production to areas with abundant water, preserving long-term availability.

These findings may seem surprising. Despite the prominent examples of depletion in California and India, and pervasive market failures surrounding water use, specialization in water-intensive agriculture closely follows water abundance. Without property rights, markets, or prices for most water users, how does this specialization occur? We show that specialization in water-intensive activity corresponds to water availability because extraction costs depend on water scarcity. Regions with deeper water tables and less accessible surface water face higher extraction costs, as revealed in our estimation through farmers’ land-use choices and consistent with the basic physics of groundwater extraction ([Burlig, Preonas, and Woerman, 2021](#)). Thus, even without formal markets or tradable rights, water’s effective input price partially reflects scarcity. Despite significant externalities, the natural environment partially substitutes for functioning markets by increasing procurement costs where water is scarce.

Our third key finding is that although global trade typically reallocates water use productively, certain agricultural policy reforms can worsen resource depletion and lower long-term productivity. We find that the Uruguay Round of WTO negotiations—the largest agricultural market liberalization to date—caused agriculture to shift from water-abundant to water-scarce countries, exacerbating depletion in regions with higher extraction costs. Under WTO rules, many wealthy, water-

abundant countries significantly reduced domestic agricultural support. Simultaneously, many lower-income countries removed agricultural disincentives originally established through import-substitution policies aimed at industrialization ([Anderson, Rausser, and Swinnen, 2013](#)).

Our simulations show that these policy reforms reduced water use in many water-abundant regions, such as Western Europe, but increased use in some water-scarce ones, such as parts of sub-Saharan Africa. These reforms slightly worsened average depletion across global aquifers and especially increased it in many dry countries. By contrast, removing remaining domestic agricultural market distortions, nearly all of which subsidize agriculture, would modestly reduce depletion risks globally and in most dry areas. Agricultural production would become less water-intensive without these subsidies. These results highlight the second-best nature of this setting. Input market distortions render the long-term water impacts of trade liberalization ambiguous, so reducing output market distortions does not necessarily improve outcomes in the long run.

This paper builds on related work across several literatures within and beyond economics. In the literature on the economics of water, most existing papers focus on the efficacy of input market reforms and related policies that take place in a single location, such as California, India, or southeastern Australia ([Ayres, Meng, and Plantinga, 2021](#); [Bruno and Jessoe, 2021](#); [Ryan and Sudarshan, 2022](#); [Rafey, 2023](#)). A small number of empirical papers consider the role of international trade in agriculture, including [Carleton \(2021\)](#), which estimates the impact of agricultural and trade policies on trends in water resources, and [Sekhri \(2022\)](#), which investigates trade promotion and groundwater depletion in northern India. The paper with the most relevant empirical work to the facts presented here is [Debaere \(2014\)](#), which uses country-level data to show that water-intensive exports correlate with water-abundance, though less so than is observed for other inputs.

To our knowledge, this paper is the first quantitative spatial analysis of the allocation of global water resources. This work builds on a growing recent economics literature at the intersection of trade, spatial, and the environment, which is summarized in a review article by [Copeland, Shapiro, and Taylor \(2022\)](#). The model in this paper builds most closely on [Costinot, Donaldson, and Smith \(2016\)](#), though we add water resources and dynamics. Most papers in the spatial environmental literature focus on climate change and air pollution, but a small number consider natural resources in the context of forests. [Hsiao \(2025\)](#) investigates the effects of import tariffs on deforestation for palm oil production in Indonesia and Malaysia, and [Domínguez-Iino \(2025\)](#) considers the land use and deforestation implications of market power in agricultural supply chains in South America. The most similar work to this paper is [Farrokhi, Kang, Pellegrina, and Sotelo \(2023\)](#), which uses a global dynamic spatial equilibrium model to study the effects of agricultural trade on deforestation. The context of forests differs from water in a number of critical ways, including most notably that the CO<sub>2</sub> externality is global rather than local,

and the marginal cost of extraction does not vary systematically with the magnitude of the externality across space.

As mentioned above, this paper also relates to an older theoretical literature on trade and natural resources. Chichilnisky (1994) uses a static, two-country model to illustrate that the resource depletion and welfare effects of trade liberalization are ambiguous when one country has ill-defined property rights over the resource. In a series of papers, Brander and Taylor (1997a,b, 1998) further develop this point in dynamic models of small open economies and North-South trade. Taylor (2011) finds empirical support for their framework in the near-extinction of the North American bison.

In the natural sciences, several papers consider the implications of “virtual water trade” for a wide range of topics such as groundwater depletion (Dalin et al., 2017), inequality across countries (Carr, Seekell, and D’Odorico, 2015), and climate change (Konar et al., 2013). Since these papers do not contain economic models of supply, demand, and trade, however, they quantify volumes of water implicitly traded across countries, but do not investigate counterfactual policies, equilibrium reallocation, or long-run dynamics.

The paper proceeds as follows. Section 2 uses a wide array of geospatial data to establish a set of stylized facts that frame the analysis. Section 3 lays out the model, and Section 4 shows how we calibrate it to match the data. Section 5 shows results from the policy counterfactuals, and Section 6 concludes.

## 2 Stylized facts

We assemble and harmonize data from 16 distinct geospatial and panel datasets to compile what constitutes, to our knowledge, the largest collection of global data on water and agriculture yet to be used in economics. The data document water resources and trends, agricultural activity, and land characteristics at a granular spatial resolution for the entire surface of the earth. We complement the spatial data with country-level measures of agricultural output, prices, trade flows, and policies. Table 1 summarizes the data, and Appendix A provides a full description of each dataset. Here, we combine these data with the relevant scientific and institutional context to establish five key facts about water and agriculture that frame our quantitative analysis.

### Fact 1: Water availability varies widely across space

We start by summarizing global variation in water availability. The main determinant of water extraction costs is the depth of the water table, which can be at ground level (surface water) or below ground (groundwater). Water table depth evolves according to a standard water balance equation (Viessman et al., 1977): for

any aquifer  $q$ ,

$$\Delta\text{Depth}_{qt} = \rho_q[\text{Consumption}_{qt} - \text{Recharge}_{qt}] \text{ given Depth}_{q0}, \quad (1)$$

where  $\rho_q$  – known as the specific yield – converts changes in water volumes into changes in water table depth based on local soil characteristics. Figure 1 shows how three components of this equation—initial depth, recharge, and changes in depth—differ across space.<sup>1</sup> We describe the global landscape of each of these variables below.

First, initial water table depth varies widely. Figure 1a maps gridded estimates that interpolate, using a hydrologic model, between observations from more than 1.6 million wells circa 2000 (Fan, Li, and Miguez-Macho, 2013). About 15% of all land is covered by surface water (e.g., rivers, lakes, inundated wetlands) usable for irrigation, and 8% of arable land has groundwater within one meter of the surface.<sup>2</sup> In contrast, 64% of arable land lies above water tables deeper than eight meters, a threshold beyond which submersible pumps must be used instead of lower-cost centrifugal pumps (Sekhri, 2014). The deepest water tables exceed 75 meters and are found beneath the arable lands of the American West, the South American Pacific coast, and North and Southern Africa—all relatively arid regions.<sup>3</sup> Note that this measure of distance from the surface to the top of the water table beneath it constitutes the primary determinant of the costs of water extraction for farmers, as we discuss in Section 3.

Second, precipitation, the main observable component of recharge, varies by nearly two orders of magnitude across the earth’s arable lands. Figure 1b maps gridded data from GMFD v3 (Sheffield, Goteti, and Wood, 2006). The data show that the median arable 5-arcminute grid cell receives 7,021 cubic meters per hectare ( $m^3/ha$ ) of precipitation per year, with the 1<sup>st</sup> to 99<sup>th</sup> percentile ranging from 44 to 33,208  $m^3/ha$ . For context, rice requires about 8,790  $m^3/ha$  annually, while millet requires roughly 4,300  $m^3/ha$ . Based on these benchmarks, less than 42% of arable land receives enough precipitation to support full coverage with rice, and the driest 31% receives too little to fully support millet without lowering water table depths.<sup>4</sup> Across space, average annual precipitation is positively correlated with the avail-

---

<sup>1</sup>All three maps are shown at the finest common resolution, which comprises equal-area grid cells that measure  $1^\circ \times 1^\circ$  at the equator.

<sup>2</sup>We define *arable lands* as locations where crops or pasture are detected at 5-arcminute resolution in the M3-Crops gridded land cover dataset (Monfreda, Ramankutty, and Foley, 2008).

<sup>3</sup>Although we measure water table depth as the distance below ground level (a nonnegative number), we maintain the convention that *lowering* the water table means *increasing* this number.

<sup>4</sup>These are conservative estimates, since a substantial share of precipitation is lost to runoff or returns to storage through return flow and cannot be productively used by crops. While no global estimates of runoff rates exist, accounting for runoff would lower our estimates of the extent of arable land with sufficient rainfall to support water-intensive crop production. That said, these figures are not meant to represent strict limits on where crops can be grown: farmers can plant on a subset of land or supplement with irrigation.

ability of ground and surface water, taking its highest values on the arable lands of Southeast Asia, coastal West Africa, and parts of the Amazon.

Third, medium-run trends in water table depth also vary across regions. Figure 1c shows the trend in total water storage ( $\Delta\text{TWS}$ ) recovered from the Gravity Recovery and Climate Experiment (GRACE) satellite over the period 2003–2016. Total water storage is defined as the aggregate volume of water in a location, including groundwater, soil moisture, surface water, snow, and ice (Tapley et al., 2004).<sup>5</sup> The data show tremendous heterogeneity throughout the world, at both regional scales—with broad patterns of gain or loss across Europe and the Middle East—and at more local scales—with diverging subnational patterns within the United States, India, and Australia.<sup>6</sup> For the world overall, we calculate that water losses and gains on arable land have been in near-perfect balance. Over the satellite record, 51.2 percent of arable acreage lost water, while 48.8 percent gained.<sup>7</sup> Moreover, regardless of sign, the trends were relatively modest in magnitude when compared to annual inflows of water: changes in storage across arable land ranged from  $-224$  to  $+188 \text{ m}^3/\text{ha}$  per year—as compared to median annual rainfall of  $7,021 \text{ m}^3/\text{ha}$ .

In general, heterogeneity in input abundance across locations governs farmer costs of water-intensive production and thus the potential benefits of trade. Given the considerable variation in the static and dynamic measures of water availability across the world, the data suggest a strong role for the spatial allocation of production of water-intensive tradable goods in maximizing the present and future value of the world’s water resources.

## Fact 2: Agriculture dominates global human water consumption

Recent work suggests that human water use is heavily concentrated in agriculture, which accounts for approximately 70% of global water withdrawals by humans (Dubois et al., 2011). Agriculture is responsible for an even larger share of water actually *consumed* by humans because crops evapotranspire a large share of applied moisture, such that it is lost to the local environment. In contrast, other water-extracting activities, like power plant cooling, return much of the water they withdraw to local water storage. Thus, Hoekstra and Mekonnen (2012) estimate that agriculture accounts for 92% of global water *consumption* by humans.<sup>8</sup> The remainder is split between industrial production (4.4%) and domestic supply (3.6%).

To show how this consumption is distributed across space, we combine gridded land cover data from M-3 Crops (Monfreda, Ramankutty, and Foley, 2008) with

<sup>5</sup>The corresponding change in water table depth in a given location can be calculated by multiplying the change in total water storage by the conversion factor  $\rho_q$  in Equation (1).

<sup>6</sup>Carleton, Crews, and Nath (2024) characterize the regions gaining and, in particular, losing water in more detail.

<sup>7</sup>Stable water supplies on arable land can be reconciled with large transfers of water from land to the oceans by evidence that the latter comprises mostly melting ice from mountain ranges and glaciers (Chen, Wilson, and Tapley, 2013).

<sup>8</sup>See Appendix A.2 for details on how these estimates are constructed.

estimated “virtual water content” from [Mekonnen and Hoekstra \(2011\)](#) for a sample of 126 crops that account for 88% of global planted acreage. For each 5-arcminute grid cell, we weight the virtual water content of each crop by its share of total planted acreage in that grid cell and then sum. Figure 2a maps the resulting global geographic distribution of agricultural water consumption. Consumption is highly concentrated in a few regions: agriculture in Uttar Pradesh consumes  $7,480 \text{ m}^3/\text{ha}$  per year, for example, while in Kenya the figure is just  $578 \text{ m}^3/\text{ha}$ . Across all arable land, the 1<sup>st</sup> to 99<sup>th</sup> percentile ranges from 0 (pasture) to  $3,759 \text{ m}^3/\text{ha}$ .<sup>9</sup>

The substantial variation here and in [Fact 1](#) has clear implications for trade: countries with limited water could, in theory, rely on imports of water-intensive crops. To examine whether they do, we first estimate “virtual water trade” by tracing virtual water content through crop-specific trade flows from Comtrade in 2009. Figure 2b maps the resulting net virtual water imports by country. Globally, we find that 21% of agricultural water consumption is embedded in international trade, consistent with earlier estimates ([Hoekstra and Mekonnen, 2012](#)).<sup>10</sup> In the driest countries, virtual water imports seem to play an indispensable role in offsetting local water scarcity: over 70% of agricultural water consumption in Egypt, Yemen, Israel, Jordan, and Kuwait is embedded in imports. But, in general, the map does not show a strong pattern of water flowing from water-abundant to water-scarce countries. This is consistent with work by [Debaere \(2014\)](#), which finds that although relatively water abundant countries tend to export more water-intensive products, water explains a much smaller share of global trade flows than labor and physical capital.<sup>11</sup>

However, country-level trade flows may not be the most relevant metric to evaluate potential water savings from trade, given the substantial local-level variation in water resources shown in [Fact 1](#). Instead, water endowments may be shaping global agricultural specialization and trade patterns as predicted by standard trade theory, but at a more granular spatial scale that better captures resource abundance. This paper brings together the high-resolution data necessary to examine specialization at the grid-cell, rather than the country level. We do so below in [Fact 5](#), which brings together the data on regional water availability from [Fact 1](#) with the measure of agricultural water use in [Fact 2](#). While no data at the grid cell level corresponds

---

<sup>9</sup>While some pasture lands are irrigated and consume meaningful quantities of water ([Boser et al., 2024](#)), this is rare globally and [Mekonnen and Hoekstra \(2011\)](#) do not include estimates of pasture water consumption. Therefore, we only account for crop water use in this calculation.

<sup>10</sup>A large literature studies virtual water trade. See, for example, [Dalin et al. \(2012\)](#); [Carr et al. \(2013\)](#); [d'Odorico et al. \(2019\)](#). [Dalin et al. \(2017\)](#) estimate that 11% of groundwater overdraft is embedded in agricultural exports, mostly from India, Pakistan, and the United States.

<sup>11</sup>Differences in relative agricultural productivity and relative endowments of arable land can drive the pattern of specialization instead, leading virtual water to flow from scarce countries to abundant ones. [Kumar and Singh \(2005\)](#) first documented that virtual water often flows out of water-poor, arable land-rich countries (e.g., Malawi) to arable land-poor, water-rich countries (e.g., Norway). See [Ansink \(2010\)](#) for a helpful discussion of virtual water trade through the lens of the Heckscher-Ohlin model.

exactly to country-level trade flows, we can test whether specialization at high spatial scales follows from the predictions of the Heckscher-Ohlin-Vanek theorem.<sup>12</sup> But, before doing so, we must recognize important reasons why predictions from the standard model might fail. In particular, widespread distortions in water use and agricultural markets could obscure or even reverse patterns suggested by water abundance alone. We turn to these next in [Facts 3–4](#).

### **Fact 3: Water is almost always extracted under open access**

Water is often extracted under open access, with few limits on use and no market price ([Libecap, 2008](#)). When property rights are undefined or poorly enforced, farmers draw from a shared resource without bearing the full social cost, raising extraction costs for others both now and in the future. Even when rights exist, they are often based on historical claims or institutional rules that do not allow water to flow to its highest-value uses. In the few places where water markets function well, prior work estimates that the gains are large: water is reallocated efficiently and total water withdrawals are reduced ([Ayres, Meng, and Plantinga, 2021](#); [Bruno and Jessoe, 2021](#); [Rafey, 2023](#); [Hagerty, 2024](#)).

Still, despite these documented benefits, tradable water rights are rare in practice. We conduct an extensive review of the literature on agricultural water markets and find that at least 94% of the world’s agricultural output occurs in regions with no formal mechanisms for farmers to trade water ([Appendix Figure C.1](#)). Fully-established markets exist in only a handful of countries: Australia, Chile, Mexico, Spain, South Africa, Oman, and several western U.S. states.<sup>13</sup> Taken together, these areas account for only about 6% of global agricultural production value—and that estimate assumes full market coverage, which is rarely the case.

Some informal water trading occurs in parts of India, Pakistan, and China, but without clear rules to address the externality ([Saleth, 2004](#); [Jacoby, Murgai, and Rehman, 2004](#); [Zhang, Wang, Huang, and Rozelle, 2008](#)).<sup>14</sup> Some places, including India, have adopted rationing schemes that reduce overuse without improving efficiency ([Ryan and Sudarshan, 2022](#)), though such regulatory approaches remain rare ([Richter, 2016](#)).

---

<sup>12</sup>A large literature has tested this theorem. See, in particular, [Trefler \(1993, 1995\)](#); [Davis \(1995\)](#); [Davis and Weinstein \(2001\)](#); [Romalis \(2004\)](#); [Morrow \(2010\)](#).

<sup>13</sup>U.S. states with formal water markets for farmers include Arizona, California, Colorado, Idaho, Montana, Nevada, New Mexico, Oregon, Texas, Utah, Washington, and Wyoming ([Griffin and Characklis, 2002](#); [Phillips and Teng, 2020](#); [Schwabe, Nemati, Landry, and Zimmerman, 2020](#)). For more information on water markets outside the U.S., see [Young \(2013\)](#) and [Rafey \(2023\)](#) on Australia, [Donoso \(2013\)](#) on Chile, [Hearne and Trava \(1997\)](#) and [Kloezen \(1998\)](#) on Mexico, [Palomo-Hierro, Gómez-Limón, and Riesgo \(2015\)](#) and [Donna and Espín-Sánchez \(2023\)](#) on Spain, and [Easter and Huang \(2014\)](#) and [Grafton, Libecap, McGlennon, Landry, and O’Brien \(2011\)](#) for broad global overviews.

<sup>14</sup>China has also established a national water exchange for interprovincial transfers and small pilot programs for farmer-to-farmer trade ([Wang and Yang, 2018](#)).

Even where water markets exist on paper, they often face implementation challenges. Transaction costs remain high in many settings, and actual trade volumes are low. In drought years, water trading accounts for over 20% of extraction in Australia and Chile, but just 5% in Spain and less than 1% in South Africa (Grafton et al., 2011).<sup>15</sup> Institutional barriers undermine the functioning of many nominal markets (Easter, Rosegrant, and Dinar, 1999; Debaere et al., 2014; Ferguson, 2024).

In short, the market failures that characterize water input use seem pervasive and broadly intractable.<sup>16</sup> With that in mind, our policy exercises will focus on second-best interventions that take existing failures in input markets for water as given and instead focus on policy in agricultural output markets, which also play a key role in driving global water use, as we document next.

#### Fact 4: Water consumption responds to agricultural policy

A large literature in agricultural economics shows that subsidies, taxes, tariffs, and other price interventions strongly affect farmer decisions, including land use, crop choice, and technology adoption.<sup>17</sup> Because crop production is the main driver of global water consumption, these policies also influence where and how much water is consumed.

Carleton (2021) provides direct evidence of this link. The paper measures the global effects of agricultural price interventions, summarized by the World Bank's Nominal Rate of Assistance (NRA), on trends in total water storage ( $\Delta\text{TWS}$ ) from GRACE. Using panel regressions that leverage the interaction between spatial variation in land use and temporal variation in policy, the study finds that a 10 percentage point increase in net agricultural subsidy lowers annual water storage by about  $45 \text{ m}^3/\text{ha}$ . This effect is roughly equivalent to moving from the median global parcel of arable land to the 25<sup>th</sup> or 75<sup>th</sup> percentile in water storage trend. Similarly, Chatterjee, Lamba, and Zaveri (2022) and Sekhri (2022) find that domestic price supports and export promotion policies, respectively, significantly accelerated groundwater depletion in India.

These findings suggest that even modest changes in agricultural policy can have lasting effects on water availability. And such policies are indeed widespread: Anderson, Rausser, and Swinnen (2013) document that, although they have converged toward zero in the last 50 years, average NRAs to agricultural tradables in high-income countries were still close to 20% in 2005–09. National NRAs for agricultural

<sup>15</sup> Based on similar measurements, Rafey (2023) estimates that traded water rights account for no more than 1% of global freshwater withdrawals each year.

<sup>16</sup> Endo, Kakinuma, Yoshikawa, and Kanae (2018) document the full set of countries and regions where water markets could *potentially* be instituted, based on a review of 296 current water laws implemented by governments throughout the world. Less than half of the cases they consider satisfy all three legal conditions necessary to support water markets.

<sup>17</sup> See, for example, Roberts and Schlenker (2013); Hendricks, Smith, and Sumner (2014); Scott (2014); Hendricks, Smith, and Villoria (2018).

tradables varied from around  $-30\%$  for several African countries to over  $100\%$  for a few high-income countries such as South Korea and Norway. This substantial heterogeneity impinges most on global markets: trade-policy instruments account for at least  $60\%$  of agricultural NRAs globally, which further underlines our focus on second-best interventions through international trade.

### **Fact 5: Water-abundant arable lands tend to specialize in water-intensive crops**

In the absence of distortions, we would expect water-intensive crops to be grown in water-abundant locations. As discussed above in [Facts 2](#), this prediction follows from the standard Heckscher-Ohlin model, in which factor abundance drives comparative advantage. In our dynamic setting, regions with greater water availability can sustain more water-intensive cropping over time without lowering local water tables. While water is only one among many determinants of crop suitability—including climate, soil, and technology—an efficient global allocation would tend to concentrate water-intensive production in water-rich areas.

In practice, as the last two facts showed, agricultural markets are distorted on both sides. Whether specialization follows factor abundance is therefore an empirical question. To quantify this pattern at high spatial resolution, we use detailed data on crop-level water requirements, land use, and water availability. For each 5-arcminute parcel of global arable land, we compute an index of the water intensity of land use by calculating a planted hectare-weighted average of crop-level water intensities using data from [Mekonnen and Hoekstra \(2011\)](#) and [Monfreda, Ramankutty, and Foley \(2008\)](#). As above, pasture land is treated as requiring no human-applied water, so the measure captures both the intensive and extensive margins of water use. Figure 3 maps agricultural water intensity alongside depth to the water table, rainfall, and long-run changes in total water storage ( $\Delta TWS$ ).

The data show that water-intensive production is strongly concentrated in water-abundant regions. The maps in panels (a) and (c) show that areas with low water tables and low rainfall—such as the western United States, Australia, and arid parts of North Africa—tend to exhibit very low water use. In contrast, water-rich regions such as Southeast Asia, the midwestern U.S., and the Amazon grow more water-intensive crops on more land. These patterns are also visible in the decile plots in panels (b) and (d): on average, land in the top quintile of groundwater access is more than three times as water-intensive as land in the bottom quintile. For rainfall, the difference is more than fivefold. These differences reflect both area planted and crop choice. When conditioning on cropped acreage, the top quintile of rainfall regions select crops that use twice as much water per hectare as those in the bottom quintile.<sup>18</sup> Thus, these cross-sectional measures of land use and

---

<sup>18</sup>This result aggregates over highly heterogeneous patterns across water-intensive crops. Rice, for example, is especially concentrated in the wettest parts of the world, while almonds, also highly

water availability suggest a strong role for resource abundance driving patterns of specialization, consistent with the Heckscher-Ohlin hypothesis.

The correlation between water-intensive land use and the dynamic measure of water availability – trends in total water storage – shows a somewhat different pattern. Panels (e) and (f) show that the regions *losing* water most rapidly over the 2003–2016 period—such as northern India, Turkey, and northeastern China—have the *highest* water intensity of agricultural land use. The global average is 2,400 m<sup>3</sup>/ha, but in the bottom decile of  $\Delta\text{TWS}$ , the average is over 3,000 m<sup>3</sup>/ha, and in the bottom 1%, nearly 3,500 m<sup>3</sup>/ha. Carleton, Crews, and Nath (2024) examine the characteristics of these regions, and show that they tend to be highly populated, water-scarce, and have relatively low agronomic potential. As one especially extreme example, Northeastern India ranks in the bottom 1% of  $\Delta\text{TWS}$ , has crops planted on over 91% of arable land, and uses more than three times the global average amount of water per hectare. Total water storage in the region is declining at a rate equivalent to annual rainfall approximately every twenty years.

Still, these regions are rare. Only about 6.8% of the world’s arable land lies in the intersection of low rainfall, deep water tables, and declining  $\Delta\text{TWS}$ , and water use in these regions is modest (Appendix Figure C.3). The final panel of Figure 3 shows that, once the bottom decile of  $\Delta\text{TWS}$  is excluded, water intensity is again increasing in trends in water availability. With the exception of a small number of regions, global agricultural water use is concentrated not only in locations with abundant existing resources, but also those with stable to increasing trends in water availability.

In sum, water-intensive agricultural production is largely concentrated in water-abundant regions. While the country-level patterns of agricultural trade we document in Fact 2 do not show a strong correlation between water abundance and water-intensive exports, the high-resolution spatial data compiled in this paper reveal a more granular picture in which the dominant global pattern is indeed consistent with comparative advantage in water playing a central role in driving specialization, even in the presence of strong distortions. The following sections investigate how the causes and consequences of this fact relate to global agricultural trade and trade policy.

### 3 Model

We extend the model in Costinot, Donaldson, and Smith (2016) by allowing agricultural productivity to depend on local water table depth. Depth, in turn, evolves with local agricultural water consumption according to the water balance equation in Equation (1). This structure allows us to quantify how trade and policy shape patterns of agricultural production and water use over time. The rest of this section describes the full model.

---

water-intensive, are grown primarily in dry areas, such as California (Appendix Figure C.2).

### 3.1 Basic environment

Time is discrete and indexed by  $t \in \mathbb{N}$ . The world economy consists of multiple countries, indexed by  $i \in \mathcal{I} \equiv \{1, \dots, I\}$ , where consumption and production take place, and multiple aquifers, indexed by  $q \in \mathcal{Q} \equiv \{1, \dots, Q\}$ , from which water is extracted to be used in production.<sup>19</sup> Motivated by Fact 3, we assume that the water in each aquifer is an open access resource, available at the cost of extraction to any that cultivate the land above that aquifer.

Land is divided into heterogeneous fields, indexed by  $f \in \mathcal{F} \equiv \{1, \dots, F\}$ , each of which is within some country  $i$  and above some aquifer  $q$ .<sup>20</sup> Fields comprise a continuum of heterogeneous parcels, indexed by  $\omega$ . All fields correspond to 5-arcminute grid cells. Because the surface of the earth is curved, grid cells at different latitudes cover different areas, with larger grid cells closer to the equator. We let  $h^f$  denote the area in hectares of field  $f$ .

Atomistic laborers in each country can choose to either farm their assigned parcel, earning the revenue from their harvest, or work for a wage  $w_i$  producing an outside good, which we think of as a composite of manufactured goods.<sup>21</sup> A farmer uses his own labor to extract water, which he combines with his land and remaining time to produce one of multiple crops, indexed by  $k \in \mathcal{K} \equiv \{1, \dots, K\}$ .

#### 3.1.1 Preferences

In each country  $i$  there is a representative household who lives hand-to-mouth and derives utility in each period from consuming the outside good,  $C_{it}^o$ , and an agricultural composite,  $C_{it}$ :

$$U_{it} = C_{it}^o + \zeta_i \ln C_{it}. \quad (2)$$

Since the upper-level utility function in Equation (2) is quasilinear, there are no income effects. The total demand for crops depends only on a country-specific demand shifter,  $\zeta_i \geq 0$ .

The agricultural composite,  $C_{it}$ , depends on the consumption of each crop,  $C_{it}^k$ , which itself depends on the consumption of varieties from different origins,  $C_{jiti}^k$ :

$$C_{it} = \left[ \sum_{k \in \mathcal{K}} \left( \zeta_i^k \right)^{\frac{1}{\kappa}} \left( C_{it}^k \right)^{\frac{\kappa-1}{\kappa}} \right]^{\frac{\kappa}{\kappa-1}} \quad (3)$$

and

$$C_{it}^k = \left[ \sum_{j \in \mathcal{I}} \left( \zeta_{ji}^k \right)^{\frac{1}{\sigma}} \left( C_{jiti}^k \right)^{\frac{\sigma-1}{\sigma}} \right]^{\frac{\sigma}{\sigma-1}}, \quad (4)$$

---

<sup>19</sup>Aquifers occur naturally and therefore need not be circumscribed by country borders.

<sup>20</sup>Accordingly, objects that vary at the field level will not have country- or aquifer-specific subscripts. When we need to refer to the country in which field  $f$  is located, we will write  $i(f)$ . Likewise, we will write  $q(f)$  for the aquifer below field  $f$ .

<sup>21</sup>Because laborers are assigned to parcels one-to-one, we sometimes use  $\omega$  as an index of laborers.

where  $\kappa > 0$  denotes the elasticity of substitution between different crops (e.g., corn vs. soybeans) and  $\sigma > 0$  denotes the elasticity of substitution between different varieties of a given crop (e.g., Chinese vs. American soybeans). The last preference parameters,  $\zeta_i^k \geq 0$  and  $\zeta_{ji}^k \geq 0$ , are crop- and crop-origin-specific demand shifters for country  $i$ .

### 3.1.2 Technology

In the agricultural sector, we assume that the farmer of each parcel  $\omega$  has access to a Cobb-Douglas technology for each crop  $k$  that combines some fraction of his labor endowment,  $H_t^{fk}(\omega)$ , with a Leontief bundle of land,  $L_t^{fk}(\omega)$ , and water,  $G_t^{fk}(\omega)$ ,

$$Q_t^{fk}(\omega) = A^{fk}(\omega) \left[ H_t^{fk}(\omega) \right]^\alpha \times \left[ \min \left\{ L_t^{fk}(\omega), \frac{G_t^{fk}(\omega)}{\phi^k} \right\} \right]^{1-\alpha}, \quad (5)$$

where  $A^{fk}(\omega) \geq 0$  denotes the total factor productivity of parcel  $\omega$  in field  $f$  if allocated to crop  $k$ , and  $\phi^k$  measures how much water per unit of land is required to grow crop  $k$ . Without loss, we normalize the size of parcels such that each farmer is endowed with one unit of land.<sup>22</sup>

Analogous to the approach in [Eaton and Kortum \(2002\)](#), we assume that TFP is independently drawn for each parcel  $\omega$  from a field-specific Fréchet distribution:

$$\mathbb{P} \left\{ A^{f1}(\omega) \leq a^1, \dots, A^{fK}(\omega) \leq a^K \right\} = \exp \left\{ -\gamma \sum_{k \in \mathcal{K}} \left( \frac{a^k}{A^{fk}} \right)^{-\theta} \right\} \quad (6)$$

where  $\theta > 1$  measures the extent of technological heterogeneity within each field and the constant  $\gamma$  is set such that  $A^{fk} = \mathbb{E}[A^{fk}(\omega)]$ .<sup>23</sup> The term  $A^{fk} \geq 0$  measures the comparative and absolute advantage of a field  $f$  in producing crop  $k$ .

To extract the water needed to irrigate his parcel  $\omega$ , a farmer must allocate the remaining fraction  $1 - H_t^{fk}(\omega)$  of his labor endowment. Water is extracted under constant returns to scale in the farmer's labor only.<sup>24</sup> His productivity in extraction, however, is assumed to vary with the current depth of the water table below his parcel. Intuitively, it requires more labor to draw up one cubic meter of water from an aquifer with a deep water table than from an aquifer with a shallow

<sup>22</sup>The main restriction of the technology in Equation (5) is instead that each farm is endowed with a fixed amount of labor per unit of land. This restriction, along with the Leontief assumption, is nevertheless consistent with the underlying agronomic models that we use to calibrate the parameters of this technology in Section 4. Appendix B.1.5 discusses a generalization to a nested CES technology.

<sup>23</sup>Formally, we set  $\gamma \equiv \Gamma[(\theta - 1)/\theta]^{-\theta}$ , where  $\Gamma(\cdot)$  denotes the gamma function.

<sup>24</sup>A linear extraction technology is standard, dating back to the canonical Gordon-Schaefer model of renewable resource use ([Gordon, 1954](#); [Schaefer, 1954](#)). See [Brown \(2000\)](#) and [Stavins \(2011\)](#) for reviews. [Brander and Taylor \(1997a,b, 1998\)](#) embed this model into open economy settings.

one. In particular, let  $D_{qt}$  denote the depth of the water table in aquifer  $q$  in period  $t$ . Then the corresponding labor productivity in water extraction is given by

$$A_q^w(D_{qt}) = \Upsilon_q D_{qt}^{-v}. \quad (7)$$

The extraction productivity conditional on water table depth,  $\Upsilon_q$ , is allowed to vary across aquifers to account for, among other things, differences in pumping technology and the prevalence of surface water.<sup>25</sup>

The outside good is produced under constant returns to scale using labor only. The productivity of each worker in the outside sector,  $A_i^o(\omega)$ , is also drawn independently from a Fréchet distribution with the same shape parameter  $\theta$ :

$$\mathbb{P}\{A_i^o(\omega) \leq a^o\} = \exp\left\{-\gamma\left(\frac{a^o}{A_i^o}\right)^{-\theta}\right\} \quad (8)$$

where  $A_i^o = \mathbb{E}[A_i^o(\omega)]$  is the average labor productivity in country  $i$ 's outside sector. Importantly, draws from this distribution are independent of the crop-specific productivity draws for the parcel the worker would otherwise cultivate.<sup>26</sup>

### 3.1.3 Market structure and trade costs

All markets are perfectly competitive. The outside good is freely traded and is used as the numeraire. International trade in crops, on the other hand, is subject to iceberg trade costs: In order to sell one unit of crop  $k$  to the representative consumer in country  $j$ , farmers in country  $i$  must ship  $\delta_{ij}^k$  units. The usual no-arbitrage condition then requires that the price of crop  $k$  produced in country  $i$  and sold in country  $j$  be equal to

$$p_{ijt}^k = \delta_{ij}^k p_{it}^k, \quad (9)$$

where  $p_{it}^k$  denotes the local consumer price of the domestic variety of crop  $k$  in country  $i$ .

In addition to trade costs, crops are subject to policy distortions. Each national government sets a proportional tax  $\tau_{it}^k$  for each crop  $k$  at each date  $t$ .<sup>27</sup> With  $p_{it}^k$  denoting the price paid by local consumers, the distorted farm gate price received by

---

<sup>25</sup>In principle, the model can directly account for surface water with depth at or near zero. In practice, however, the spatial scale of a surface water body is typically much smaller than that of its underlying aquifer. Because we model water tables at the resolution of aquifers, two water tables that are both near zero depth on average may still be associated with varying shares of surface water. Variation in the parameters  $\{\Upsilon_q\}$ , which will be estimated as structural residuals in Section 4, can account for this.

<sup>26</sup>This model is observationally equivalent to one in which it is the laborers themselves that vary in farming productivity across parcels within a field. The assumption is then that the idiosyncratic deviations of a laborer's productivity from its corresponding task-specific mean are uncorrelated across tasks. Note, however, that the empirical correlation between those means is left completely unrestricted.

<sup>27</sup>If  $\tau_{it}^k < 1$ , the policy is a net tax on that commodity; if  $\tau_{it}^k > 1$ , it is a net subsidy.

farmers is  $\tau_{it}^k p_{it}^k$ . Agricultural policies are funded by lump-sum taxes on the domestic consumer such that the government's budget is always balanced.

### 3.1.4 Evolution of local water resources

The depth of the water table in aquifer  $q$  follows the law of motion from Equation (1), reformulated here as

$$D_{qt+1} = D_{qt} + \rho_q[(1 - \psi)X_{qt} - R_q] \quad (10)$$

where  $X_{qt}$  is the total amount of water extracted from aquifer  $q$  in period  $t$ ,  $R_q$  is the natural recharge of the aquifer,  $\psi$  is the constant rate of return flow,<sup>28</sup> and  $\rho_q$  is an aquifer-specific conversion factor between volume and depth that depends on the local soil type.

## 3.2 Competitive equilibrium

In a competitive equilibrium, all consumers maximize their utility, all laborers maximize their returns (either by cultivating the revenue-maximizing crop on their parcel or by working in the outside sector), and all markets clear in each period.

### 3.2.1 Utility maximization

Given Equations (2), (3), (4), and (9), utility maximization by the representative household in each country requires that

$$C_{jit}^k = \zeta_i \frac{\zeta_i^k (P_{it}^k)^{1-\kappa}}{\sum_{\ell \in \mathcal{K}} \zeta_i^\ell (P_{it}^\ell)^{1-\kappa}} \frac{\zeta_{ji}^k (\delta_{ji}^k p_{jt}^k)^{-\sigma}}{\sum_{n \in \mathcal{I}} \zeta_{ni}^k (\delta_{ni}^k p_{nt}^k)^{1-\sigma}} \quad \text{for all } i, j \in \mathcal{I}, k \in \mathcal{K}, \quad (11)$$

where

$$P_{it}^k = \left[ \sum_{n \in \mathcal{I}} \zeta_{ni}^k (\delta_{ni}^k p_{nt}^k)^{1-\sigma} \right]^{\frac{1}{1-\sigma}}$$

denotes the CES price index associated with crop  $k$  in country  $i$  at time  $t$ .<sup>29</sup>

### 3.2.2 Revenue maximization and labor choice

Each laborer chooses to either cultivate his parcel or work in the outside sector. In the outside sector, profit maximization requires that workers are paid their marginal

---

<sup>28</sup>When water is applied to a cultivated area, the crop evapotranspires only a fraction of that water. The rest soaks back into the soil and, ultimately, back into the aquifer. The parameter  $\psi$  accounts for the latter fraction. Only the volume  $(1 - \psi)X_{qt}$ , then, is actually *consumed* by crops above aquifer  $q$  in period  $t$ . This corresponds to Consumption <sub>$qt$</sub>  in Equation (1).

<sup>29</sup>See Appendix B.1.1 for derivation.

products whenever the outside good is produced. Throughout this paper, we assume that labor endowments are large enough and expenditure shares on agricultural goods are low enough that the outside good is always produced in all countries.

Should he choose to cultivate his parcel, a farmer selects the crop that maximizes his revenue. Revenue maximization requires that, for any crop  $k$ , the farmer allocates his labor optimally between extracting water and tending the crop. One can show that his optimal output of crop  $k$  can then be written as

$$Q_t^{fk}(\omega) = A^{fk}(\omega)M(\phi^k, D_{q(f)t}) \quad (12)$$

and his corresponding revenue as

$$r_t^{fk}(\omega) = \tau_{i(f)t}^k p_{i(f)t}^k A^{fk}(\omega) M(\phi^k, D_{q(f)t}),$$

where  $M$  is bounded between zero and one and is decreasing in both the water intensity of the crop,  $\phi^k$ , and the current water table depth,  $D_{q(f)t}$ .<sup>30</sup> Because  $M$  is bounded between zero and one, it can be interpreted as a *yield gap* relative to  $A^{fk}(\omega)$ , which itself can be interpreted as the maximum *potential yield* for crop  $k$  on that parcel. This is consistent with our calibration strategy in Section 4.

We assume that laborers know their outside labor productivity and their vectors of crop-specific productivities in each period before they select in which sector to work. It follows that a laborer assigned to parcel  $\omega$  in field  $f$  cultivates crop  $k$  on his parcel in period  $t$  with probability

$$\pi_t^{fk} \equiv \mathbb{P} \left\{ r_t^{fk}(\omega) = \max \{A_{i(f)}^o(\omega), r_t^{f1}(\omega), \dots, r_t^{fK}(\omega)\} \right\}.$$

Since there is a continuum of parcels within each field,  $\pi_t^{fk}$  also corresponds to the share of parcels on which crop  $k$  is cultivated in field  $f$  in period  $t$ . Because TFP and labor productivity in the outside sector are both independently distributed Fréchet with a common shape parameter according to Equations (6) and (8), standard algebra implies that for all  $f \in \mathcal{F}$  and  $t \in \mathbb{N}$ ,

$$\pi_t^{fk} = \frac{\left( \tau_{i(f)t}^k p_{i(f)t}^k A^{fk} M(\phi^k, D_{q(f)t}) \right)^\theta}{\left( A_{i(f)}^o \right)^\theta + \Pi_t^f}, \quad (13)$$

where

$$\Pi_t^f = \sum_{\ell \in \mathcal{K}} \left( \tau_{i(f)t}^\ell p_{i(f)t}^\ell A^{f\ell} M(\phi^\ell, D_{q(f)t}) \right)^\theta$$

summarizes the profitability of cultivating field  $f$  at time  $t$ .<sup>31</sup> Looking at the expression in Equation (13), one sees that the higher a crop's farm-gate price,  $\tau_{i(f)t}^k p_{i(f)t}^k$ ,

---

<sup>30</sup>See the definition and derivation of  $M$  in Appendix B.1.2.

<sup>31</sup>See Appendix B.1.3 for derivation.

or mean productivity,  $A^{fk}$ , the higher is the share of a given field allocated to that crop. The higher the crop-specific water requirements,  $\phi^k$ , however, the lower is the share of that field allocated to crop  $k$ . The lower the labor productivity in water extraction due to a deep water table,  $D_{q(f)t}$ , or the higher the mean labor productivity in the outside sector,  $A_{i(f)}^o$ , the lower is the share of a given field allocated to *any* crops, as laborers are more likely to leave their parcels fallow to work in the outside sector. Finally, the larger the shape parameter  $\theta$ , the less heterogeneity there is across parcels within a field, so the more sensitive farmers are to cross-crop differences in prices or average productivity.

Let  $\mathcal{F}_i = \{f : i(f) = i\}$  denote the set of all fields in country  $i$  so that

$$Q_{it}^k = \sum_{f \in \mathcal{F}_i} \int_0^{h^f} Q_t^{fk}(\omega) d\omega$$

denotes the total output of crop  $k$  in country  $i$ . By Equation (12) and the law of iterated expectations, it must be that

$$Q_{it}^k = \sum_{f \in \mathcal{F}_i} h^f \pi_t^{fk} M(\phi^k, D_{q(f)t}) \mathbb{E} \left[ A^{fk}(\omega) \middle| r_t^{fk}(\omega) = \max \{A_{i(f)}^o(\omega), r_t^{f1}(\omega), \dots, r_t^{fK}(\omega)\} \right].$$

Given our distributional assumptions, one can check that<sup>32</sup>

$$\mathbb{E} \left[ A^{fk}(\omega) \middle| r_t^{fk}(\omega) = \max \{A_{i(f)}^o(\omega), r_t^{f1}(\omega), \dots, r_t^{fK}(\omega)\} \right] = A^{fk} \left( \pi_t^{fk} \right)^{-\frac{1}{\theta}}.$$

Because of the endogenous selection of fields into crops, the average productivity conditional on a crop being produced is strictly greater than the unconditional average. Combining the two previous expressions with Equation (13), we obtain the following expression for the supply of crop  $k$  in country  $i$ :

$$Q_{it}^k = \sum_{f \in \mathcal{F}_i} h^f A^{fk} M(\phi^k, D_{q(f)t}) \left( \pi_t^{fk} \right)^{\frac{\theta-1}{\theta}} \quad (14)$$

for all  $i \in \mathcal{I}$  and  $k \in \mathcal{K}$ .

### 3.2.3 Market clearing and feasibility

Since trade in crops is subject to iceberg trade costs, market clearing for all varieties of all crops requires

$$Q_{it}^k = \sum_{j \in \mathcal{I}} \delta_{ij}^k C_{ijt}^k \quad \text{for all } i \in \mathcal{I} \text{ and } k \in \mathcal{K}. \quad (15)$$

---

<sup>32</sup>See Appendix B.1.4 for derivation.

Let  $\mathcal{F}_q = \{f : q(f) = q\}$  denote the set of all fields above aquifer  $q$ . Then total water extracted from aquifer  $q$  in period  $t$  is

$$X_{qt} = \sum_{f \in \mathcal{F}_q} \sum_{k \in \mathcal{K}} h^f x_t^{fk} \pi_t^{fk}, \quad (16)$$

where  $x_t^{fk}$  is optimal water extraction to grow crop  $k$  on field  $f$ .<sup>33</sup>

Finally, under the assumption that the outside good is produced in all countries, the amount of labor demanded by the outside sector adjusts to guarantee labor market clearing at a unit wage per efficiency unit of labor.

### 3.2.4 Definition and well-posedness of the competitive equilibrium

A competitive equilibrium in this environment is a feasible path, starting from an initial vector of water table depths, along which consumers maximize their utility, laborers maximize their returns, and all markets clear.

**Definition 1.** Given a set of agricultural policies,  $\{\tau_{it}^k\}$ , and an initial vector of water table depths,  $\{D_{q0}\}$ , a *competitive equilibrium* is a path of consumption,  $\{C_{jxt}^k\}$ , output,  $\{Q_{it}^k\}$ , prices,  $\{p_{it}^k\}$ , shares,  $\{\pi_t^{fk}\}$ , water table depths,  $\{D_{qt}\}$ , and water extractions,  $\{X_{qt}\}$ , such that Equations (10), (11), (13), (14), (15), and (16) hold.<sup>34</sup>

Conditions for the existence and uniqueness of an equilibrium are established in Appendix B.2. A key feature of the equilibrium is that it can be decomposed into a sequence of static sub-equilibria connected only through the law of motion in Equation (10). This is not because laborers are assumed to be myopic ad hoc; instead, it follows naturally from the fact that the water in each aquifer is treated as an open access resource, the stock of which is always large relative to the farms that draw from it.<sup>35</sup> Accordingly, laborers do not consider how their choice of activity—and the water that must be extracted to do said activity—will affect the water table depth below their parcel in the future. Instead of solving a dynamic program, then, each laborer just solves a sequence of static problems. This is what makes estimation feasible at the fine spatial scales we have in our data, which we turn to next.<sup>36</sup>

---

<sup>33</sup>See the definition and derivation of  $x_t^{fk}$  in Appendix B.1.2.

<sup>34</sup>There is nothing about the outside sector in this definition because that sector acts like a residual claimant on the resources of the economy once agricultural markets clear. See Appendix B.2.4 for discussion.

<sup>35</sup>That the representative consumers are assumed to be hand-to-mouth is also necessary.

<sup>36</sup>Dynamic spatial models are notoriously hard to solve (Rossi-Hansberg, 2019). The framework developed in Desmet, Nagy, and Rossi-Hansberg (2018) has recently been put to great use tackling environmental questions (see, e.g., Desmet, Kopp, Kulp, Nagy, Oppenheimer, Rossi-Hansberg, and Strauss, 2021; Cruz and Rossi-Hansberg, 2024). Like ours, that framework relies on assumptions around agents' decision problems that ensure those problems are always static. In our case, the assumption is on the market structure (or lack thereof) for water; in their case, the assumption is on the returns to investment.

## 4 Estimation

To simulate the model described in Section 3, we require estimates of a host of parameters governing the demand, supply, and hydrology blocks of the model. We cover each in turn. But, before doing so, we briefly describe the data we use and the sample restrictions that we impose on the inputs to our estimation procedure. Details on the datasets used can be found in Appendix A. We conclude by showing the model’s fit to the data.

### 4.1 Data and sample selection

We choose 2009 as the base year for our analysis because it is the midpoint of the GRACE satellite period and the earliest year that postdates all water table depths reported in Fan, Li, and Miguez-Macho (2013). It also marks the start of the FAO’s Global Agro-Ecological Zones v4 (GAEZ) reference period, which targets 2009–11 FAOSTAT data on agricultural production and land use.

To construct our sample, we select 52 countries ( $i \in \mathcal{I}$ ) that account for 94% of global GDP, 97% of global agricultural production value, and 99% of global agricultural laborers in the base year (see Figure 4a).<sup>37</sup> Within these countries, we model land use at the resolution of 5-arcminute grid cells to match the resolution of the GAEZ dataset. There are approximately 1.9 million grid cells that overlap with our selected countries. We make two further adjustments to this sample. First, using the Global Land Cover-SHARE database (Latham et al., 2014) at 30-arcsecond resolution, we exclude from each grid cell any non-arable acreage.<sup>38</sup> Second, using the GCI30 database (Zhang et al., 2021) at 30m resolution, we scale each field’s arable acreage by the estimated number of growing seasons per year. The resulting sample has approximately 1.1 million fields ( $f \in \mathcal{F}$ ) with non-zero arable acreage.

From the set of 41 non-fodder crops for which GAEZ reports potential yields, we select 22 crops ( $k \in \mathcal{K}$ ) that account for 78% of global agricultural production and 82% of global water consumption (see Figure 4b). Our sample of crops includes major staples such as wheat, rice, and maize; water-intensive cash crops such as coffee, cotton, and oil palm; and regional staples for many drier low-income regions such as cassava, chickpeas, and yams. Importantly, the selected crops span a wide range of water intensities, from 3,014 m<sup>3</sup>/ha for buckwheat to 21,740 m<sup>3</sup>/ha for bananas.

We construct aquifers ( $q \in \mathcal{Q}$ ) as clusters of contiguous GRACE grid cells. Following Richey et al. (2015), we first overlay a map of the 37 largest global aquifer

<sup>37</sup>Coverage shares are reported relative to totals for which data is available from both GAEZ and FAOSTAT in the base year.

<sup>38</sup>We define as *arable* any land that is currently covered by crops or pasture. We therefore exclude forest, permanent snow, glaciers, surface water, and artificial surfaces (e.g., cities). Our counterfactuals hold fixed the total amount and spatial distribution of arable land. Land use changes on the extensive margin consist exclusively of converting pasture to cropland and vice versa. See Gouel and Laborde (2021) for related discussion.

systems obtained from the Worldwide Hydrogeological Mapping and Assessment Program (WHYMAP) and group GRACE grid cells into clusters if they are all at least partially contained within the borders of a single aquifer. We then overlay a map of 180 NASA-delineated water basins and group the *remaining* GRACE grid cells into clusters according to the basin in which they lie. These basins are defined based on their hydrologic connectivity—within each basin, precipitation exits from the same location—so we take this as a useful measure of the geographic extent of the open access externality. This procedure yields 278 clusters that partition global land area. We finish by discarding all GRACE grid cells that lie fully outside the arable lands within our sample countries. The surviving 199 clusters comprise our set of aquifers in the model (see Figure 4c).

## 4.2 Demand

To estimate the demand block, we closely follow the procedure described in Costinot, Donaldson, and Smith (2016, §V.A). We proceed in three steps, moving outward from the innermost nest of the demand system in Equation (11). First, we use data on prices,  $p_j^k$ , and bilateral trade flows by crop,  $E_{ji}^k$ , to estimate the elasticity of substitution  $\sigma$  between different varieties of a given crop and to invert a composite of the crop-origin-specific demand shifters,  $\zeta_{ji}^k$ , and trade costs,  $\delta_{ji}^k$ .<sup>39</sup> Second, we use the previous estimates to construct price indices at the crop level,  $P_i^k$ , and combine them with data on crop expenditures,  $E_i^k = \sum_{j \in \mathcal{I}} E_{ji}^k$ , to estimate the elasticity of substitution  $\kappa$  between crops and to invert the crop-specific demand shifters,  $\zeta_i^k$ . Finally, we use data on total crop expenditures,  $E_i = \sum_{k \in \mathcal{K}} E_i^k$ , to invert the uppermost demand shifters,  $\zeta_i$ . Throughout, we make repeated use of the identity

$$E_{ji}^k = (\delta_{ji}^k p_j^k) C_{ji}^k = \zeta_i \frac{\zeta_i^k (P_i^k)^{1-\kappa}}{\sum_{\ell \in \mathcal{K}} \zeta_i^\ell (P_i^\ell)^{1-\kappa}} \frac{\zeta_{ji}^k (\delta_{ji}^k p_j^k)^{1-\sigma}}{\sum_{n \in \mathcal{I}} \zeta_{ni}^k (\delta_{ni}^k p_n^k)^{1-\sigma}}, \quad (17)$$

which defines the value of exports of crop  $k$  from country  $j$  to country  $i$ .

### Step 1: Estimating preferences across varieties of a given crop

With 52 countries and 22 crops, some crop-specific bilateral flows are zero. To rationalize these observations, whenever  $E_{ji}^k = 0$  we set  $\zeta_{ji}^k (\delta_{ji}^k)^{1-\sigma} = 0$ .<sup>40</sup> Whenever

---

<sup>39</sup>Prices are measured in current U.S. dollars per tonne in 2009 from FAOSTAT. Where no U.S. dollar price was reported, we converted from local currency units using the exchange rates provided by FAOSTAT. Where no price was reported, we followed Costinot, Donaldson, and Smith (2016) in imputing the price from the fitted values of a regression of log prices on a country and crop fixed effect *before* imposing our sample restrictions. Trade flows are measured in current U.S. dollars in 2009 from Comtrade. We compute autoconsumption,  $E_{ii}^k$ , as the difference between country  $i$ 's total production from FAOSTAT and total exports of crop  $k$ .

<sup>40</sup>Note that, in counterfactuals where these preference-adjusted trade costs remain finite, there will then be zero trade flow of crop  $k$  from country  $j$  to country  $i$  by construction.

$E_{ji}^k > 0$ , on the other hand, we take logs and rearrange Equation (17) as

$$\ln \left( \frac{E_{ji}^k}{E_i^k} \right) = m_i^k + (1 - \sigma) \ln p_j^k + \varepsilon_{ji}^k, \quad (18)$$

where the first term

$$m_i^k = -\ln \left[ \sum_{n \in \mathcal{I}} \zeta_{ni}^k (\delta_{ni}^k p_n^k)^{1-\sigma} \right]$$

is captured by an importer-crop fixed effect, and the last term  $\varepsilon_{ji}^k \equiv \ln[\zeta_{ji}^k (\delta_{ji}^k)^{1-\sigma}]$  is a structural error accounting for trade costs and unobserved variety-specific demand shifters. Without loss of generality, we normalize the demand shifters such that

$$\sum_{j \in \mathcal{I}} \varepsilon_{ji}^k = 0. \quad (19)$$

By definition, the equilibrium prices are correlated with the structural errors. We instrument for prices using the log of the arithmetic average of the GAEZ potential yield of crop  $k$  across all fields in country  $j$ ,

$$Z_j^k \equiv \ln \left( \frac{1}{|\mathcal{F}_j|} \sum_{f \in \mathcal{F}_j} A_j^{fk} \right).$$

The instrument  $Z_j^k$  should be correlated with crop prices,  $p_j^k$ , because higher productivity leads farmers in  $j$  to supply more of crop  $k$ . We assume that it is uncorrelated with the demand shifters and trade costs.<sup>41</sup>

From Equation (18), we estimate  $\sigma = 5.32$  (with a standard error of 1.34 when clustered at the crop-importer and crop-exporter levels). Preference-adjusted trade costs  $\zeta_{ji}^k (\delta_{ji}^k)^{1-\sigma}$  are then backed out from the prediction errors of the regression while imposing the normalization in Equation (19). These composites will be sufficient to construct equilibria—observed and counterfactual—in what follows.

## Step 2: Estimating preferences across crops

The second step looks much like the first, but instead of instrumenting for observed prices, we need to instrument for a price index that we construct ourselves,

$$P_i^k = \left[ \sum_{j \in \mathcal{I}} \zeta_{ji}^k (\delta_{ji}^k p_j^k)^{1-\sigma} \right]^{\frac{1}{1-\sigma}},$$

---

<sup>41</sup>Formally, the exclusion restriction is  $\mathbb{E}[Z_j^k \varepsilon_{ji}^k] = 0$ .

using the data and estimates from the previous step. With that index in hand, we rearrange Equation (17) as

$$\ln\left(\frac{E_i^k}{E_i}\right) = m_i + (1 - \kappa) \ln P_i^k + \varepsilon_i^k \quad (20)$$

where the first term

$$m_i = -\ln \left[ \sum_{\ell \in \mathcal{K}} \zeta_i^\ell (P_i^\ell)^{1-\kappa} \right]$$

is captured by an importer fixed effect, and the last term  $\varepsilon_i^k \equiv \ln \zeta_i^k$  is a structural error accounting for unobserved crop-specific demand shifters. Without loss of generality, we again normalize the demand shifters such that

$$\sum_{\ell \in \mathcal{K}} \varepsilon_i^\ell = 0. \quad (21)$$

The same endogeneity concerns from the first step are present here, so we instrument for the price index,  $P_i^k$ , with the corresponding arithmetic average of potential yields for crop  $k$ ,  $Z_i^k$ .

From Equation (20), we estimate  $\kappa = 3.81$  (with a standard error of 0.29 when clustered at the importer level). As in the first step, the demand shifter  $\zeta_i^k$  can then be inverted from the prediction error of the regression while imposing the normalization in Equation (21).

### Step 3: Estimating preferences across sectors

The third step is the easiest: the utility function in Equation (2) implies that  $\zeta_i = E_i$  for all  $i \in \mathcal{I}$ . Across all three steps, our procedure for inverting the demand shifters allows us to exactly match observed expenditures by each importer on each exporter-specific variety of crop in our sample.

## 4.3 Supply

To estimate the supply block, we note first that the mean potential yield for each crop-field pair,  $A^{fk}$ , has already been estimated by GAEZ. Crucially, this estimate exists even for a crop  $k$  that was never actually observed growing on field  $f$  in the reference FAOSTAT data. The GAEZ project estimates these potential yields for multiple climate scenarios, irrigation methods, and input levels.<sup>42</sup> We consider only the baseline climate scenario, defined as average historical conditions over the period

---

<sup>42</sup>Potential yields are always reported in dry-weight tonnes per hectare; we convert them to fresh-weight using the provided table to match FAOSTAT units (Fischer et al., 2021). For rice, GAEZ reports two varieties (dryland rice and wetland rice), but FAOSTAT only reports the aggregate category, rice. We therefore use the maximum yield over the two varieties for each field.

1961–1990.<sup>43</sup> We take a weighted average of irrigated and rainfed yields using estimates of land equipped for irrigation at 5-arcminute resolution from the Global Map of Irrigation Areas (Siebert et al., 2015). We use high-input yields everywhere, which assume market-oriented and fully-mechanized farming with optimal application of nutrients and chemical pest, disease, and weed control.<sup>44</sup> Even with the yield gaps  $M$  specified in the model, though, these potential yields can deviate substantially from average realized yields in FAOSTAT (Adamopoulos and Restuccia, 2022). Because of that, we follow Gouel and Laborde (2021, Appx. B) in rescaling our chosen GAEZ estimates to match average realized yields at the country level.

We calibrate another subset of supply-side parameters to estimates from the literature. First, we set  $1-\alpha=0.25$  to match the typical value-added share of land in agricultural production as computed in Boppart, Kiernan, Krusell, and Malmberg (2023). Second, to quantify the crop-specific water intensities,  $\phi^k$ , we convert the estimates reported by Mekonnen and Hoekstra (2011) from cubic meters per tonne to cubic meters per hectare using data on average yields from FAOSTAT. Third, we set the elasticity of labor productivity with respect to depth in the pumping technology to  $v=1$  in order to accord with Burlig, Preonas, and Woerman (2021), who specify a cost function for water extraction that is linear in the vertical distance over which the water must be lifted.

The supply-side parameters that remain to be estimated are the extent of within-field heterogeneity in potential yields,  $\theta$ , each country’s average labor productivity in the outside sector,  $\mathbf{A}^o \equiv \{A_i^o\}$ , and each aquifer’s scale of labor productivity in water extraction,  $\boldsymbol{\Upsilon} \equiv \{\Upsilon_q\}$ . In the final step, we jointly estimate these parameters to best fit three sets of empirical moments, each of which in some manner aggregates data on cropped area shares at 5-arcminute resolution from the M-3 Crops data (Monfreda, Ramankutty, and Foley, 2008).

Let  $\hat{\pi}^{fk}$  denote the *observed* share of field  $f$  allocated to crop  $k$  in the base year from M-3 Crops. Define the corresponding *predicted* share as a function of the parameters  $(\theta, \mathbf{A}^o, \boldsymbol{\Upsilon})$ ,

$$\pi^{fk}(\theta, \mathbf{A}^o, \boldsymbol{\Upsilon}) \equiv \frac{(\tau_i^k p_i^k A^{fk} M(\phi^k, D_{q(f)}))^{\theta}}{(A_i^o)^{\theta} + \sum_{\ell \in \mathcal{K}} (\tau_i^{\ell} p_i^{\ell} A^{f\ell} M(\phi^{\ell}, D_{q(f)}))^{\theta}},$$

where the dependence on  $\boldsymbol{\Upsilon}$  is through the yield gap,  $M$ . Note that this function encodes an equilibrium for a given set of agricultural policies,  $\{\tau_i^k\}$ . We set these to match the nominal rates of assistance (NRAS) reported for 2009 by the World Bank DAI project.<sup>45</sup>

---

<sup>43</sup>See Costinot, Donaldson, and Smith (2016) and Gouel and Laborde (2021) for analyses of how land use change and international trade aid adaptation to climate change.

<sup>44</sup>Low-input yields assume labor-intensive, subsistence farming with no application of nutrients or chemical pest, disease, and weed control. See Farrokhi and Pellegrina (2023) for a model of trade, agriculture, and technology adoption that endogenizes the choice of input levels.

<sup>45</sup>Nominal rates of assistance are reported in percentage terms, so  $\tau_i^k = 1 + \text{NRAS}_i^k$ . NRAS

We use these observed and predicted shares to construct three sets of moments. The first two sets, by which  $\mathbf{A}^o$  and  $\boldsymbol{\Upsilon}$  are primarily identified, target total cropped acreage in each country and total water extraction from each aquifer, respectively, in the base year. Define observed and predicted total cropped acreage in each country  $i \in \mathcal{I}$  as, respectively,

$$\hat{L}_i \equiv \sum_{k \in \mathcal{K}} \sum_{f \in \mathcal{F}_i} h^f \hat{\pi}^{fk} \quad \text{and} \quad L_i(\theta, \mathbf{A}^o, \boldsymbol{\Upsilon}) \equiv \sum_{k \in \mathcal{K}} \sum_{f \in \mathcal{F}_i} h^f \pi^{fk}(\theta, \mathbf{A}^o, \boldsymbol{\Upsilon}),$$

and observed and predicted total water extraction from each aquifer  $q \in \mathcal{Q}$  as, respectively,

$$\hat{X}_q \equiv \sum_{k \in \mathcal{K}} \sum_{f \in \mathcal{F}_q} h^f \phi^k \hat{\pi}^{fk} \quad \text{and} \quad X_q(\theta, \mathbf{A}^o, \boldsymbol{\Upsilon}) \equiv \sum_{k \in \mathcal{K}} \sum_{f \in \mathcal{F}_q} h^f x^{fk} \pi^{fk}(\theta, \mathbf{A}^o, \boldsymbol{\Upsilon}).$$

The intuition is straightforward: A higher  $A_i^o$ , by increasing the expected value of the non-agricultural option for laborers in country  $i$ , must decrease the total cropped area share of each constituent field. Likewise, a higher  $\Upsilon_q$ , by increasing the productivity of water extraction in aquifer  $q$ , must reduce the yield gap on each constituent field, which will increase their total cropped area shares in turn. A higher  $\Upsilon_q$  will also induce reallocation of cropped area toward more water-intensive crops within any constituent field, which would further affect the total water extracted from aquifer  $q$ . <sup>46</sup> The costs of water extraction are then, in some sense, inferred from the revealed preference of farmers: Where farmers use more land to grow more water-intensive crops, we infer, all else equal, that the cost of water extraction is lower.

The final moment, by which  $\theta$  is primarily identified, directly targets the within-field dispersion in land use across all fields in the sample. Define observed and predicted dispersion as, respectively,

$$\begin{aligned} \hat{\mathcal{S}} &\equiv \sum_{f \in \mathcal{F}} \left( \frac{h^f}{\sum_{f \in \mathcal{F}} h^f} \right) \text{SD}(\hat{\pi}^f) \\ \mathcal{S}(\theta, \mathbf{A}^o, \boldsymbol{\Upsilon}) &\equiv \sum_{f \in \mathcal{F}} \left( \frac{h^f}{\sum_{f \in \mathcal{F}} h^f} \right) \text{SD}(\pi^f(\theta, \mathbf{A}^o, \boldsymbol{\Upsilon})), \end{aligned}$$

where  $\text{SD}(\cdot)$  is the sample standard deviation of elements of a vector, and  $\boldsymbol{\pi}^f \equiv \{\pi^{f1}, \dots, \pi^{fK}, \pi^{fo}\}$  is a vector of land use shares for field  $f$  across all crops ( $k \in \mathcal{K}$ ) and the outside good ( $o$ ), the last of which corresponds to parcels being left fallow. Intuitively, as  $\theta$  increases, productivity differences across parcels within a field

---

are not reported for every country-crop pair in 2009. Where no NRA was reported, we set  $\tau_i^k$  to the “general” value that summarizes country  $i$ ’s assistance across agricultural products in 2009, if available. Where no general value was reported, we set  $\tau_i^k = 1$ .

<sup>46</sup>Both of these statements condition on equilibrium prices and all other parameters being held fixed.

shrink. This makes land use choices more sensitive to prices and mean productivities, pushing more land toward the most profitable activities for the average assigned laborer. As a result, the standard deviation of land use shares within a field ought to rise with  $\theta$ , as more area is allocated to top-ranked activities.

Formally, we jointly estimate  $(\theta, \mathbf{A}^0, \mathbf{T})$  as the vector that minimizes the sum of squared percentage deviations between the observed and predicted moments. This procedure produces an estimate of  $\theta=1.98$ , which aligns closely with estimates reported previously in the literature.<sup>47</sup>

#### 4.4 Hydrology

We close the calibration of the model by specifying the remaining hydrologic parameters that govern the law of motion in Equation (10). We assume a common return flow rate across crops and aquifers,  $\psi = 0.25$ , which is the central value reported by Dewandel et al. (2008). For each aquifer  $q$ , we set its initial depth,  $D_{q0}$ , to the median value across constituent grid cells as reported in Fan, Li, and Miguez-Macho (2013), expressed in centimeters from the surface. To convert from a change in volume in aquifer  $q$  (coming in part from extraction,  $X_{qt}$ ) to a change in depth,  $\Delta D_{qt}$ , we calibrate the parameter  $\rho_q$ , which accounts for two characteristics of the aquifer. First, and most plainly, its *area*, which can be computed easily from the underlying GRACE grid cells and expressed in squared meters. Second, its *specific yield*, which is the space available in the soil for water mass to be gained or lost. Specific yield depends on the porosity of the soil type, which itself depends on location and depth.<sup>48</sup> Accordingly, we use maps of soil type from Hengl et al. (2017) and estimates of specific yield by soil type from Loheide, Butler, and Gorelick (2005) to calibrate  $\rho_q$ .

The final component is the natural recharge rate for each aquifer  $q$ ,  $R_q$ , expressed in cubic meters. We calibrate recharge in order to match the average annual change in total water volume for each aquifer implied by GRACE trends from 2003 to 2016, given what the model implies about water extraction for crop use. This captures the dominant source of recharge—rainfall—but also accounts for runoff between aquifers or any other unobserved variation in the global hydrological system.<sup>49</sup>

#### 4.5 Goodness of fit

We consider how well the model fits its targets of country-level cropped acreage and aquifer-level water extraction. Figures 5a and 5b compare the observed and

---

<sup>47</sup>Costinot, Donaldson, and Smith (2016), targeting total output from FAOSTAT for each country-crop pair, estimate  $\theta=2.46$  with a bootstrapped 95-percent confidence interval of [2.28, 2.62]. Sotelo (2020), using Peruvian data on crop output disaggregated at the district level, estimates  $\theta=2.06$ .

<sup>48</sup>For example, clay is among the least porous types of soil; gravel, among the most porous.

<sup>49</sup>Note that, with this procedure, we may calibrate a negative recharge rate for some aquifers. This is possible despite strictly positive rainfall if there is enough runoff and crop consumption to outweigh rainfall.

predicted values of cropped acreage and water extraction, respectively. For cropped acreage, the model reproduces the global patterns almost exactly, with a simulation error under 2.5% for all 52 countries. For water extraction, the simulation error is under 5% for 117 (out of 199) aquifers, which cover 73% of the arable land represented in the sample.

Figures 5c and 5d show that the model generally captures the global pattern of water-intensive land use, which is concentrated in south and southeast Asia, southern Europe, and west Africa. Most remaining gaps between the model and the data occur in aquifers with low water use, as shown in Figure 5b. There are two main reasons for the remaining mismatch. First, the model includes only 22 crops—limited by available GAEZ data on potential yields—while the targeted data on land use shares (Monfreda, Ramankutty, and Foley, 2008) and water intensities (Mekonnen and Hoekstra, 2011) cover 126 crops. Second, GAEZ and M-3 Crops sometimes disagree on which grid cells within a country are best suited for farming particular crops. This can cause the model to allocate cropped area in different aquifers within a country than is indicated in the M-3 land use data.

Overall, the model closely matches the global distribution of cropped area and water use. By construction, it also reproduces other targeted moments: the average within-field dispersion in crop shares, initial water table depths, trends in water resources from 2003 to 2016, and bilateral crop expenditures in 2009. In the next section, we use the quantified model to consider counterfactual policy scenarios.

## 5 Counterfactuals

We now present results from several counterfactual policy simulations, which we compare with the calibrated baseline. For each scenario, we report differences in initial outcomes, such as cropped acreage and water use, and track how those variables evolve over time as water table depths adjust. Table 2 summarizes the key results.

### 5.1 Autarky

We begin by asking how global trade affects long-run water use and agricultural production. To do so, we simulate a world without trade by setting preference-adjusted trade costs,  $\zeta_{ji}^k(\delta_{ji}^k)^{1-\sigma}$ , to infinity for all crops  $k$  and all country pairs  $\{ij : i \neq j\}$ . We then compare the baseline and autarky scenarios over a 30-year horizon, tracking how water table depths and productivity evolve as production shifts and aquifers adjust.

Figure 6 compares global outcomes in the baseline and autarky scenarios over 30 years, starting in 2003. Panel (a) shows that global cropped acreage nearly doubles in the first year under autarky. This reflects the static efficiency gains from trade: when crops can be produced far from where they are consumed, the most productive

regions can produce a disproportionate share of the world’s food. Without trade, however, each country must meet its own demand, even if that means using low-yield land. This reallocation lowers global average yields by 44% in the first year, with even sharper drops for crops that currently concentrate heavily in highly suitable exporting regions.<sup>50</sup> With potential yields fixed and initial water table depths—and thus yield gaps—unchanged across scenarios, this drop in realized yields must occur entirely through changes in *which* crops are grown on *what* land.

Panel (b) shows that global water extraction increases by 60.7% in the first year of autarky—evidence of the global aggregate water savings from trade. Notably, the increase in global water extraction is well below the 99.8% increase in global cropped acreage. This difference reflects substitution toward less water-intensive crops in the simulation: with more land under cultivation in lower productivity regions, countries shift their cropping mix to reduce water use. As a result, the water intensity of cropped land is about 20% lower in the first year under autarky than in the baseline as the share of low water-intensity crops in the global consumption basket grows in the absence of trade.

Panel (c) shows the 30-year path of global average aquifer depth under baseline and autarky. In the baseline, global water table depths remain stable, consistent with observed trends in total water storage from GRACE.<sup>51</sup> Under autarky, however, average depth falls by 12 meters over 30 years—a 70.2% decline from the initial level. Meeting food demand without trade requires more land and more water, causing rapid depletion of the world’s water resources.

We now decompose the global changes in land and water use into regional patterns. Figure 7 maps the rise in water use in the first year of autarky, showing that the increase in extraction is most severe in dry regions. While global extraction rises by 60.7% in the first year, Panel (a) shows increases above 300% in the southern U.S., Mexico, eastern Brazil, South Africa, and Australia. Panel (b) confirms this pattern: aquifers in the bottom quartile of water table depth or rainfall see more than double the global average increase in water use.

In contrast, regions with abundant water see smaller increases—or even declines in water extraction. For those in the top quartile of initial depth, extraction rises by only half the global average in the first year of autarky. Some major exporters—such as China, Southeast Asia, northern India, and the U.S. Great Plains—use *less* water in the first year of autarky than they would have under baseline conditions. These include many water-abundant regions, but also California’s Central Valley, whose aquifer depletes especially rapidly in the baseline, where rainfall is low, and where concerns over trade causing local water depletion are widespread (Dalin et al., 2017). However, the dominant pattern globally reflects the correlation identified in

---

<sup>50</sup>For example, banana yields fall by 67% under autarky as production shifts out of current high-yield exporters.

<sup>51</sup>Fact 1 showed that global arable land is evenly split between locations gaining and losing water. We match the average trend in total water storage when we calibrate the model.

**Fact 5:** In the baseline, wetter regions export water-intensive crops to drier regions, allowing production to relocate away from places that can least sustain it in the long run.

Figure 8 maps 30-year change in water table depth in the baseline and autarky. In the baseline, even the most rapidly depleting regions (e.g., northern India, southern Argentina) see depth declines of only 1–3 meters over 30 years. Under autarky, the global average decline is 12 meters. About 29% of global arable land sees depth fall by more than 10 meters, a pace far beyond anything observed in the historical record.

While most regions deplete faster under autarky, some do not. In a few cases, drawdowns slow or reverse entirely. These include the U.S. Midwest, where water is already stable, but also areas of known concern—most notably, the Central Valley of California and parts of northeastern India, including Uttar Pradesh and Uttarakhand. In the baseline data, these are among the most rapidly depleting agricultural regions in the world (Figure 1c). Yet in autarky, their depletion slows or stops. This pattern is consistent with prior evidence, including Sekhri (2022), that links water-intensive exports to local scarcity. Still, these exceptions highlight the rule: for most of the world, trade alleviates rather than worsens long-run water loss.

The effects of autarky on agriculture and water use have major consequences for human welfare. Table 2 shows that population-weighted median food prices rise by 1,410% in the first year of autarky relative to the baseline.<sup>52</sup> This surge reflects the loss of spatial efficiency when countries can no longer rely on trade to exploit comparative advantage. Price increases are steepest in water-scarce food importers: the top quartile of net virtual water importers see a 3,550% increase, compared to a 2% decline in the top quartile of exporters. Non-agricultural production also falls by 15.5% as land and labor shift toward food production—consistent with the “food problem” mechanism studied by Tombe (2015) and Nath (2025).<sup>53</sup>

Water depletion under autarky also reduces agricultural productivity over time. In the model, as aquifers decline, water becomes harder to extract and yields fall. Over the 30 years in autarky, yields decline further beyond the initial drop for 20 of the 22 crops in the simulation. The average loss is 1.8%, but it is 4% for rice, the most water-intensive staple, and upwards of 4.5% for crops like coffee and oil palm.<sup>54</sup> Figure 6b shows that farmers respond by planting fewer water-intensive

---

<sup>52</sup>We compute the population-weighted median across the set of agricultural consumption price indices  $\{P_{it}\}$  as defined in Appendix B.1.1. Because agricultural expenditure in each country  $i$  remains fixed at  $\zeta_i$ , the median quantity of the agricultural consumption basket must fall proportionally.

<sup>53</sup>Given the quasilinear preferences in Equation (2), the agricultural CPI and the level of non-agricultural consumption are sufficient statistics for welfare. Because we estimate non-agricultural productivity to best fit observed agricultural land use and not non-agricultural GDP, though, we cannot interpret aggregate welfare levels. Nevertheless, we can generically *sign* the welfare effect of a change whenever a country’s agricultural CPI and its non-agricultural consumption negatively co-move in response.

<sup>54</sup>These losses are relative to yields in the first year of autarky, which are already 37.4% lower

crops over time: the average water intensity of cropped land declines an additional 10% over 30 years in autarky. Feeding the world without trade requires shifting away from water-intensive crops—and doing so even more as water becomes scarcer over time.

## 5.2 Global agricultural policy reforms

We now turn from autarky to consider specific policy reforms. Because water consumption is unpriced, changes in output market policies may either ease or worsen existing inefficiencies. We examine two cases: one based on the reforms that followed the Uruguay Round of World Trade Organization (WTO) negotiations, and one that removes all remaining agricultural output market distortions.

The Uruguay Round, which concluded in 1994 with the agreement of 123 countries, marked the most significant liberalization of global agricultural markets to date. Before the agreement, agriculture was largely excluded from the General Agreement on Tariffs and Trade (GATT), and governments used a range of tools—subsidies, import restrictions, exchange controls—to distort production and trade (Healy, Pearce, and Stockbridge, 1998). The reforms heavily reduced these distortions in many countries.

To evaluate the long-run effects of these policy changes, we simulate a counterfactual in which country-by-crop Nominal Rates of Assistance (NRAs;  $\tau_i^k$  in Section 3) are fixed at their average levels from the Uruguay Round negotiation period (1986–1994). We compare this to the baseline, which uses 2009 NRA values. In the second counterfactual, we set all NRA values to zero.

Figures 9a and 9b illustrate that the Uruguay Round reforms and the removal of remaining agricultural distortions have markedly different spatial patterns. Prior to 1994, high-income countries provided substantial support to agriculture, while many lower-income countries employed import-substitution policies intended to promote industrialization, such as export taxes and currency controls, that implicitly taxed agricultural production (Anderson, Rausser, and Swinnen, 2013). Consequently, the Uruguay Round led to reductions in NRAs in regions such as the United States, Europe, and Australia, but increases in India, Brazil, and much of sub-Saharan Africa (Figure 9a). In contrast, the remaining global policy distortions in 2009 consist almost entirely of net subsidies, such that their removal lowers production incentives across nearly all regions (Figure 9b).

Figures 9c and 9d report the regional impacts of these policy changes on water extraction. The Uruguay Round reforms reduced water use in high-income, water-abundant regions that scaled back subsidies, such as western Europe and the United States, but increased extraction in many lower-income, water-scarce countries that lifted restrictions on agricultural production, including China and relatively-arid

---

for rice and 55.6% lower for coffee compared to the baseline, because of how production reallocates across space.

parts of East Africa. In aggregate, these reforms raised global extraction by 3.4% and shifted the sign of the trend in global average aquifer depth from slightly positive to slightly negative (Table 2). The effects were disproportionately concentrated in vulnerable regions: extraction increased by approximately 7.5%—twice the global average—in regions comprising the bottom quartile of observed water resource trends, and average aquifer depth declined by 2.2 meters over 30 years in the driest decile, compared to just 0.3 meters globally. These spatial shifts in production also reduced global average crop yields by 9.2% in the initial period, with further declines over time as cultivation expanded into regions with limited and draining water resources.

By contrast, eliminating all remaining agricultural distortions reduces water use and slows depletion in most regions (Figure 9d).<sup>55</sup> Globally, extraction falls by 3.7%, with larger reductions in dry regions. After 30 years, average water table depth is 2.5% shallower. Global crop yields rise by 4.1% in the first year and increase another 0.8% in the 30 years thereafter as water tables stabilize and production reallocates toward more suitable land. Although food prices increase modestly (by 2.1%) due to the removal of subsidies, non-agricultural output rises slightly, and the overall water intensity of global agriculture declines. These patterns are particularly pronounced in drier regions, where reductions in water-intensive production mitigate long-run productivity losses.

Taken together, these findings underscore the importance of policy design in the presence of input market failures. While the autarky counterfactual points to large economic and environmental gains from trade—both through static efficiency and dynamic conservation—we find that the most significant agricultural liberalization to date, the Uruguay Round, increased global water stress and reduced productivity in many regions over time. And yet, the removal of all remaining output distortions would, in general, produce the opposite effects. These results, combined with the earlier finding that autarky preserves water in a few severely stressed regions, highlight that agricultural trade is not unconditionally beneficial for local water resources or productivity. In a world with unpriced inputs, the spatial structure of output policies plays a critical role in shaping long-run outcomes.

## 6 Conclusion

This paper considers the implications of global agricultural trade for regional water scarcity and long-run agricultural productivity. In a setting where farmers generally extract water under open access, it is possible for trade to exacerbate the input market failure, worsen depletion, and reduce long-run productivity (Chichilnisky, 1994; Brander and Taylor, 1997a). In the absence of strong property rights for water

---

<sup>55</sup>One notable exception is Argentina, where agricultural export taxes continue to suppress production incentives (Anderson, Rausser, and Swinnen, 2013).

as an input, trade need not channel water-intensive production toward locations with true underlying comparative advantage.

We show that, in the case of water, global agricultural specialization closely follows resource abundance despite the lack of functioning input markets. This pattern of specialization follows from a natural mapping between the physical scarcity of water into its effective input price: where water tables are deep and rainfall scarce, farmer extraction costs rise, even if no market operates. While market failures remain, we show empirically that this mapping leads water-rich locations to, on average, specialize in water-intensive production and drier places to import their agricultural consumption and preserve local water resources.

Using a calibrated dynamic spatial equilibrium model, we find that global trade in agriculture reduces global cropped area by half and global water consumption by nearly two-fifths. We estimate that global crop yields under autarky would be 44% lower than in the baseline due to a reallocation of crop production toward less suitable land, even as the productivity of each individual plot is initially unchanged. Without trade, global water tables decline precipitously throughout the world, with especially large drops in dry locations that currently rely on food imports. Global average food prices rise sharply under autarky, with unequal incidence across regions. Food prices increase by over 3500% in the largest virtual water importers, while major agricultural exporters see little change. Despite the broadly beneficial role of trade in mediating global water consumption, we also show that some rapidly depleting exporting regions—most notably parts of California and northern India—experience more stable water resources under autarky, and that some historical trade liberalizations have reduced agricultural productivity and exacerbated regional water scarcity.

A natural question is whether the findings about trade preventing depletion of water resources can be generalized to the cases of other open access natural resources. Given the mechanism for the primary results in this paper, we conjecture that a key factor determining the relationship between trade and resource depletion is whether there exists a physical mechanism for the resource’s scarcity to map into its marginal cost of extraction. If so, it may be the case that nature can, at least partially, compensate for nonfunctional input markets in governing the allocation. If not, it may not be that trade is helpful at all—and indeed could be harmful—for preserving the long-run availability of the resource. Thus, we might expect to see different results for the effects of global trade on the management of forests, for which the marginal cost of extraction is generally independent of the existing stock of forests, and the management of fisheries, for which the marginal cost of extraction depends strongly on the existing local stock of fish.

We conclude with two suggestions for future research. First, the results in this paper speak to the effects of agricultural trade policy in the presence of input market failures. However, solving for the socially optimal allocation that removes both input and output market distortions is beyond the scope of the approach taken

here. Future work that considers such a global social planner’s problem could shed further light on *optimal* output market policy and on the interactions and complementarities between establishing strong property rights for water and liberalizing agricultural markets. Second, this paper does not consider the emerging effects of climate change on agricultural productivity, regional water resources, and crop water demand (Rodell et al., 2018). We view analysis of the relationship between global warming, changing precipitation patterns, shifting comparative advantage, and evolving water resource dynamics as an important area for future work.

## References

- Adamopoulos, Tasso and Diego Restuccia. 2014. “The size distribution of farms and international productivity differences.” *American Economic Review* 104 (6):1667–97. (Cited on page 62.)
- . 2022. “Geography and agricultural productivity: Cross-country evidence from micro plot-level data.” *Review of Economic Studies* 89 (4):1629–1653. (Cited on page 25.)
- Allan, John A. 1998. “Virtual water: A strategic resource.” *Ground water* 36 (4):545–547. (Cited on page 1.)
- Allan, Tony. 2011. *Virtual water: Tackling the threat to our planet’s most precious resource*. London: I. B. Tauris. (Cited on page 1.)
- Allen, Treb, Costas Arkolakis, and Yuta Takahashi. 2020. “Universal gravity.” *Journal of Political Economy* 128 (2):393–433. (Cited on page 71.)
- Alvarez, Fernando and Robert E. Lucas, Jr. 2007. “General equilibrium analysis of the Eaton–Kortum model of international trade.” *Journal of Monetary Economics* 54 (6):1726–1768. (Cited on page 71.)
- Anderson, Kym, Marianne Kurzweil, Will Martin, Damiano Sandri, and Ernesto Valenzuela. 2008. “Methodology for measuring distortions to agricultural incentives.” Tech. Rep. 2, World Bank. (Cited on page 62.)
- Anderson, Kym, Gordon Rausser, and Johan Swinnen. 2013. “Political economy of public policies: Insights from distortions to agricultural and food markets.” *Journal of Economic Literature* 51 (2):423–77. (Cited on pages 1, 5, 11, 31, 32, and 62.)
- Ansink, Erik. 2010. “Refuting two claims about virtual water trade.” *Ecological Economics* 69 (10):2027–2032. (Cited on page 9.)

- Ayres, Andrew B., Kyle C. Meng, and Andrew J. Plantinga. 2021. “Do environmental markets improve on open access? Evidence from California groundwater rights.” *Journal of Political Economy* 121 (10). (Cited on pages 5 and 10.)
- Boppert, Timo, Patrick Kiernan, Per Krusell, and Hannes Malemberg. 2023. “The macroeconomics of intensive agriculture.” Working Paper 31101, National Bureau of Economic Research. (Cited on pages 25 and 69.)
- Boser, Anna, Kelly Taylor, Ashley Larsen, Madeleine Pascolini-Campbell, John T. Reager, and Tamma Carleton. 2024. “Field-scale crop water consumption estimates reveal potential water savings in California agriculture.” *Nature Communications* 15 (1). (Cited on page 9.)
- Brander, James A. and M. Scott Taylor. 1997a. “International trade and open-access renewable resources: The small open economy case.” *Canadian Journal of Economics* 30 (3):526. (Cited on pages 6, 15, and 32.)
- . 1997b. “International trade between consumer and conservationist countries.” *Resource and Energy Economics* 19 (4):267–297. (Cited on pages 6 and 15.)
- . 1998. “Open access renewable resources: Trade and trade policy in a two-country model.” *Journal of International Economics* 44 (2):181–209. (Cited on pages 6 and 15.)
- Brown, Gardner M. 2000. “Renewable natural resource management and use without markets.” *Journal of Economic Literature* 38 (4):875–914. (Cited on page 15.)
- Bruno, Ellen M. and Katrina Jessoe. 2021. “Missing markets: Evidence on agricultural groundwater demand from volumetric pricing.” *Journal of Public Economics* 196. (Cited on pages 5 and 10.)
- Burlig, Fiona, Louis Preonas, and Matt Woerman. 2021. “Energy, groundwater, and crop choice.” Working Paper 28706, National Bureau of Economic Research. (Cited on pages 4 and 25.)
- Carleton, Tamma. 2021. “The global water footprint of distortionary agricultural policy.” (Cited on pages 5, 11, and 58.)
- Carleton, Tamma, Levi Crews, and Ishan Nath. 2024. “Is the world running out of fresh water?” *AEA Papers and Proceedings* 114:31–35. (Cited on pages 8 and 13.)
- Carr, J. A., David A. Seekell, and P. D’Odorico. 2015. “Inequality or injustice in water use for food?” *Environmental Research Letters* 10 (2). (Cited on page 6.)
- Carr, Joel A., Paolo D’Odorico, Francesco Laio, and Luca Ridolfi. 2013. “Recent history and geography of virtual water trade.” *PLoS ONE* 8 (2). (Cited on page 9.)

- Chatterjee, Shoumitro, Rohit Lamba, and Esha Zaveri. 2022. “The role of farm subsidies in changing India’s water footprint.” *Nature Communications* . (Cited on page 11.)
- Chen, J. L., C. R. Wilson, and B. D. Tapley. 2013. “Contribution of ice sheet and mountain glacier melt to recent sea level rise.” *Nature Geoscience* 6 (7):549–552. (Cited on pages 8 and 58.)
- Chichilnisky, Graciela. 1994. “North-south trade and the global environment.” *American Economic Review* 84 (4):851–874. (Cited on pages 1, 6, and 32.)
- Copeland, Brian R., Joseph S. Shapiro, and M. Scott Taylor. 2022. “Globalization and the environment.” In *Handbook of International Economics*, vol. 5, edited by Gita Gopinath, Elhanan Helpman, and Kenneth Rogoff, chap. 2. Elsevier, 61–146. (Cited on page 5.)
- Costinot, Arnaud, Dave Donaldson, and Cory Smith. 2016. “Evolving comparative advantage and the impact of climate change in agricultural markets: Evidence from 1.7 million fields around the world.” *Journal of Political Economy* 124 (1):205–248. (Cited on pages 5, 13, 22, 25, 27, and 61.)
- Cruz, José-Luis and Esteban Rossi-Hansberg. 2024. “The economic geography of global warming.” *Review of Economic Studies* 91 (2):899–939. (Cited on page 20.)
- Dalin, Carole, Megan Konar, Naota Hanasaki, Andrea Rinaldo, and Ignacio Rodriguez-Iturbe. 2012. “Evolution of the global virtual water trade network.” *Proceedings of the National Academy of Sciences* 109 (16):5989–5994. (Cited on page 9.)
- Dalin, Carole, Yoshihide Wada, Thomas Kastner, and Michael J. Puma. 2017. “Groundwater depletion embedded in international food trade.” *Nature* 543 (7647):700–704. (Cited on pages 1, 6, 9, and 29.)
- Davis, Donald R. 1995. “Intra-industry trade: A Heckscher-Ohlin-Ricardo approach.” *Journal of International Economics* 39 (3):201–226. (Cited on page 10.)
- Davis, Donald R. and David E. Weinstein. 2001. “An account of global factor trade.” *American Economic Review* 91 (5):1423–1453. (Cited on page 10.)
- Debaere, Peter. 2014. “The global economics of water: Is water a source of comparative advantage?” *American Economic Journal: Applied Economics* 6 (2):32–48. (Cited on pages 5 and 9.)
- Debaere, Peter, Brian D. Richter, Kyle Frankel Davis, Melissa S. Duvall, Jessica Ann Gephart, Clark E. O'Bannon, Carolyn Pelnik, Emily Maynard Powell, and Tyler William Smith. 2014. “Water markets as a response to scarcity.” *Water Policy* 16 (4):625–649. (Cited on page 11.)

- Desmet, Klaus, Robert E. Kopp, Scott A. Kulp, Dávid Krisztián Nagy, Michael Oppenheimer, Esteban Rossi-Hansberg, and Benjamin H. Strauss. 2021. “Evaluating the economic cost of coastal flooding.” *American Economic Journal: Macroeconomics* 13 (2):444–486. (Cited on page 20.)
- Desmet, Klaus, Dávid Kristián Nagy, and Esteban Rossi-Hansberg. 2018. “The geography of development.” *Journal of Political Economy* 126 (3):903–983. (Cited on page 20.)
- Dewandel, B., J.-M. Gandolfi, D. de Condappa, and S. Ahmed. 2008. “An efficient methodology for estimating irrigation return flow coefficients of irrigated crops at watershed and seasonal scale.” *Hydrological Processes* 22 (11):1700–1712. (Cited on page 27.)
- d’Odorico, Paolo, Joel Carr, Carole Dalin, Jampel Dell’Angelo, Megan Konar, Francesco Laio, Luca Ridolfi, Lorenzo Rosa, Samir Suweis, Stefania Tamea, and Marta Tuminetti. 2019. “Global virtual water trade and the hydrological cycle: Patterns, drivers, and socio-environmental impacts.” *Environmental Research Letters* 14 (5). (Cited on pages 9 and 61.)
- Domínguez-Iino, Tomás. 2025. “Efficiency and redistribution in environmental policy: An equilibrium analysis of agricultural supply chains.” (Cited on page 5.)
- Donna, Javier and José-Antonio Espín-Sánchez. 2023. “The illiquidity of water markets: Efficient institutions for water allocation in southeastern Spain.” (Cited on page 10.)
- Donoso, Guillermo. 2013. “The evolution of water markets in Chile.” In *Water Trading and Global Water Scarcity*, edited by Josefina Maestu, chap. 7. Routledge, 131–149. (Cited on page 10.)
- Dubois, Olivier et al. 2011. *The state of the world’s land and water resources for food and agriculture: Managing systems at risk*. London: Earthscan. (Cited on page 8.)
- Easter, K. William and Qiuqiong Huang. 2014. “Water markets: How do we expand their use?” In *Water markets for the 21<sup>st</sup> century: What have we learned?, Global Issues in Water Policy*, vol. 11, edited by K. William Easter and Qiuqiong Huang, chap. 1. Springer, 1. (Cited on page 10.)
- Easter, K. William, Mark W. Rosegrant, and Ariel Dinar. 1999. “Formal and informal markets for water: Institutions, performance, and constraints.” *The World Bank Research Observer* 14 (1):99–116. (Cited on page 11.)
- Eaton, Jonathan and Samuel Kortum. 2002. “Technology, geography, and trade.” *Econometrica* 70 (5):1741–1779. (Cited on page 15.)

- Endo, Takahiro, Kaoru Kakinuma, Sayaka Yoshikawa, and Shinjiro Kanae. 2018. “Are water markets globally applicable?” *Environmental Research Letters* 13 (3):034032. (Cited on page 11.)
- Fan, Y., H. Li, and G. Miguez-Macho. 2013. “Global patterns of groundwater table depth.” *Science* 339 (6122):940–943. (Cited on pages 7, 21, 27, 46, 48, 55, 57, 58, and 60.)
- Farrokhi, Farid, Elliot Kang, Heitor S. Pellegrina, and Sebastian Sotelo. 2023. “Deforestation: A global and dynamic perspective.” (Cited on page 5.)
- Farrokhi, Farid and Heitor S. Pellegrina. 2023. “Trade, technology, and agricultural productivity.” *Journal of Political Economy* 131 (9):2509–2555. (Cited on page 25.)
- Ferguson, Billy. 2024. “Trade frictions in surface water markets.” (Cited on page 11.)
- Fischer, G., F. O. Nachtergaele, H. T. van Velthuizen, F. Chiozza, G. Franceschini, M. Henry, D. Muchoney, and S. Tramberend. 2021. *Global Agro-Ecological Zones v4: Model documentation*. Rome: FAO. (Cited on page 24.)
- Gordon, H. Scott. 1954. “The economic theory of a common-property resource: The fishery.” *Journal of Political Economy* 62 (2):124–142. (Cited on page 15.)
- Gouel, Christophe and David Laborde. 2021. “The crucial role of domestic and international market-mediated adaptation to climate change.” *Journal of Environmental Economics and Management* 106:102408. (Cited on pages 21 and 25.)
- Grafton, R. Quentin, Gary Libecap, Samuel McGlennon, Clay Landry, and Bob O’Brien. 2011. “An integrated assessment of water markets: A cross-country comparison.” *Review of Environmental Economics and Policy* 5 (2):219–239. (Cited on pages 10 and 11.)
- Griffin, Ronald C. and Gregory W. Characklis. 2002. “Issues and trends in Texas water marketing.” *Journal of Contemporary Water Research and Education* 121 (1):29–33. (Cited on page 10.)
- Hagerty, Nick. 2024. “Transaction costs and the gains from trade in water markets.” (Cited on page 10.)
- Healy, Stephen, Richard Pearce, and Michael Stockbridge. 1998. *The implications of the Uruguay Round Agreement on Agriculture for developing countries: A training manual, Training materials for agricultural planning*, vol. 41. Rome: Food and Agricultural Organization of the United Nations. (Cited on page 31.)
- Hearne, Robert R. and José L. Trava. 1997. “Water markets in Mexico: Opportunities and constraints.” Tech. Rep. DP 97-01, IIED Environmental Economics Programme. (Cited on page 10.)

- Hendricks, Nathan P. and Jeffrey M. Peterson. 2012. “Fixed effects estimation of the intensive and extensive margins of irrigation water demand.” *Journal of Agricultural and Resource Economics* 37 (1):1–19. (Cited on page 57.)
- Hendricks, Nathan P., Aaron Smith, and Daniel A. Sumner. 2014. “Crop supply dynamics and the illusion of partial adjustment.” *American Journal of Agricultural Economics* 96 (5):1469–1491. (Cited on page 11.)
- Hendricks, Nathan P., Aaron D. Smith, and Nelson B. Villoria. 2018. “Global agricultural supply response to persistent price shocks.” (Cited on page 11.)
- Hengl, Tomislav, Jorge Mendes de Jesus, Gerard B. M. Heuvelink, Maria Ruiperez Gonzalez, Milan Kilibarda, Aleksandar Blagotić, Wei Shangguan, Marvin N. Wright, Xiaoyuan Geng, Bernhard Bauer-Marschallinger, Mario Antonio Guevara, Rodrigo Vargas, Robert A. MacMillan, Niels H. Batjes, Johan G. B. Leenaars, Eloi Ribeiro, Ichsanı Wheeler, Stephan Mantel, and Bas Kempen. 2017. “SoilGrids250m: Global gridded soil information based on machine learning.” *PLOS ONE* 12 (2). (Cited on pages 27, 55, and 60.)
- Hoekstra, Arjen Y. and Mesfin M. Mekonnen. 2012. “The water footprint of humanity.” *Proceedings of the National Academy of Sciences* 109 (9):3232–3237. (Cited on pages 8, 9, and 47.)
- Hsiao, Allan. 2025. “Coordination and commitment in international climate action: Evidence from palm oil.” (Cited on page 5.)
- Jacob, Thomas, John Wahr, W. Tad Pfeffer, and Sean Swenson. 2012. “Recent contributions of glaciers and ice caps to sea level rise.” *Nature* 482 (7386):514–518. (Cited on page 58.)
- Jacoby, Hanan G., Rinku Murgai, and Saeed Ur Rehman. 2004. “Monopoly power and distribution in fragmented markets: The case of groundwater.” *Review of Economic Studies* 71 (3):783–808. (Cited on page 10.)
- Kloezen, Wim H. 1998. “Water markets between Mexican water user associations.” *Water Policy* 1 (4):437–455. (Cited on page 10.)
- Konar, Megan, Zekarias Hussein, Naota Hanasaki, Denise L. Mauzerall, and Ignacio Rodriguez-Iturbe. 2013. “Virtual water trade flows and savings under climate change.” *Hydrology and Earth System Sciences* 17 (8):3219–3234. (Cited on page 6.)
- Kumar, M. Dinesh and O. P. Singh. 2005. “Virtual water in global food and water policy making: Is there a need for rethinking?” *Water Resources Management* 19 (6):759–789. (Cited on page 9.)

- Latham, John, Renato Cumani, Ilaria Rosati, and Mario Bloise. 2014. “Global Land Cover SHARE (GLC-SHARE) database: Beta-Release v1.0.” Tech. rep., FAO. (Cited on page 21.)
- Libecap, Gary D. 2008. *Transaction costs, property rights, and the tools of the new institutional economics: Water rights and water markets*, chap. 13. Cambridge: Cambridge University Press, 272–291. (Cited on pages 1 and 10.)
- Lipsey, R. G. and Kelvin Lancaster. 1956. “The general theory of second best.” *Review of Economic Studies* 24 (1):11–32. (Cited on page 1.)
- Loheide, Steven P., James J. Butler, and Steven M. Gorelick. 2005. “Estimation of groundwater consumption by phreatophytes using diurnal water table fluctuations: A saturated-unsaturated flow assessment.” *Water Resources Research* 41 (7). (Cited on pages 27, 55, and 60.)
- Long, Di, Bridget R. Scanlon, Laurent Longuevergne, Alexander Y. Sun, D. Nelun Fernando, and Himanshu Save. 2013. “GRACE satellite monitoring of large depletion in water storage in response to the 2011 drought in Texas.” *Geophysical Research Letters* 40 (13):3395–3401. (Cited on page 59.)
- Loomis, B. D., S. B. Luthcke, and T. J. Sabaka. 2019. “Regularization and error characterization of GRACE mascons.” *Journal of geodesy* 93:1381–1398. (Cited on page 59.)
- Mas-Colell, Andreu, Michael D. Whinston, and Jerry R. Green. 1995. *Microeconomic theory*. Oxford: Oxford University Press. (Cited on page 71.)
- Mekonnen, M. M. and A. Y. Hoekstra. 2011. “The green, blue and grey water footprint of crops and derived crop products.” *Hydrology and Earth System Sciences* 15 (5):1577–1600. (Cited on pages 1, 9, 12, 25, 28, 48, 55, 61, 62, and 79.)
- Melton, Forrest S., Justin Huntington, Robyn Grimm, Jamie Herring, Maurice Hall, Dana Rollison, Tyler Erickson, Richard Allen, Martha Anderson, Joshua B. Fisher et al. 2022. “OpenET: Filling a critical data gap in water management for the western United States.” *Journal of the American Water Resources Association* 58 (6):971–994. (Cited on page 59.)
- Monfreda, Chad, Navin Ramankutty, and Jonathan A. Foley. 2008. “Farming the planet: Geographic distribution of crop areas, yields, physiological types, and net primary production in the year 2000.” *Global Biogeochemical Cycles* 22 (1). (Cited on pages 7, 8, 12, 25, 28, 46, 47, 55, 60, 61, and 78.)
- Morrow, Peter M. 2010. “Ricardian-Heckscher-Ohlin comparative advantage: Theory and evidence.” *Journal of International Economics* 82 (2):137–151. (Cited on page 10.)

- Nath, Ishan. 2025. “Climate change, the food problem, and the challenge of adaptation through sectoral reallocation.” *Journal of Political Economy* 133 (6):1705–1756. (Cited on page 30.)
- Neely, Wesley R., Adrian A. Borsa, Jennifer A. Burney, Morgan C. Levy, Francesca Silverii, and Michelle Sneed. 2021. “Characterization of groundwater recharge and flow in California’s San Joaquin Valley from InSAR-observed surface deformation.” *Water Resources Research* 57 (4). (Cited on page 59.)
- Palomo-Hierro, Sara, José A. Gómez-Limón, and Laura Riesgo. 2015. “Water markets in Spain: Performance and challenges.” *Water* 7 (2):652–678. (Cited on page 10.)
- Pekel, Jean-François, Andrew Cottam, Noel Gorelick, and Alan S. Belward. 2016. “High-resolution mapping of global surface water and its long-term changes.” *Nature* 540:418–422. (Cited on pages 55 and 60.)
- Phillips, Keith R. and Judy Teng. 2020. “Groundwater markets slowly evolve in ever-thirstier Texas.” *Southwest Economy* (First Quarter):7–11. (Cited on page 10.)
- Portmann, Felix T., Stefan Siebert, and Petra Döll. 2010. “MIRCA2000—Global monthly irrigated and rainfed crop areas around the year 2000: A new high-resolution data set for agricultural and hydrological modeling.” *Global Biogeochemical Cycles* 24 (1). (Cited on page 58.)
- Potapov, Peter, Svetlana Turubanova, Matthew C. Hansen, Alexandra Tyukavina, Viviana Zalles, Ahmad Khan, Xiao-Peng Song, Amy Pickens, Quan Shen, and Jocelyn Cortez. 2022. “Global maps of cropland extent and change show accelerated cropland expansion in the twenty-first century.” *Nature Food* 3 (1):19–28. (Cited on page 60.)
- Proctor, Jonathan, Tamma Carleton, and Sandy Sum. 2023. “Parameter recovery using remotely sensed variables.” Working Paper 30861. (Cited on page 60.)
- Rafey, Will. 2023. “Droughts, deluges, and (river) diversions: Valuing market-based water reallocation.” *American Economic Review* 113 (2):430–471. (Cited on pages 5, 10, and 11.)
- Richey, Alexandra S., Brian F. Thomas, Min-Hui Lo, John T. Reager, James S. Famiglietti, Katalyn Voss, Sean Swenson, and Matthew Rodell. 2015. “Quantifying renewable groundwater stress with GRACE.” *Water resources research* 51 (7):5217–5238. (Cited on pages 21 and 59.)
- Richter, B. 2016. “Water share: Using water markets and impact investment to drive sustainability.” Tech. rep., The Nature Conservancy, Washington, D.C. (Cited on page 10.)

- Roberts, Michael J. and Wolfram Schlenker. 2013. “Identifying supply and demand elasticities of agricultural commodities: Implications for the US ethanol mandate.” *American Economic Review* 103 (6):2265–95. (Cited on page 11.)
- Rodell, M., J. S. Famiglietti, D. N. Wiese, J. T. Reager, H. K. Beaudoing, F. W. Landerer, and M.-H. Lo. 2018. “Emerging trends in global freshwater availability.” *Nature* 557 (7707):651–659. (Cited on pages 1, 34, and 59.)
- Rodell, Matthew, Isabella Velicogna, and James S. Famiglietti. 2009. “Satellite-based estimates of groundwater depletion in India.” *Nature* 460 (7258):999–1002. (Cited on pages 58 and 59.)
- Romalis, John. 2004. “Factor proportions and the structure of commodity trade.” *American Economic Review* 94 (1):67–97. (Cited on page 10.)
- Rossi-Hansberg, Esteban. 2019. “Geography of growth and development.” In *Oxford Research Encyclopedia of Economics and Finance*. Oxford University Press. (Cited on page 20.)
- Ryan, Nicholas and Anant Sudarshan. 2022. “Rationing the commons.” *Journal of Political Economy* 130 (1):210–257. (Cited on pages 5 and 10.)
- Saleth, Rathinasamy Maria. 2004. “Strategic analysis of water institutions in India: Application of a new research paradigm.” Tech. Rep. 79, International Water Management Institute. (Cited on page 10.)
- Schaefer, Milner B. 1954. “Some aspects of the dynamics of populations important to the management of commercial marine fisheries.” *Bulletin of the Inter-American Tropical Tuna Commission* 1 (2):27–56. (Cited on page 15.)
- Schwabe, Kurt, Mehdi Nemati, Clay Landry, and Grant Zimmerman. 2020. “Water markets in the Western United States: Trends and opportunities.” *Water* 12 (1):233. (Cited on page 10.)
- Scott, Paul. 2014. “Dynamic discrete choice estimation of agricultural land use.” Tech. Rep. TSE-526, Toulouse School of Economics. (Cited on page 11.)
- Sekhri, Sheetal. 2014. “Wells, water, and welfare: The impact of access to groundwater on rural poverty and conflict.” *American Economic Journal: Applied Economics* 6 (3):76–102. (Cited on page 7.)
- . 2022. “Agricultural trade and depletion of groundwater.” *Journal of Development Economics* 156. (Cited on pages 1, 4, 5, 11, and 30.)
- Sheffield, Justin, Gopi Goteti, and Eric F. Wood. 2006. “Development of a 50-year high-resolution global dataset of meteorological forcings for land surface modeling.” *Journal of Climate* 19 (13):3088–3111. (Cited on pages 7, 46, 48, 55, and 60.)

- Siebert, S., M. Kummu, M. Porkka, P. Döll, N. Ramankutty, and B. R. Scanlon. 2015. “A global data set of the extent of irrigated land from 1900 to 2005.” *Hydrology and Earth System Sciences* 19 (3):1521–1545. (Cited on page 25.)
- Sotelo, Sebastian. 2020. “Domestic trade frictions and agriculture.” *Journal of Political Economy* 128 (7):2690–2738. (Cited on page 27.)
- Stavins, Robert N. 2011. “The problem of the commons: Still unsettled after 100 years.” *American Economic Review* 101 (1):81–108. (Cited on page 15.)
- Tapley, Byron D., Srinivas Bettadpur, John C. Ries, Paul F. Thompson, and Michael M. Watkins. 2004. “GRACE measurements of mass variability in the earth system.” *Science* 305 (5683):503–505. (Cited on pages 8, 58, and 59.)
- Taylor, Charles A. 2025. “Irrigation and climate change: Long-run adaptation and its externalities.” (Cited on page 58.)
- Taylor, M. Scott. 2011. “Buffalo hunt: International trade and the virtual extinction of the North American bison.” *American Economic Review* 101 (7):3162–3195. (Cited on page 6.)
- Tombe, Trevor. 2015. “The missing food problem: Trade, agriculture, and international productivity differences.” *American Economic Journal: Macroeconomics* 7 (3):226–258. (Cited on page 30.)
- Trefler, Daniel. 1993. “International factor price differences: Leontief was right!” *Journal of Political Economy* 101 (6):961–987. (Cited on page 10.)
- . 1995. “The case of the missing trade and other mysteries.” *American Economic Review* 85 (5):1029–1046. (Cited on page 10.)
- Viessman, Warren, Jr., John W. Knapp, Gary L. Lewis, and Terence E. Harbaugh. 1977. *Introduction to hydrology*. New York: Harper & Row, second ed. (Cited on page 6.)
- Wahr, John M., Steven R. Jayne, and Frank O. Bryan. 2002. “A method of inferring changes in deep ocean currents from satellite measurements of time-variable gravity.” *Journal of Geophysical Research: Oceans* 107 (C12). (Cited on page 58.)
- Wang, Xin and Shizhong Yang. 2018. “Research on status quo of water rights trading in China.” In *IOP Conference Series: Earth and Environmental Science*, vol. 171. (Cited on page 10.)
- Young, Mike. 2013. “Trading into and out of trouble: Australian’s water allocation and trading experience.” In *Water Trading and Global Water Scarcity*, edited by Josefina Maestu, chap. 6. Routledge, 114–130. (Cited on page 10.)

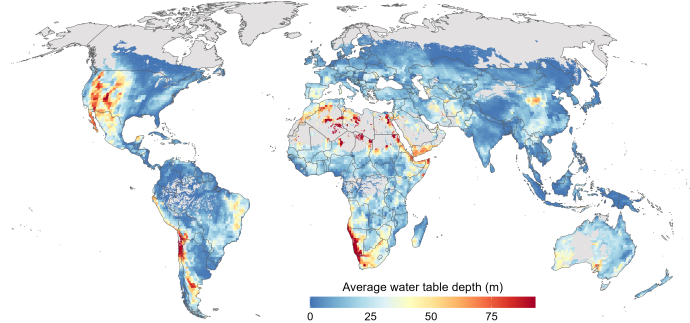
Zhang, Lijuan, Jinxia Wang, Jikun Huang, and Scott Rozelle. 2008. “Development of groundwater markets in China: A glimpse into progress to date.” *World Development* 36 (4):706–726. (Cited on page 10.)

Zhang, M., B. Wu, H. Zeng, G. He, C. Liu, S. Tao, Q. Zhang, M. Nabil, F. Tian, J. Bofana, A. N. Beyene, A. Elnashar, N. Yan, Z. Wang, and Y. Liu. 2021. “GCI30: A global dataset of 30m cropping intensity using multisource remote sensing imagery.” *Earth System Science Data* 13 (10):4799–4817. (Cited on pages 21 and 55.)

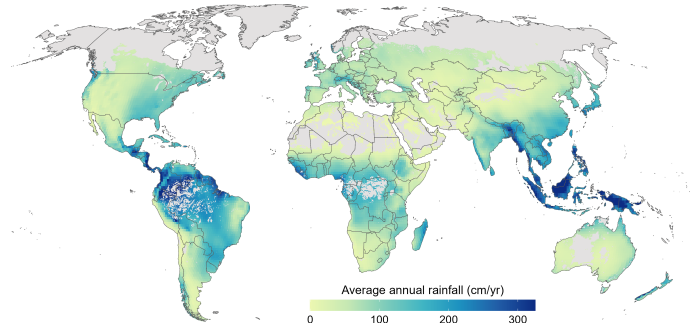
## Tables and Figures

**Figure 1:** Summary of global data on water resources

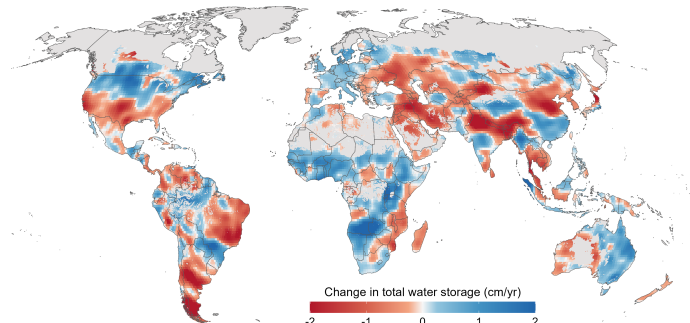
(a) Average water table depth (meters below land surface)



(b) Average rainfall (centimeters/year)



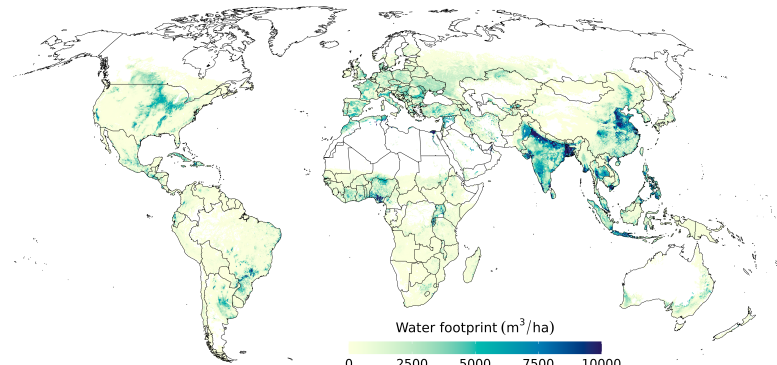
(c) Change in total water storage (centimeters/year)



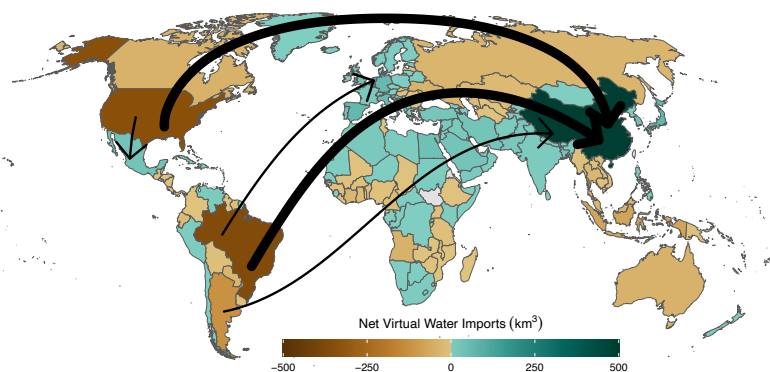
**Notes:** Panel (a) maps average groundwater depth from [Fan, Li, and Miguez-Macho \(2013\)](#). Panel (b) maps average precipitation from [Sheffield, Goteti, and Wood \(2006\)](#). Panel (c) maps changes in total water storage from the Gravity Recovery and Climate Experiment (GRACE). All variables are aggregated from their native resolutions to the equal-area grid ( $1^\circ \times 1^\circ$  at the equator) of the GRACE data, but are shown only over arable lands as defined using the 5-arcminute resolution grid from [Monfreda, Ramankutty, and Foley \(2008\)](#). Details are in Appendix A.

**Figure 2:** Agricultural water consumption and virtual water trade

(a) The spatial distribution of agricultural water consumption

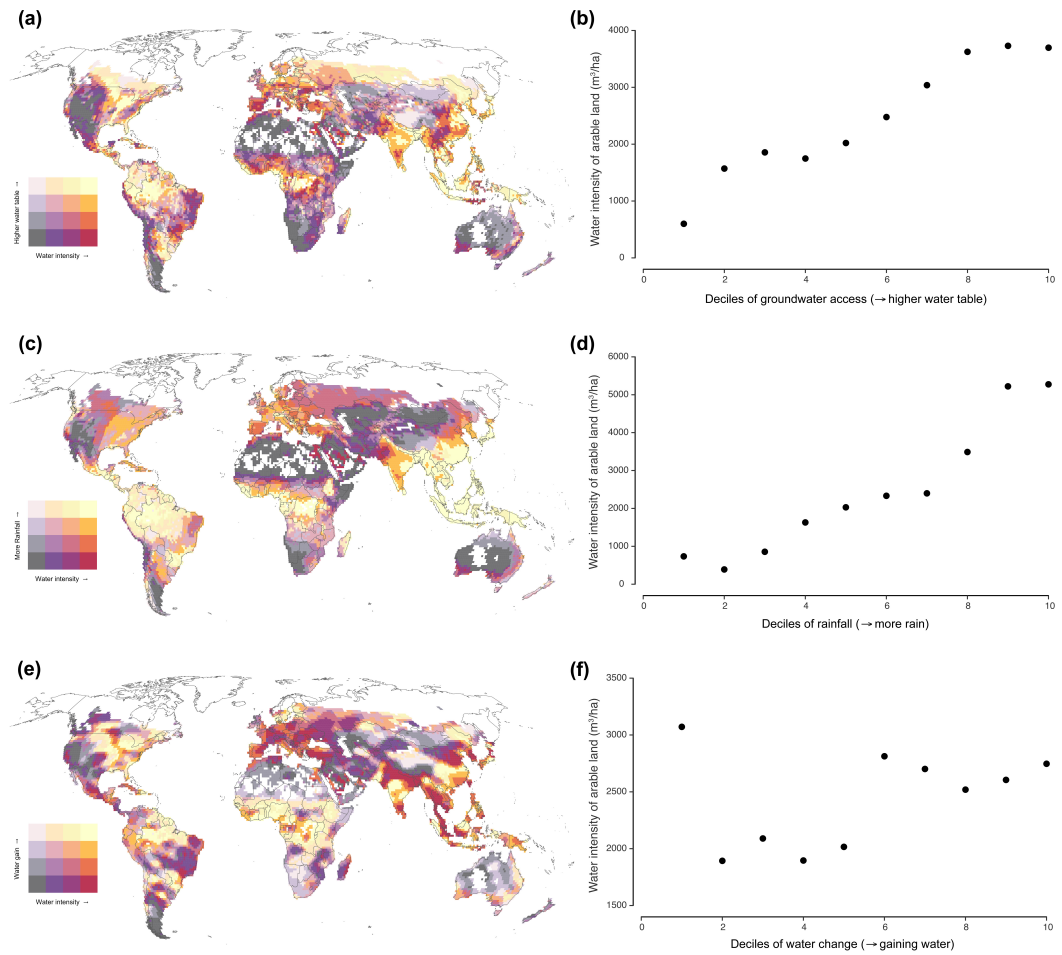


(b) Virtual water trade



**Notes:** Panel (a) maps estimated water consumption in agriculture over arable lands, constructed by combining agronomic estimates of crop-specific water consumption from Hoekstra and Mekonnen (2012) with gridded data on crop-specific planted area from Monfreda, Ramankutty, and Foley (2008). Panel (b) maps imports minus exports of agricultural “virtual water”—water consumed in the production of agricultural goods. Estimates combine water consumption measures shown in (a) with Comtrade data from 2009. Positive values indicate that imports of water embedded in traded goods exceeds exports. The five largest bidirectional flows are shown with arrows, where arrow width indicates flow magnitude.

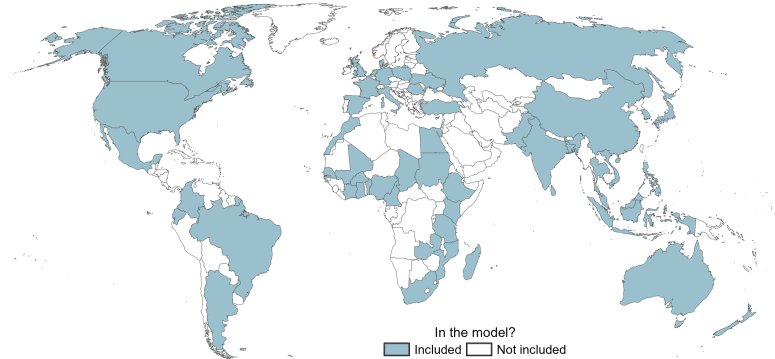
**Figure 3:** Correlations of water intensity of arable land use and relative water abundance



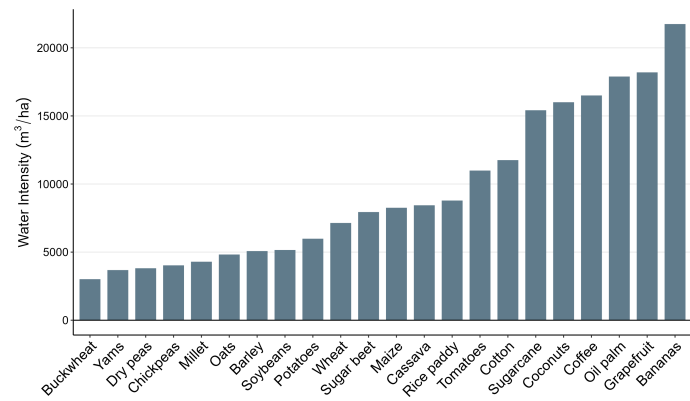
**Notes:** Maps show water intensity of arable lands against: (a) depth to groundwater from [Fan, Li, and Miguez-Macho \(2013\)](#); (c) total annual rainfall from [Sheffield, Goteti, and Wood \(2006\)](#); and (e) trends in total water storage from the GRACE satellite. Scatter plots in (b), (d), and (f) show the average water intensity of arable land for each decile of water table depth, precipitation, and change in total water storage, respectively. Arable land is defined as land that is cropped or pastured. The water intensity measures are calculated using data from [Mekonnen and Hoekstra \(2011\)](#), and water variable data sources are detailed in Appendix A.

**Figure 4:** Selected sample of countries crops and aquifers

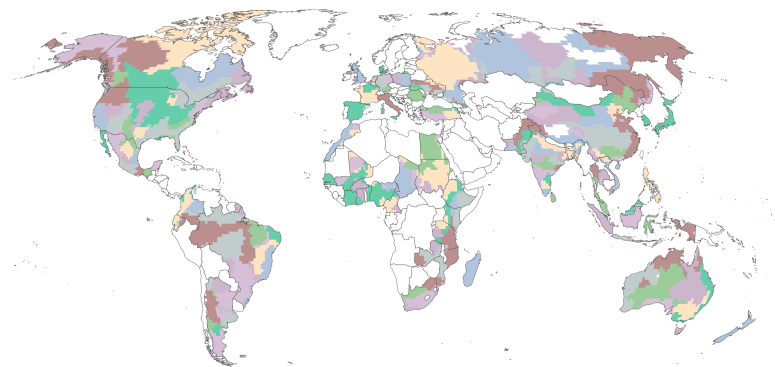
(a) 52 countries included in the model



(b) Water intensity of 22 crops included in the model

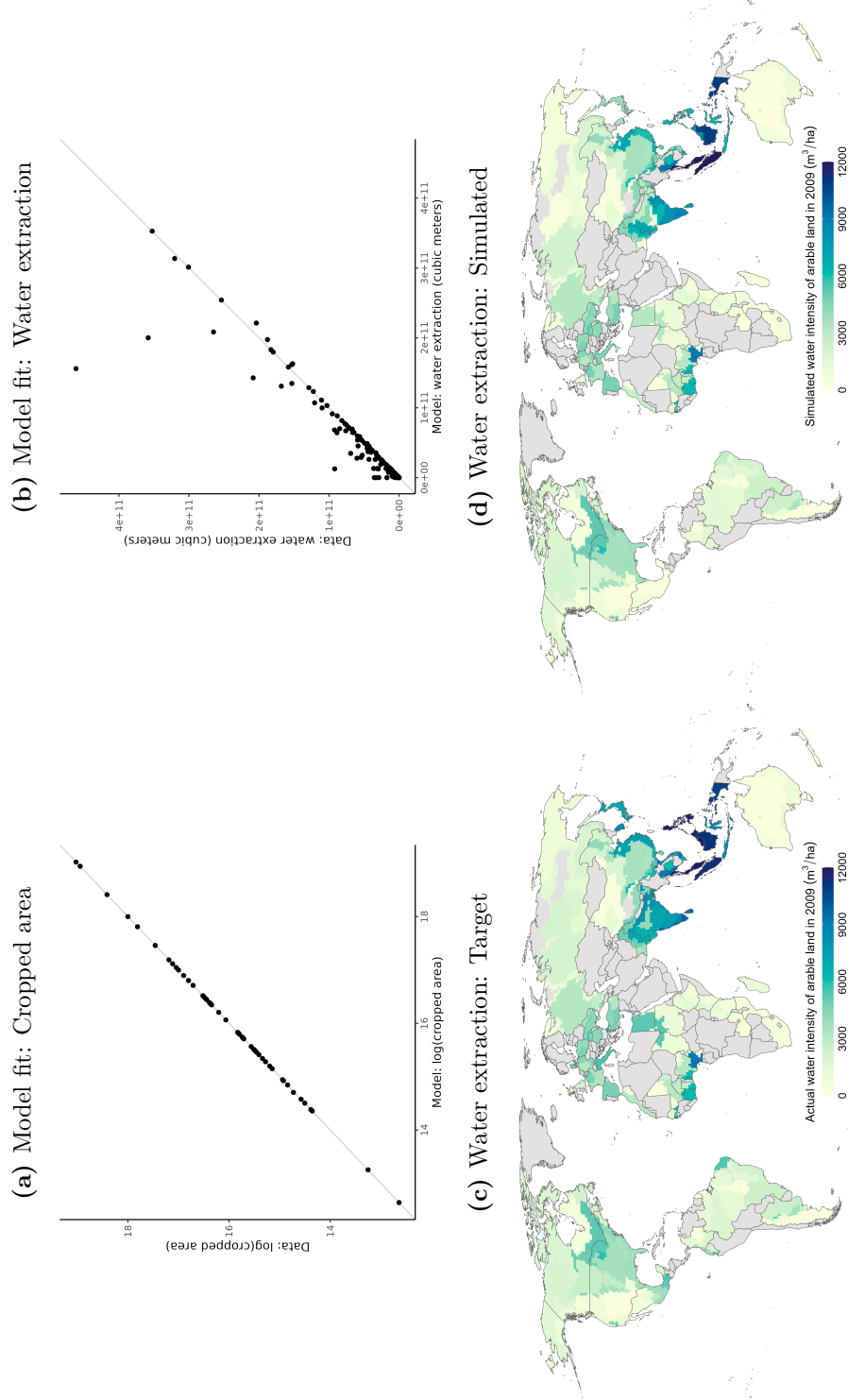


(c) 199 global aquifers included in the model



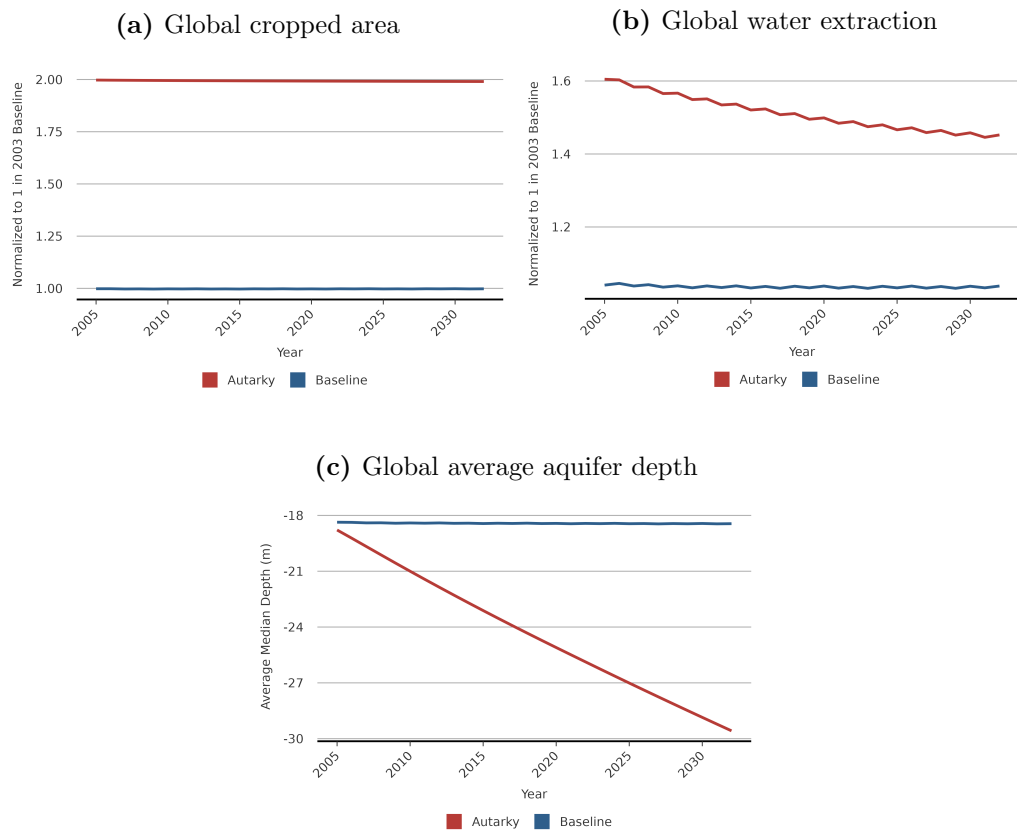
**Notes:** Panel (a) maps the 52 countries included in the model. Panel (b) shows the water intensity in cubic meters per hectare of the 22 crops included in the model. Panel (c) maps 278 global aquifers, 199 of which overlap with the countries shown in panel (a) and are therefore included in the model. Details on sample selection are provided in Section 4.1.

**Figure 5:** Simulated model fit for cropped area and water extraction



**Notes:** Panel (a) maps the percentage difference between model-simulated and observed county-level cropped area. Negative values indicate that the model simulation is under-estimating cropped area. Panel (b) maps the percentage difference between model-simulated and observed aquifer-level total water extraction. Negative values indicate that the model simulation is under-estimating water extraction. Panels (c)–(d) map aquifer-level observed (c) and model simulated (d) water intensity of arable land.

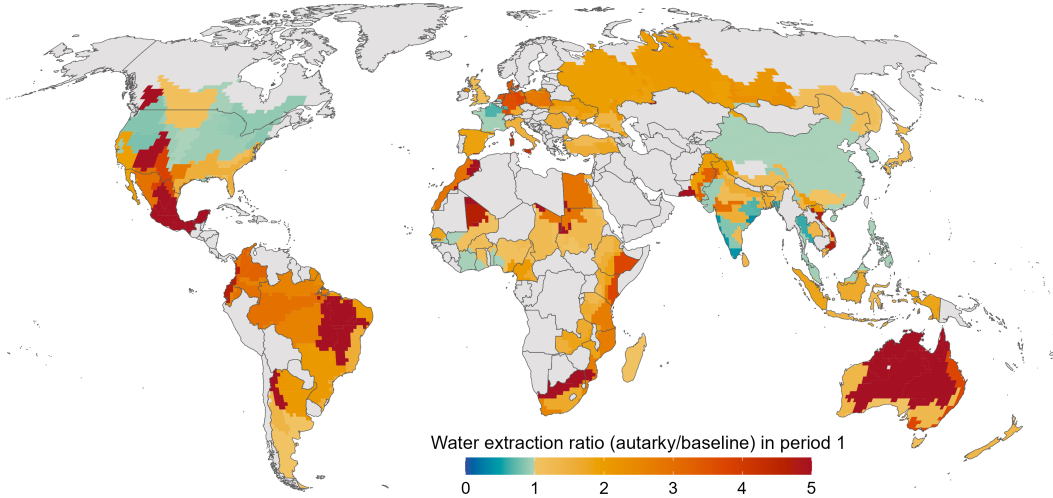
**Figure 6:** Simulated impact of agricultural trade on global agriculture water and welfare over time



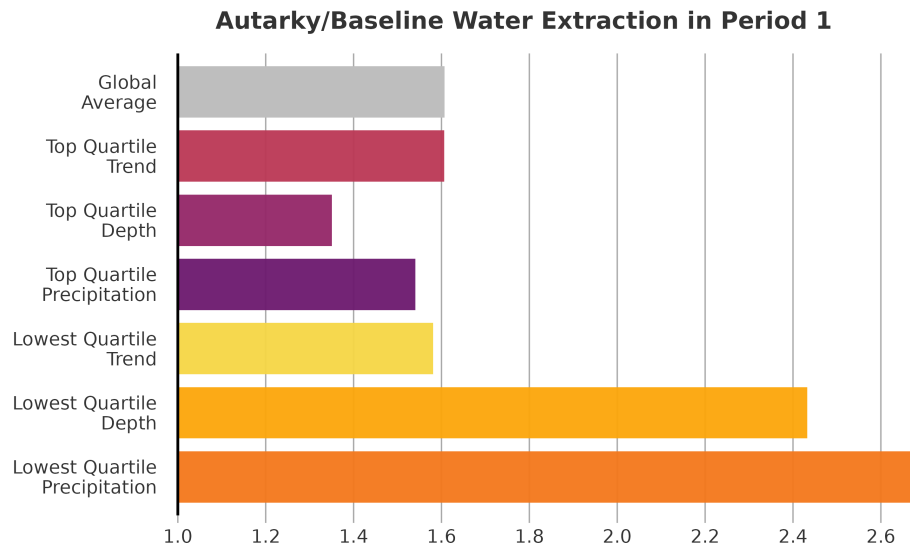
**Notes:** Each panel shows model simulated output under the baseline calibration (in blue) and a counterfactual autarky simulation (in red) in which trade costs for all crops and all country pairs are infinite. All values are three year backward-looking moving averages.

**Figure 7:** Relative water extraction under autarky—by initial water availability

(a) Global distribution

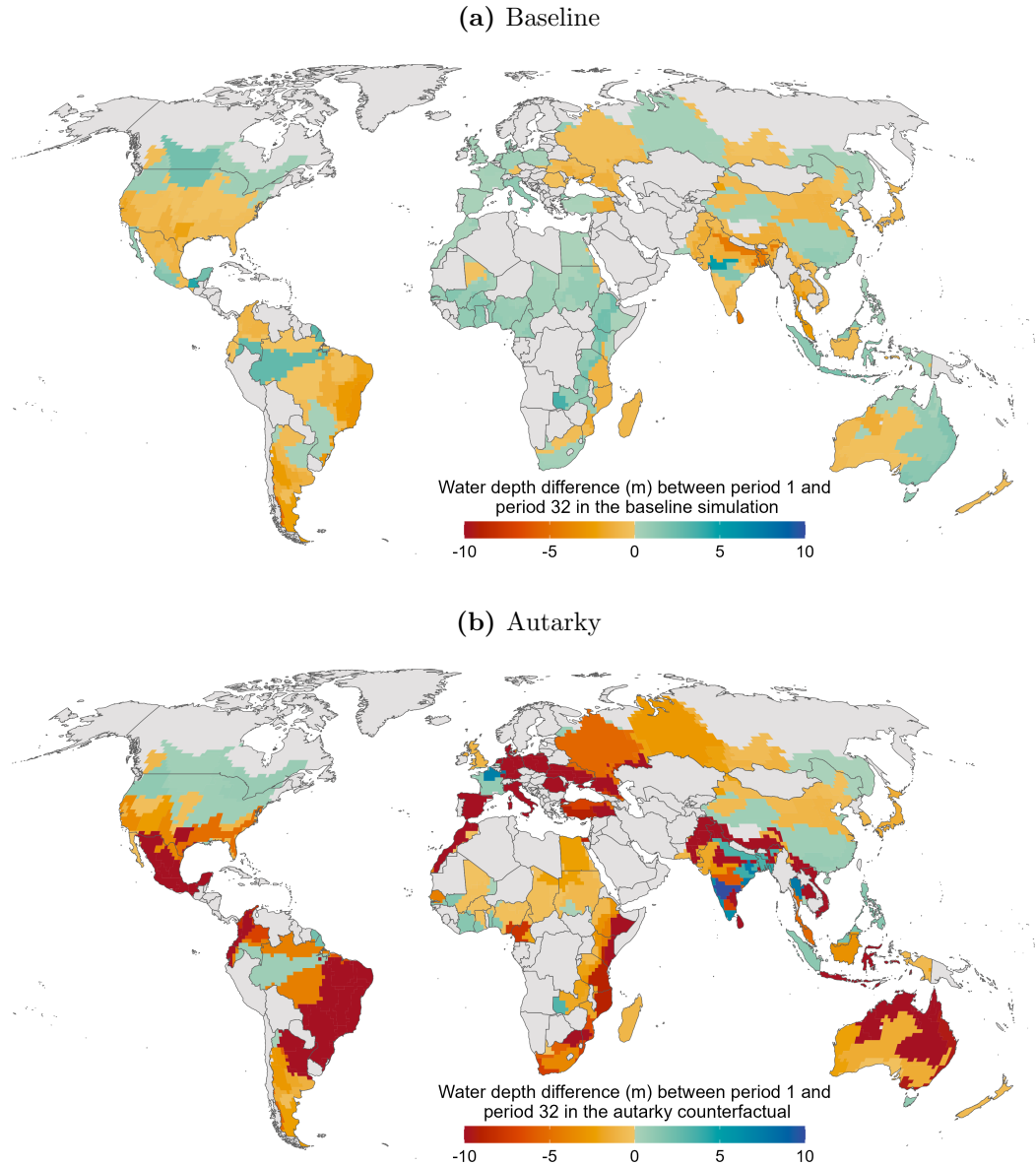


(b) Heterogeneity by initial water resource characteristics



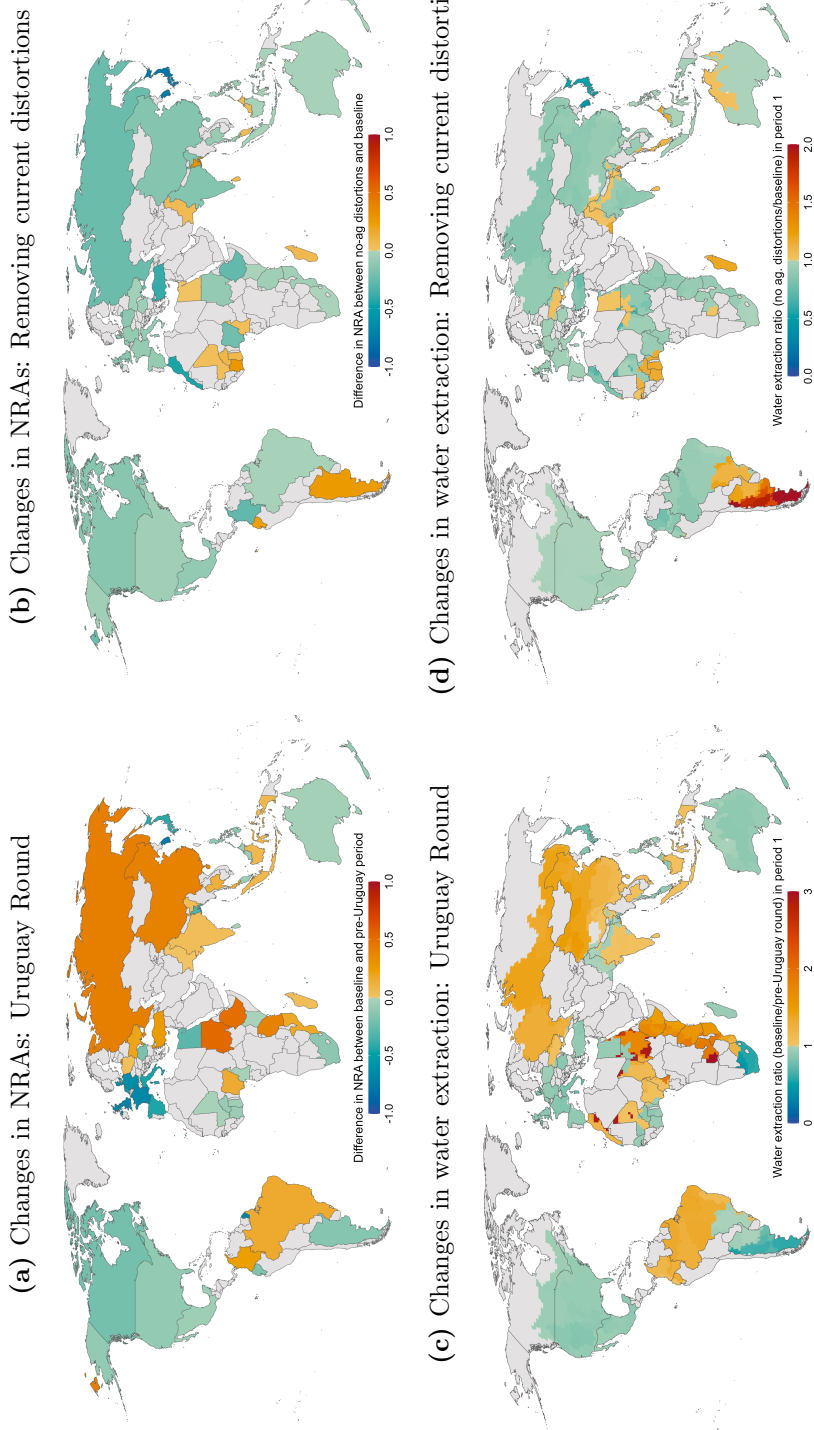
**Notes:** Map shows the ratio of water extraction under autarky to that under the baseline simulation, at the aquifer level. Ratios above one indicate water extraction rates in autarky that exceed those simulated under baseline agricultural production and trade.

**Figure 8:** Simulated trends in water tables over time



**Notes:** Map shows the projected 30-year change in water table depth in the baseline simulation in panel (a) and in the autarky counterfactual in panel (b). Changes in water table depth depend on water extraction, recharge, and the specific yield of the soil in each region. Calibrated recharge is held fixed across years and counterfactuals, and Figure 7 shows the ratio of extraction in autarky versus the baseline.

**Figure 9:** Nominal rates of assistance (NRA) and simulated water extraction under alternative policy simulations



**Notes:** Panels (a)–(b) show the difference in country-level average Nominal Rates of Assistance (NRA) between (a) after and before the Uruguay Round of World Trade Organization negotiations, which concluded in 1994 and dramatically liberalized agricultural production and trade (negative values indicate that the Uruguay Round lowered subsidies to agriculture); and (b) after versus before removing all baseline (2009) period agricultural distortions (negative values indicate that removing current distortions would lower agricultural subsidies to agriculture). Panels (c)–(d) show global water extraction on impact under these two counterfactual simulations.

**Table 1:** Global geospatial and administrative datasets used throughout the analysis

	Source	Scale	Process
<b>Hydrological spatial</b>			
Aquifer boundaries	WHYMAP	37 aquifers	Compilation of national, regional and global groundwater sources
Water table depth	Fan, Li, and Miguez-Macho (2013)	1km grid	Hydrological model used to interpolate between observations from 1.6 million wells
Change in total water storage	GRACE	~1° equal-area grid	Satellite-based measurements of anomalies in Earth's gravitational field used to infer changes in water mass
Precipitation and temperature	Sheffield, Goteti, and Wood (2006)	0.25° grid	Reanalysis product combining a climate model with observational records
Presence of surface water	Pekel, Cottam, Gorelick, and Belward (2016)	30m grid	Machine learning classification of over three million Landsat satellite images
Soil type	Hengl et al. (2017)	250m grid	Machine learning predictions trained on 150,000 soil samples
Specific yield	Loheide, Butler, and Gorelick (2005)	14 soil types	Literature meta-analysis
<b>Agricultural spatial</b>			
Agricultural land use	Monfreda, Ramankutty, and Foley (2008)	~10km grid × 178 crops	Census data combined with remote sensing-based downscaling
Potential crop yields	GAEZ	~10km grid × 38 crops	Agronomic modeling using a wide array of climate, soil, and geography input datasets
Area equipped for irrigation	Global Map of Irrigation Areas	~10 km grid	Administrative records combined with geospatial and remote sensing-based downscaling
Water intensity of production	Mekonnen and Hoekstra (2011)	126 crops	Agronomic and hydrologic modeling using a wide array of input data on climate, soil, and farmer inputs and techniques
Land cover	GLC-SHARE	30 arcsec grid	Compilation of high resolution national and sub-national land cover databases
Cropping intensity	Zhang et al. (2021)	30m grid	Machine learning classification using Landsat and Sentinel-2 satellite images
<b>Country-level</b>			
Agricultural output, prices, and trade	FAOSTAT & Comtrade	~200 crops × >200 countries	Direct reporting in administrative records
Distortions to agricultural incentives	World Bank	80 crops × 82 countries	Direct reporting in administrative records combined with a small open economy model

**Table 2:** Summary of global and regional model counterfactual results

	<u>Cropped Acreage</u>		<u>Water Extraction</u>		<u>Water Table Depth</u>		<u>Food Prices</u>		<u>Non-ag Production</u>	
	2003 <i>Level</i> (ha)	2003 → 30 <i>Growth Rate</i>	2003 <i>Level</i> (m <sup>3</sup> )	2003 → 30 <i>Growth Rate</i>	2003 <i>Level</i> (m)	2003 → 30 <i>Growth Rate</i>	2003 <i>Level</i> (Index)	2003 → 30 <i>Growth Rate</i>	2003 <i>Level</i> (\$)	2003 → 30 <i>Growth Rate</i>
Global Baseline	<b>1.07e+09</b>	0.002%	<b>7.67e+12</b>	0.033%	<b>17.1</b>	0.048%	<b>5.86e-07</b>	0.007%	<b>3.9e+08</b>	0%
Autarky	99.8%	-0.014%	60.7%	-0.329%	-	2.34%	1410%	0.009%	-15.5%	0.01%
pre-Uruguay Round	-3.74%	0.003%	-3.41%	0.115%	-	0.026%	0.361%	-0.071%	-0.185%	-0.001%
Zero ag. distortions	-3.37%	-0.005%	-3.7%	0.1%	-	-0.007%	2.06%	-0.039%	0.125%	0%
Top 25% Net Water Exports Baseline	<b>6.32e+08</b>	0%	<b>4.74e+12</b>	-0.029%	<b>15.6</b>	0.005%	<b>5.11e-07</b>	0.01%	<b>1.78e+08</b>	0%
Autarky	85.5%	-0.003%	27.5%	-0.456%	-	1.47%	-2.11%	0.043%	-16%	0.008%
China	-1.09%	-0.012%	-0.941%	-0.186%	-	0.176%	-2.11%	0.043%	0.933%	0.008%
India	108%	0%	1.53%	-0.066%	-	1.82%	4420%	-0.479%	-98.4%	0.05%
Thailand	-36.3%	-0.016%	-40.6%	-0.472%	-	1.1%	-13.9%	0.173%	9.12%	0.002%
U.S.A.	36%	-0.004%	10.9%	-0.156%	-	0.308%	-4.54%	0.003%	-10.5%	0.001%
Bot. 25% Net Water Exports Baseline	<b>1.87e+08</b>	-0.017%	<b>1.02e+12</b>	-0.057%	<b>23.5</b>	0.005%	<b>1.3e-06</b>	0.003%	<b>1.97e+12</b>	-0.001%
Autarky	150%	-0.045%	217%	-0.175%	-	3.66%	3550%	0%	-15.1%	0.015%
Australia	484%	-0.06%	385%	-0.31%	-	1.09%	205%	0.097%	-15.1%	0.015%
Egypt	39.1%	0%	197%	-0.002%	-	0.168%	3550%	0%	-60%	0.001%
Ghana	11.2%	0.032%	6.6%	0.179%	-	-0.094%	1010%	-0.013%	-1.94%	-0.006%
Pakistan	75.8%	0%	706%	-0.004%	-	18.7%	4510%	0%	-80.3%	0.001%

**Notes:** Table displays starting period (2003) levels and annual trends across the baseline calibration and counterfactual simulations. For rows indicating “Baseline,” each variable’s left column shows the 2003 level of the variable globally or in the specified region (in bold). In all other rows, the left column shows the percent change in the 2003 level of the variable induced by switching from the baseline to the indicated counterfactual simulation. These 2003 percent changes are omitted for water table depth because depths are fixed in the first period of simulation. The right column shows, for both the baseline and counterfactuals, the growth rate of the variable in each region from 2003 to 2030, represented as the average annual change as a percentage of the variable’s 2003 level. The top panel describes the global baseline values and their evolution in the three counterfactuals indicated in the leftmost column. The remaining two panels detail the implications of switching to autarky in regions made up of countries in the top and bottom quartile of net virtual water exports, as displayed in Figure 2b. Within each region, rows labeled with individual country names contain percent changes and growth rates for specific countries within each quartile.

## Appendix—For Online Publication

### A Data Appendix

---

A.1 Global hydrological spatial data . . . . .	57
A.2 Global agricultural spatial data . . . . .	60
A.3 Global country-level data . . . . .	62

---

We compile a wide array of geospatial datasets to assemble what constitutes, to our knowledge, the largest collection of global data on water and agriculture yet to be used in economics. The compiled dataset is summarized in Table 1, and each component dataset is detailed below.

#### A.1 Global hydrological spatial data

Our analysis of the spatial allocation of water resources draws primarily on two scientific datasets that provide information on levels and trends, respectively, of water availability throughout the world.

##### Water table depth

We collect globally comprehensive data on a cross-sectional measure of water table depth from Fan, Li, and Miguez-Macho (2013).<sup>56</sup> This scientific paper begins by compiling water table depth observations published in government or scientific sources from over 1.6 million wells located across all six populated continents. The paper proceeds to create a continuous spatial dataset by interpolating between well observations using a hydrological model calibrated to detailed spatial data on climate, geology, elevation, and soil characteristics. Together, the empirical observations and model simulations are used to produce global estimates of the depth of the water table in meters from the surface at a 30 arcsecond (approximately 1km) resolution.

This dataset provides estimates of the water available to farmers from both groundwater and surface water. For farmers who irrigate their crops using groundwater, well depth plays a critical role in their costs of extraction since it is costlier to pump water from further underground.<sup>57</sup> Other farmers irrigate crops from surface water, which is typically lower cost where available. Approximately 37% of global

---

<sup>56</sup>Note that we use the updated version of the dataset accessed [here](#), which corrects for some known errors in the 2013 version.

<sup>57</sup>See Hendricks and Peterson (2012) for analysis of how extraction costs vary with well depth.

irrigated land relies on groundwater, and 63% on surface water.<sup>58</sup> The data from the hydrological model simulations in [Fan, Li, and Miguez-Macho \(2013\)](#) provides information on the presence of surface water by marking these areas with water table depth readings of less than zero. The paper estimates that 15% of global land area is covered by lakes, rivers, and inundated wetlands.<sup>59</sup>

The data on both water table depth and surface water availability play a critical role in the calibration of the costs of water extraction described in Section 4 of the main text. The drawback of this dataset, however, is that it contains only cross-sectional information on water availability, limiting its ability to inform about water resource dynamics that exist in the world and are represented in the model.<sup>60</sup>

### Trends in total water storage

The Gravity Recovery and Climate Experiment (GRACE) satellite mission was launched in 2002 by the U.S. National Aeronautics and Space Administration (NASA) and the German Deutsche Forschungsanstalt für Luft und Raumfahrt (DLR). The first mission ended in 2016.<sup>61</sup> GRACE missions are designed to measure changes in Earth's gravitational pull. Each mission consists of two identical spacecraft flying 220 km apart in the same orbital plane about 500 km above the Earth. As the pair passes over regions on Earth's surface with greater mass, they face stronger gravitational pull, affecting the distance between the lead and trailing satellites. Instruments on board generate precise measurements of the changing distance between the two satellites while in orbit, accurate up to one micrometer ( $\mu\text{m}$ ) per second ([Tapley et al., 2004](#)).

Because water moves in large quantities through the hydrologic cycle at a rate far faster than other processes that move mass across the Earth's surface, mass variations uncovered by GRACE each month are mostly attributable to changes in water content as it cycles between ocean, atmosphere, continents, glaciers, and polar ice caps ([Tapley et al., 2004](#)). These variations have been used to study ocean currents ([Wahr, Jayne, and Bryan, 2002](#)), measure ground water storage on land ([Rodell, Velicogna, and Famiglietti, 2009](#)), and document exchanges between ice sheets or glaciers and the oceans ([Jacob et al., 2012; Chen, Wilson, and Tapley, 2013](#)), among many other applications.<sup>62</sup> GRACE "solutions" convert monthly changes in the distance between satellites into estimates of changing mass. These solutions are available in gridded form across the globe. We use the Goddard Space Flight Center

---

<sup>58</sup>This statistic comes from our calculations using data from the Monthly Irrigated and Rainfed Crop Areas (MIRCA2000) dataset produced by [Portmann, Siebert, and Döll \(2010\)](#).

<sup>59</sup>This proportion excludes oceans, seas, and other large water bodies such as the Great Lakes.

<sup>60</sup>The exact years of water table depth observations in [Fan, Li, and Miguez-Macho \(2013\)](#) vary across regions but end in 2009.

<sup>61</sup>A follow-on mission to extend the satellite record was launched in 2018 and is ongoing. Our analysis uses data from the first mission only.

<sup>62</sup>Their use in economics, however, has been much more limited. The two exceptions are recent work by [Carleton \(2021\)](#) and [Taylor \(2025\)](#).

(GSFC) mass concentration solution RL06v2.0, which yields changes in centimeters of equivalent water height for 41,168 equal-area blocks, called mascons, which measure  $1^\circ \times 1^\circ$  ( $\sim 111.11 \text{ km} \times 111.11 \text{ km}$ ) at the equator (Loomis, Luthcke, and Sabaka, 2019).<sup>63</sup>

Following a large scientific literature (e.g., Rodell, Velicogna, and Famiglietti, 2009; Richey et al., 2015; Rodell et al., 2018), we assume that changes in mass recovered by GRACE can be treated as changes in total water storage ( $\Delta \text{TWS}$ ), which is composed of the following elements:

$$\begin{aligned}\Delta \text{TWS} = & \Delta \text{groundwater} + \Delta \text{surface water} \\ & + \Delta \text{soil moisture} + \Delta \text{snow water equivalent}.\end{aligned}$$

Throughout our analysis, we abstract from any decomposition of  $\Delta \text{TWS}$  and directly use this aggregate measure of water storage.<sup>64</sup> We use the raw monthly  $\Delta \text{TWS}$  observations to compute grid-cell specific trends in total water storage (in centimeters of equivalent height lost or gained per year) using time series regressions of  $\Delta \text{TWS}$  on day-of-sample, including monthly fixed effects to remove the role of seasonality.

GRACE has the important advantage of providing global-scale estimates of changes in total water availability; no other data product comes close to presenting such a comprehensive picture of changing water resources. Like all remotely sensed data, however, there are many important limitations of the data. First, all changes in Earth's gravitational field are recovered in GRACE, not only those due to changing water resources. For example, large landslides, mass human migrations, and large-scale mining activities, among other factors, can plausibly drive variation in gravitational pull. In our analyses, all of these changes are interpreted as changes in water resources. Nevertheless, prior research has documented that water dominates the overall variation in GRACE (Tapley et al., 2004), and that land surface and/or hydrologic models that are used to isolate specific components of GRACE (e.g., groundwater) are highly sensitive to difficult-to-calibrate model parameters (Long et al., 2013). We therefore follow a large literature in interpreting gravitational anomalies from GRACE as changes in water resources and analyzing only aggregate TWS measures.

Second, the relatively low spatial resolution of GRACE ( $1^\circ \times 1^\circ$ ) makes it valuable for global-scale analysis, but of limited use for many local water resource management questions. Other remotely sensed datasets, such as OpenET for measuring evapotranspiration (Melton et al., 2022) or InSAR for measuring recharge (Neely et al., 2021), are available in some regions of the world and are undoubtedly more appropriate for certain applications.

---

<sup>63</sup>Equivalent water height is defined as the depth of water that would be present were it to be spread evenly across the entire surface of a grid cell. Other GRACE solutions, such as the mascons processed by NASA's Jet Propulsion Laboratory, are equal-angle rather than equal-area.

<sup>64</sup>Because we restrict our analysis to arable land, we do not suppose that changes in snow water equivalent play a meaningful role.

Finally, GRACE gives a measure of *changes* in water storage, but not estimates of available water *stocks*. Changes in gravitational pull are estimated from GRACE by taking a residual relative to a modeled estimate of the geoid—the hypothetical shape of the Earth. The data are represented as *anomalies* in the average gravitational field, which prohibits any interpretation of output in levels. Moreover, because this method relies heavily on the modeled geoid, there is undoubtedly measurement error that may influence downstream empirical estimation (Proctor, Carleton, and Sum, 2023).

### Other hydrological data

We supplement the two primary datasets on water availability described above with a range of other relevant global spatial hydrological datasets. We use data on cumulative precipitation at  $0.25^\circ \times 0.25^\circ$  resolution from the Global Meteorological Forcing Dataset (GMFD) version 3 from Princeton University (Sheffield, Goteti, and Wood, 2006). We also collect satellite data on the presence of surface water at a 30-meter resolution from Pekel et al. (2016) as a complement to the measure available from Fan, Li, and Miguez-Macho (2013).

We collect several datasets relevant to calibrating the law of motion for local water table depths in the model (Equation (10)). These include global spatial data on soil type from Hengl et al. (2017) and specific yield by soil type from Loheide, Butler, and Gorelick (2005). Specific yield is the volume of water that can be drained from porous media by gravity, relative to the total volume of the media. This value, between zero and one, indicates the space available in the soil for water mass to be gained or lost. Thus, we use soil type information from Hengl et al. (2017) with specific yield by soil type from Loheide, Butler, and Gorelick (2005) to estimate the average specific yield at grid cell level across the globe. This then enables us to map changes in the volume of water in a given location into changes in water table depth in model simulations.

## A.2 Global agricultural spatial data

### Agricultural land use

We use global spatial data on agricultural land use at a  $10\text{km} \times 10\text{km}$  resolution compiled by Monfreda, Ramankutty, and Foley (2008). These data use a combination of remote sensing and census records from national and subnational government entities to estimate the fraction of land area in each grid cell allocated to planting each of 175 crops, and to pasture land, in the year 2000.<sup>65</sup> In this paper, we use the union of cropped area and pasture land as the definition of arable land with the potential for cultivation.

---

<sup>65</sup>While more recent products exist for aggregate cropped area, such as Potapov et al. (2022), updated estimates of crop- and pasture-specific areas are not available.

We supplement the data on crop choice and land use with additional spatial data that measures the proportion of agricultural land equipped for irrigation. This dataset is called the Global Map of Irrigation Areas, and is compiled by the United Nations Food and Agriculture Organization (FAO) and Rheinische Friedrich-Wilhelms University. The data comes at the 5-arcminute resolution and contains estimates for the year 2005.

### Potential yields

The second global spatial agricultural dataset comes from the FAO's Global Agro-Ecological Zones (GAEZ v4). This data contains potential yields for 41 non-fodder crops at 5-arcminute resolution, estimated using an agronomic model that incorporates detailed local information on soils, geography, and climate. The model provides crop-specific estimates of the maximum yield attainable under a range of possible assumptions about farmer inputs and climate conditions.

Critically, this data provides estimates of potential yields for all crops in all locations, including those that have not been historically observed in a given place. This allows for a rich representation of regional comparative advantage in agriculture and for counterfactual model simulations in which crop choice can shift meaningfully across location. [Costinot, Donaldson, and Smith \(2016\)](#) pioneered the use of this data in quantitative trade models. In our implementation, we follow their work in using the high-input yield estimates, but restrict attention to the historical climate scenario that uses average weather from 1961–1990. We take the weighted average of “rain-fed” and “irrigated” potential yields, using the data on the area equipped for irrigation in each location to assign weights between the two.

### Crop-specific water intensity of production

We use data from [Mekonnen and Hoekstra \(2011\)](#) to estimate the average global water intensity of each crop. These estimates are denominated in units of cubic meters of water used by the crop per tonne of output. To estimate these values, [Mekonnen and Hoekstra \(2011\)](#) trace water used in agricultural production throughout its supply chain. Specifically, the paper quantifies agricultural water consumption throughout the world at the 5-arcminute resolution using a model that combines hydrological and agronomic mechanisms with detailed spatial data on climate and soil conditions, crop planting and harvesting dates, irrigation techniques, information on farmer inputs such as nitrogen, and data on land use from [Monfreda, Ramankutty, and Foley \(2008\)](#). The quantitative findings from [Mekonnen and Hoekstra \(2011\)](#), which indicate that over 90% of humanity’s water consumption is dedicated to agricultural production as detailed in the main text in [Fact 2](#), are corroborated in a recent review article by [d’Odorico et al. \(2019\)](#).

We combine the estimates from [Mekonnen and Hoekstra \(2011\)](#) with data on the average global yield of each crop to construct a dataset of crop-specific water

intensities denominated in units of cubic meters per hectare. Note the caveat that [Mekonnen and Hoekstra \(2011\)](#) provide only an average global estimate of crop water use without any heterogeneity, so a data limitation of the current analysis is that we do not currently account for changes in water use arising from different techniques of growing a given crop, or other differences in crop-specific water intensity of production across space.

### A.3 Global country-level data

#### Production and trade

We collect data from FAOSTAT on crop-specific production in tonnes along with farm-gate prices measured in U.S. dollars per tonne. The data is available for over 200 countries from 1961–2020, though in our implementation in the model calibration we use a cross-section of the data for a subset of countries in 2009. We also use data on bilateral trade flows by crop for the same year from the UN Comtrade database.

#### Agricultural policy

Government interventions in agricultural markets play a critical role in shaping global agricultural trade patterns. Analyzing these policies in an international context, however, is complicated by the wide array of relevant policy tools with interacting and overlapping effects, including output taxes and subsidies, input subsidies, import tariffs, quotas, sanctions, and regulations. Furthermore, these policies are implemented within institutional contexts that differ substantially across countries, such that their definition and interpretation may not be consistent across locations.

We overcome these challenges by using data from the World Bank’s Distortions to Agricultural Incentives (DAI) project, which constructs an internationally-comparable measure of agricultural policy interventions that is both comprehensive and parsimonious. Included in these data is a single summary statistic, known as the *nominal rate of assistance* (NRA), measured for 80 products in 82 countries.

The NRA captures the equivalent product-specific net subsidy or tax that results from the combined effect of the full range of policies that include direct taxes and subsidies, tariff and non-tariff barriers to trade, and government manipulation of foreign exchange markets ([Anderson, Kurzweil, Martin, Sandri, and Valenzuela, 2008](#)). The NRA measure—positive for net subsidies and negative for net taxes—can be interpreted as the percentage difference between domestic farm-gate prices and international prices for the same product, excluding transportation and distribution costs. Critically, the measure does not include any water-specific policy interventions, such as subsidies for agricultural energy use or irrigation.

The DAI data has been used previously to study topics ranging from political economy ([Anderson, Rausser, and Swinnen, 2013](#)) to agricultural productivity ([Adamopoulos and Restuccia, 2014](#)). In this paper, we use this data to investigate

the spatial correlation between agricultural policy and water resources in Section 2, and to calibrate the output market distortions in the model in Section 3.

## B Theoretical Appendix

---

B.1	Derivations . . . . .	64
B.1.1	Optimal consumption bundle . . . . .	64
B.1.2	Optimal labor allocation and water use . . . . .	65
B.1.3	Crop-specific cropped area shares (by field) . . . . .	67
B.1.4	Expected productivity given crop selection . . . . .	68
B.1.5	Robustness: Nested CES agricultural technology . . . . .	69
B.2	Existence and uniqueness . . . . .	70
B.2.1	... of the trade equilibrium . . . . .	71
B.2.2	... of the steady-state equilibrium . . . . .	74
B.2.3	... of the full dynamic competitive equilibrium . . . . .	75
B.2.4	The outside sector as residual claimant . . . . .	75

---

### B.1 Derivations

#### B.1.1 Optimal consumption bundle

We wish to verify Equation (11). The representative consumer of country  $i$  chooses  $C_{it}^o$  and  $\{C_{jit}^k\}$  every period to maximize

$$U_{it} = C_{it}^o + \zeta_i \ln C_{it}$$

with the aggregators

$$C_{it} = \left[ \sum_{k \in \mathcal{K}} \left( \zeta_i^k \right)^{\frac{1}{\kappa}} \left( C_{it}^k \right)^{\frac{\kappa-1}{\kappa}} \right]^{\frac{\kappa}{\kappa-1}}$$

$$C_{it}^k = \left[ \sum_{j \in \mathcal{I}} \left( \zeta_{ji}^k \right)^{\frac{1}{\sigma}} \left( C_{jit}^k \right)^{\frac{\sigma-1}{\sigma}} \right]^{\frac{\sigma}{\sigma-1}}$$

subject to the budget constraint

$$Y_{it} = C_{it}^o + \sum_k \sum_j \delta_{ji}^k p_{jt}^k C_{jit}^k.$$

We solve the problem nest-by-nest:

- (i) what is the optimal cross-country bundle  $\{C_{jit}^k\}_j$  for a given crop-specific index  $C_{it}^k$ ?
- (ii) what is the optimal cross-crop bundle  $\{C_{it}^k\}_k$  for a given agricultural index  $C_{it}$ ?

- (iii) what is the optimal expenditure split between the outside good  $C_{it}^o$  and the agricultural index  $C_{it}$ ?

The usual CES derivations give us the following relationships for (i) and (ii):

$$C_{jit}^k = \zeta_{ji}^k \left( \delta_{ji}^k p_{jt}^k \right)^{-\sigma} \left( P_{it}^k \right)^\sigma C_{it}^k \quad \text{with price index } P_{it}^k = \left[ \sum_n \zeta_{ni}^k \left( \delta_{ni}^k p_{nt}^k \right)^{1-\sigma} \right]^{\frac{1}{1-\sigma}}$$

$$C_{it}^k = \zeta_i^k \left( P_{it}^k \right)^{-\kappa} (P_{it})^\kappa C_{it} \quad \text{with price index } P_{it} = \left[ \sum_k \zeta_i^k \left( P_{it}^k \right)^{1-\kappa} \right]^{\frac{1}{1-\kappa}}.$$

The outermost nest (iii) is simply the solution to

$$\max_{C_{it}^o, C_{it}} C_{it}^o + \zeta_i \ln C_{it} \quad \text{s.t. } Y_{it} = C_{it}^o + P_{it} C_{it},$$

which is  $P_i C_i = \zeta_i$  and  $C_{it}^o = Y_{it} - \zeta_i$ . Putting everything together:

$$\begin{aligned} C_{jit}^k &= \zeta_{ji}^k \left( \delta_{ji}^k p_{jt}^k \right)^{-\sigma} \left( P_{it}^k \right)^\sigma C_{it}^k \\ &= \zeta_{ji}^k \left( \delta_{ji}^k p_{jt}^k \right)^{-\sigma} \left( P_{it}^k \right)^\sigma \zeta_i^k \left( P_{it}^k \right)^{-\kappa} (P_{it})^\kappa C_{it} \\ &= \zeta_{ji}^k \left( \delta_{ji}^k p_{jt}^k \right)^{-\sigma} \left( P_{it}^k \right)^\sigma \zeta_i^k \left( P_{it}^k \right)^{-\kappa} (P_{it})^{\kappa-1} \zeta_i \\ &= \zeta_{ji}^k \left( \delta_{ji}^k p_{jt}^k \right)^{-\sigma} \left( P_{it}^k \right)^{\sigma-1} \zeta_i^k \left( P_{it}^k \right)^{1-\kappa} (P_{it})^{\kappa-1} \zeta_i \\ &= \frac{\zeta_{ji}^k \left( \delta_{ji}^k p_{jt}^k \right)^{-\sigma}}{\left( P_{it}^k \right)^{1-\sigma}} \frac{\zeta_i^k \left( P_{it}^k \right)^{1-\kappa}}{\left( P_{it} \right)^{1-\kappa}} \zeta_i, \end{aligned}$$

which, after reversing the order of terms and substituting in the definitions of the price indices, gives us Equation (11).

### B.1.2 Optimal labor allocation and water use

For a given crop  $k$ , the farmer solves the labor allocation problem

$$\max_{H \in [0,1]} Q^{fk}(\omega)[H] = A^{fk}(\omega) H^\alpha \left[ N^{fk}(H) \right]^{1-\alpha}$$

where  $N^{fk}(H) \equiv \min \left\{ 1, \frac{A_q^w(D_{q(f)})[1-H]}{\phi^k} \right\}$  denotes the “natural capital” (i.e., the effective bundle of land and water) the farmer can use to grow crop  $k$  if he allocates fraction  $H$  of his labor to tending the crop (hence  $1 - H$  to water extraction). An equivalent formulation of  $N^{fk}(H)$  is

$$N^{fk}(H) = \begin{cases} 1 & \text{if } H \leq 1 - \frac{\phi^k}{A_q^w(D_{q(f)})}, \\ \frac{A_q^w(D_{q(f)})}{\phi^k} (1 - H) & \text{if } H \geq 1 - \frac{\phi^k}{A_q^w(D_{q(f)})}. \end{cases}$$

Note that only in the first case would the farmer be irrigating his entire parcel.

We wish to derive the farmer's optimal policy function for labor,  $H^{fk}(\omega)$ , which in turn will determine how much water he extracts. We can prove almost immediately that the labor allocated to extracting water will be no more than  $\frac{\phi^k}{A_q^w(D_{q(f)})}$  because land and water are used in fixed proportions.

**Lemma B.1.**  $H^{fk}(\omega) \geq 1 - \frac{\phi^k}{A_q^w(D_{q(f)})}$ .

*Proof.*  $N^{fk}(H)$  is constant but  $A^{fk}(\omega)H$  is strictly increasing—hence  $Q^{fk}(\omega)[H]$  is strictly increasing—for any  $H < 1 - \frac{\phi^k}{A_q^w(D_{q(f)})}$ , so the farmer's optimal  $H$  cannot be in that range.  $\square$

Now consider the range over which  $H > 1 - \frac{\phi^k}{A_q^w(D_{q(f)})}$  and take the derivative of the farmer's objective with respect to  $H$ :

$$\begin{aligned} \frac{d}{dH} \left\{ A^{fk}(\omega)H^\alpha \left[ N^{fk}(H) \right]^{1-\alpha} \right\} \\ = A^{fk}(\omega) \left[ \alpha \left( \frac{N^{fk}(H)}{H} \right)^{1-\alpha} + (1-\alpha)(N^{fk})'(H) \left( \frac{H}{N^{fk}(H)} \right)^\alpha \right] \\ = A^{fk}(\omega) \left( \frac{A_q^w(D_{q(f)})}{\phi^k} \right)^{1-\alpha} \left[ \alpha \left( \frac{1-H}{H} \right)^{1-\alpha} - (1-\alpha) \left( \frac{H}{1-H} \right)^\alpha \right]. \end{aligned}$$

Setting this derivative equal to zero yields  $H^{fk}(\omega) = \alpha$  over that range. Combining this result with Lemma B.1, it follows that the optimal policy function for labor is

$$H^{fk} = \begin{cases} 1 - \frac{\phi^k}{A_q^w(D_{q(f)})} & \text{if } \frac{\phi^k}{A_q^w(D_{q(f)})} \leq 1 - \alpha \\ \alpha & \text{if } \frac{\phi^k}{A_q^w(D_{q(f)})} > 1 - \alpha, \end{cases} \quad (\text{B.1})$$

where we've dropped the argument  $\omega$  identifying the parcel because it proved irrelevant.

Accordingly, we can summarize the output of crop  $k$  by a farmer on parcel  $\omega$  of field  $f$  as  $A^{fk}(\omega)M(\phi^k, D_{q(f)})$ , where

$$M(\phi^k, D_{q(f)}) = \begin{cases} \left( 1 - \frac{\phi^k}{A_q^w(D_{q(f)})} \right)^\alpha & \text{if } \frac{\phi^k}{A_q^w(D_{q(f)})} \leq 1 - \alpha \\ \tilde{\alpha} \left( \frac{A_q^w(D_{q(f)})}{\phi^k} \right)^{1-\alpha} & \text{if } \frac{\phi^k}{A_q^w(D_{q(f)})} > 1 - \alpha \end{cases} \quad (\text{B.2})$$

with  $\tilde{\alpha} = \alpha^\alpha(1-\alpha)^{1-\alpha}$ . It follows that output is always decreasing in the water intensity  $\phi^k$  and the water table depth  $D$ . Moreover, for any given water intensity,  $M$  is a continuous function of depth with limits  $\lim_{D \rightarrow 0} M(\phi^k, D) = 1$  and  $\lim_{D \rightarrow \infty} M(\phi^k, D) = 0$  and a kink at the depth  $\hat{D}_q^k$  for which  $\frac{\phi^k}{A_q^w(\hat{D}_q^k)} = 1 - \alpha$  and

thus  $M(\phi^k, \hat{D}_q^k) = \alpha^\alpha$ . With  $v = 1$ , as it is calibrated in Section 4, one can further show that  $M$  is concave in depth over  $[0, \hat{D}_q^k]$  and convex over  $[\hat{D}_q^k, \infty)$ .<sup>66</sup>

Finally, the water extraction by a farmer on field  $f$  cultivating crop  $k$  is

$$x^{fk} = \begin{cases} \phi^k & \text{if } \frac{\phi^k}{A_q^w(D_{q(f)})} \leq 1 - \alpha \\ (1 - \alpha)A_q^w(D_{q(f)}) & \text{if } \frac{\phi^k}{A_q^w(D_{q(f)})} > 1 - \alpha. \end{cases} \quad (\text{B.3})$$

### B.1.3 Crop-specific cropped area shares (by field)

For convenience, assume  $i$  means  $i(f)$  and  $q$  means  $q(f)$  unless otherwise specified. We wish to verify Equation (13). The probability that crop  $k$  is grown on any given parcel  $\omega$  of field  $f$  (where  $k = o$  means the farmer works in the outside sector and leaves his parcel fallow) is the probability that the revenue from  $k$  is highest. Note that the c.d.f. of  $r_t^{fk}(\omega)$  is

$$F_t^{fk}(r) = \exp \left\{ -\gamma \left( \frac{r}{\tau_{it}^k p_{it}^k A^{fk} M(\phi^k, D_{qt})} \right)^{-\theta} \right\}$$

which follows directly from  $A^{fk}(\omega)$  being distributed Fréchet and the definition  $r_t^{fk}(\omega) \equiv \tau_{it}^k p_{it}^k A^{fk}(\omega) M(\phi^k, D_{qt})$ . Note, too, that the same can be said for the outside good  $k = o$  if we set  $p_{it}^o = 1$ ,  $A^{fo} = A_i^o$ , and  $\phi^o = 0$ . Thus, we compute

$$\begin{aligned} & \mathbb{P} \left\{ r_t^{fk}(\omega) = \max \{ A_i^o(\omega), r_t^{f1}(\omega), \dots, r_t^{fK}(\omega) \} \right\} \\ &= \int_0^\infty \prod_{\ell \neq k} F_t^{f\ell}(r) d \left[ 1 - F_t^{fk}(r) \right] \\ &= \int_0^\infty \prod_{\ell \neq k} F_t^{f\ell}(r) \times \left[ -f_t^{fk}(r) \right] dr \\ &= \int_0^\infty \prod_{\ell \in \mathcal{K} \cup \{o\}} \exp \left\{ -\gamma \left( \frac{r}{\tau_{it}^\ell p_{it}^\ell A_i^{f\ell} M(\phi^k, D_{qt})} \right)^{-\theta} \right\} \frac{-\gamma \theta}{(\tau_{it}^k p_{it}^k A^{fk} M(\phi^k, D_{qt}))^{-\theta}} r^{-\theta-1} dr \\ &= \left( \tau_{it}^k p_{it}^k A^{fk} M(\phi^k, D_{qt}) \right)^\theta \int_0^\infty -\exp \left\{ -\gamma r^{-\theta} \sum_{\ell \in \mathcal{K} \cup \{o\}} \left( \tau_{it}^\ell p_{it}^\ell A_i^{f\ell} M(\phi^k, D_{qt}) \right)^\theta \right\} \gamma \theta r^{-\theta-1} dr \\ &= \left( \tau_{it}^k p_{it}^k A^{fk} M(\phi^k, D_{qt}) \right)^\theta \int_0^\infty -\exp \left\{ -\gamma \left[ (A_i^o)^\theta + \Pi_t^f \right] r^{-\theta} \right\} \gamma \theta r^{-\theta-1} dr \\ &= \frac{\left( \tau_{it}^k p_{it}^k A^{fk} M(\phi^k, D_{qt}) \right)^\theta}{(A_i^o)^\theta + \Pi_t^f} \int_0^\infty d \left[ 1 - F_t^f(r) \right] \\ &= \frac{\left( \tau_{it}^k p_{it}^k A^{fk} M(\phi^k, D_{qt}) \right)^\theta}{(A_i^o)^\theta + \Pi_t^f} \end{aligned}$$

---

<sup>66</sup>Proof available upon request.

as claimed, where

$$1 - F_t^f(r) \equiv 1 - \exp \left\{ -\gamma \left[ (A_i^o)^\theta + \Pi_t^f \right] r^{-\theta} \right\}.$$

is the probability that the revenue for at least one use of a given parcel on field  $f$  (including leaving it fallow) exceeds  $r$ .

#### B.1.4 Expected productivity given crop selection

Continue to assume that  $i$  means  $i(f)$  and  $q$  means  $q(f)$  unless otherwise specified. We wish to show that

$$\mathbb{E} \left[ A^{fk}(\omega) \middle| r_t^{fk}(\omega) = \max \{A_i^o(\omega), r_t^{f1}(\omega), \dots, r_t^{fK}(\omega)\} \right] = A^{fk} \left( \pi_t^{fk} \right)^{-1/\theta}.$$

To compute this conditional expected value, we need to derive the corresponding conditional probability distribution. The probability that crop  $k$  is grown on field  $f$  with productivity  $a$  or less given that it is the profit-maximizing crop choice for field  $f$  can be decomposed as (i) the joint probability that crop  $k$  earns return at or below  $r_t^k(a) \equiv \tau_{it}^k p_{it}^k a M(\phi^k, D_{qt})$  and is the profit-maximizing crop choice for  $f$  divided by (ii) the unconditional probability of being the profit-maximizing crop,  $\pi_t^{fk}$ . Then,

$$\begin{aligned} & \mathbb{P} \left\{ r_t^{fk}(\omega) < r_t^k(a) \middle| r_t^{fk}(\omega) = \max \{A_i^o(\omega), r_t^{f1}(\omega), \dots, r_t^{fK}(\omega)\} \right\} \\ &= \frac{1}{\pi_t^{fk}} \int_0^{r_t^k(a)} \prod_{\ell \neq k} F_t^{f\ell}(r) d \left[ 1 - F_t^{fk}(r) \right] \\ &= \frac{1}{\pi_t^{fk}} \int_0^{r_t^k(a)} \prod_{\ell \neq k} F_t^{f\ell}(r) \times \left[ -f_t^{fk}(r) \right] dr \\ &= \frac{1}{\pi_t^{fk}} \int_0^{r_t^k(a)} \prod_{\ell \in \mathcal{K} \cup \{o\}} \exp \left\{ -\gamma \left( \frac{r}{\tau_{it}^\ell p_{it}^\ell A_i^{f\ell} M(\phi^k, D_{qt})} \right)^{-\theta} \right\} \frac{-\gamma \theta}{(\tau_{it}^k p_{it}^k A^{fk} M(\phi^k, D_{qt}))^{-\theta}} r^{-\theta-1} dr \\ &= \frac{(\tau_{it}^k p_{it}^k A^{fk} M(\phi^k, D_{qt}))^\theta}{\pi_t^{fk}} \int_0^{r_t^k(a)} -\exp \left\{ -\gamma r^{-\theta} \sum_{\ell \in \mathcal{K} \cup \{o\}} \left( \tau_{it}^\ell p_{it}^\ell A_i^{f\ell} M(\phi^k, D_{qt}) \right)^\theta \right\} \gamma \theta r^{-\theta-1} dr \\ &= \frac{(\tau_{it}^k p_{it}^k A^{fk} M(\phi^k, D_{qt}))^\theta}{\pi_t^{fk}} \int_0^{r_t^k(a)} -\exp \left\{ -\gamma \left[ (A_i^o)^\theta + \Pi_t^f \right] r^{-\theta} \right\} \gamma \theta r^{-\theta-1} dr \\ &= \frac{1}{\pi_t^{fk}} \left[ \frac{(\tau_{it}^k p_{it}^k A^{fk} M(\phi^k, D_{qt}))^\theta}{(A_i^o)^\theta + \Pi_t^f} \right] \left[ 1 - F_t^f \left( r_t^k(a) \right) \right] \\ &= 1 - F_t^f \left( r_t^k(a) \right). \end{aligned}$$

The expected value of  $r_t^{fk}(\omega)$  against this conditional distribution is

$$\begin{aligned}\mathbb{E} \left[ r_t^{fk}(\omega) \middle| r_t^{fk}(\omega) = \max\{A_i^o(\omega), r_t^{f1}(\omega), \dots, r_t^{fK}(\omega)\} \right] \\ = \int_0^\infty r d \left[ 1 - F_t^f(r) \right] \\ = \int_0^\infty -r\gamma\theta \left[ (A_i^o)^\theta + \Pi_t^f \right] r^{-\theta-1} \exp \left\{ -\gamma \left[ (A_i^o)^\theta + \Pi_t^f \right] r^{-\theta} \right\} dr,\end{aligned}$$

and now with the variable transformation  $x \equiv \gamma \left[ (A_i^o)^\theta + \Pi_t^f \right] r^{-\theta}$ ,

$$\begin{aligned}= \int_0^\infty r \left( \frac{dx}{dr} \right) \exp\{-x\} dr \\ = \int_0^\infty \left( \frac{x}{\gamma \left[ (A_i^o)^\theta + \Pi_t^f \right]} \right)^{-1/\theta} \exp\{-x\} dx \\ = \gamma^{1/\theta} \left[ (A_i^o)^\theta + \Pi_t^f \right]^{1/\theta} \int_0^\infty x^{-1/\theta} \exp\{-x\} dx \\ = \gamma^{1/\theta} \left[ (A_i^o)^\theta + \Pi_t^f \right]^{1/\theta} \Gamma \left( \frac{\theta-1}{\theta} \right) \\ = \left[ (A_i^o)^\theta + \Pi_t^f \right]^{1/\theta}.\end{aligned}$$

Now transforming from revenue to productivity:

$$\begin{aligned}\mathbb{E} \left[ A_t^{fk}(\omega) \middle| r_t^{fk}(\omega) = \max\{A_i^o(\omega), r_t^{f1}(\omega), \dots, r_t^{fK}(\omega)\} \right] &= \frac{\left[ (A_i^o)^\theta + \Pi_t^f \right]^{1/\theta}}{\tau_{it}^k p_{it}^k M(\phi^k, D_{qt})} \\ &= A^{fk} \frac{\left[ (A_i^o)^\theta + \Pi_t^f \right]^{1/\theta}}{\tau_{it}^k p_{it}^k A^{fk} M(\phi^k, D_{qt})} \\ &= A^{fk} \left( \pi_t^{fk} \right)^{-1/\theta}\end{aligned}$$

which completes the proof.

### B.1.5 Robustness: Nested CES agricultural technology

Following [Boppart et al. \(2023\)](#), who reject Cobb-Douglas technology in the agricultural sector in favor of nested CES technologies, we consider the technology (omitting sub- and superscripts for convenience)

$$Q = A \left[ \alpha^{\frac{1}{\xi_H}} H^{\frac{\xi_H-1}{\xi_H}} + (1-\alpha)^{\frac{1}{\xi_H}} \left( L^{\frac{\xi_M-1}{\xi_M}} + \left( \frac{G}{\phi^k} \right)^{\frac{\xi_M-1}{\xi_M}} \right)^{\frac{\xi_M}{\xi_M-1} \frac{\xi_H-1}{\xi_H}} \right]^{\frac{\xi_H}{\xi_H-1}}. \quad (\text{B.4})$$

One can verify that in the limit as  $\xi_H \rightarrow 1$  and  $\xi_M \rightarrow 0$ , this becomes the technology in Equation (5).

A crucial step in characterizing the equilibrium of the model is showing that agricultural output on a given parcel can be written as the product of its idiosyncratic TFP draw and a function  $M$  that is independent of the realization of that TFP draw (see Section B.1.2). From the farmer's first-order conditions with the technology in Equation (B.4), one can verify that

$$Q_t^{fk}(\omega) = A^{fk}(\omega) \tilde{M}(\phi^k, D_{q(f)t})$$

with

$$\begin{aligned} \tilde{M}(\phi^k, D_{q(f)t}) &= \left[ \alpha^{\frac{1}{\xi_H}} (\tilde{H})^{\frac{\xi_H - 1}{\xi_H}} \right. \\ &\quad \left. + (1-\alpha)^{\frac{1}{\xi_H}} \left( 1 + \left( \frac{A_q^w(D_{q(f)t})[1-\tilde{H}]}{\phi^k} \right)^{\frac{\xi_M - 1}{\xi_M}} \right)^{\frac{\xi_M}{\xi_M - 1} \frac{\xi_H - 1}{\xi_H}} \right]^{\frac{\xi_H}{\xi_H - 1}}, \end{aligned}$$

where  $\tilde{H}$  is implicitly defined by the condition

$$\tilde{H} = \frac{\alpha}{1-\alpha} \left[ \left( \frac{A_q^w(D_{q(f)t})}{\phi^k} \right)^{\frac{\xi_M - 1}{\xi_M}} (1-\tilde{H})^{-\frac{1}{\xi_M}} \left( 1 + \left[ \frac{A_q^w(D_{q(f)t})[1-\tilde{H}]}{\phi^k} \right]^{\frac{\xi_M - 1}{\xi_M}} \right)^{\frac{1}{\xi_M - 1}} \right].$$

So one can endow farmers with the technology in Equation (B.4) and define an equilibrium as before, just in terms of  $\tilde{M}$ . But doing so would require us to find the root of the preceding nonlinear equation everytime the depth of an aquifer changed, which will happen for every aquifer in every period along the equilibrium path. Moreover, to the best of our knowledge, there is no globally comprehensive data with which to estimate the elasticities  $\xi_H$  and  $\xi_M$ , nor a natural benchmark to which they can be calibrated. As such, we chose the Leontief specification presented in the main text.

## B.2 Existence and uniqueness

The goal of this section is to characterize under what conditions the competitive equilibrium given by Definition 1 exists and is unique. To that end, we'll proceed by defining and characterizing two sub-equilibria: a *trade equilibrium*, which takes the vector of aquifer depths as given, and a *steady-state equilibrium*, which imposes constant depths. Once we've characterized those two sub-equilibria, we'll characterize the *full dynamic competitive equilibrium* given by Definition 1. Because agricultural policy distortions are exogenous and act proportionally on prices, they would impose no additional complications on the arguments below, so they've been ignored to save on notation.

### B.2.1 ... of the trade equilibrium

A *trade equilibrium* asks only how goods and factors will be allocated today given depths  $\mathbf{D}$ ; it does not consider how the allocation today will affect depths tomorrow. A formal definition follows.

**Definition B.1.** Given an arbitrary vector of water table depths,  $\mathbf{D}$ , a *trade equilibrium* is a vector of consumption,  $\{C_{ji}^k\}$ , output,  $\{Q_i^k\}$ , prices,  $\{p_i^k\}$ , and shares,  $\{\pi^{fk}\}$ , such that Equations (11), (13), (14), and (15) hold.

With this reduction in scope, we've recovered a static neoclassical trade model. The presence of the outside good means that this trade block falls outside the class of gravity models that have been characterized by [Allen, Arkolakis, and Takahashi \(2020\)](#).<sup>67</sup> Instead, we'll follow [Alvarez and Lucas \(2007\)](#) in using the *aggregate excess demand function*  $\mathbf{z}(\tilde{\mathbf{p}})$ :

$$z_{ik}(\tilde{\mathbf{p}}) = \sum_{j \in \mathcal{I}} \delta_{ij}^k (p^o \zeta_j) \frac{\zeta_j^k (P_j^k)^{1-\kappa}}{\sum_{\ell \in \mathcal{K}} \zeta_j^\ell (P_j^\ell)^{1-\kappa}} \frac{\zeta_{ij}^k (\delta_{ij}^k p_i^k)^{-\sigma}}{\sum_{n \in \mathcal{I}} \zeta_{nj}^k (\delta_{nj}^k p_n^k)^{1-\sigma}}$$

$$- \sum_{f \in \mathcal{F}_i} h^f A_i^{fk} M(\phi^k, D_{q(f)}) \left( \frac{(p_i^k A_i^{fk} M(\phi^k, D_{q(f)}))^{\theta}}{(p^o A_i^o)^{\theta} + \sum_{\ell \in \mathcal{K}} (p_i^\ell A_i^{f\ell} M(\phi^\ell, D_{q(f)}))^{\theta}} \right)^{\frac{\theta-1}{\theta}}$$

and

$$z_o(\tilde{\mathbf{p}}) = \sum_i \left( \frac{Y_i}{p^o} - \zeta_i \right) - \sum_i \sum_{f \in \mathcal{F}_i} h^f A_i^o \left( \frac{(p^o A_i^o)^{\theta}}{(p^o A_i^o)^{\theta} + \sum_{\ell \in \mathcal{K}} (p_i^\ell A_i^{f\ell} M(\phi^\ell, D_{q(f)}))^{\theta}} \right)^{\frac{\theta-1}{\theta}}$$

where  $\tilde{\mathbf{p}} \equiv [\mathbf{p}, p^o]$ , with  $p^o$  being the price of the outside good (which we had been normalizing to one), and  $Y_i$  is total income  $Y_i = p^o Q_i^o + \sum_k p_i^k Q_i^k$ . By [Mas-Colell, Whinston, and Green \(1995, Ch.17\)](#), the equilibrium exists if

1.  $\mathbf{z}$  is continuous;
2.  $\mathbf{z}$  is homogeneous of degree zero in  $\tilde{\mathbf{p}}$ ;
3.  $\tilde{\mathbf{p}} \cdot \mathbf{z} = 0$  for all strictly positive price vectors (Walras' law);

---

<sup>67</sup> Considering the agricultural and outside sectors together, aggregate demand here is not CES, which violates condition C.2 of [Allen, Arkolakis, and Takahashi \(2020\)](#). One may consider only the agricultural sector, which is well-described by an Armington model of trade, but then expenditure on the outside good is isomorphic to an endogenous trade imbalance, which violates condition C.5. Note, too, that we cannot map production in each country to a representative good, which violates condition C.3.

4. there is a  $\underline{z} > 0$  such that  $z_\ell(\tilde{\mathbf{p}}) > -\underline{z}$  for every commodity  $\ell$  and all  $p$ ;
5. if  $\tilde{\mathbf{p}}^n \rightarrow \tilde{\mathbf{p}}$ , where  $\tilde{\mathbf{p}} \neq 0$  but  $\tilde{p}_\ell = 0$  for some  $\ell$ , then

$$\max\{z_1(\tilde{\mathbf{p}}^n), \dots, z_{IK+1}(\tilde{\mathbf{p}}^n)\} \rightarrow \infty;$$

and is unique if, in addition,

$$6. \frac{\partial z_\ell(\tilde{\mathbf{p}})}{\partial p_{\ell'}} > 0 \text{ for all } \ell, \ell' \text{ with } \ell \neq \ell' \text{ and all } \tilde{\mathbf{p}} \in \mathbb{R}_{++}^{IK+1} \text{ (gross substitutes).}$$

Here we're leveraging that we can identify the trade equilibrium by just the vector of prices (up to scale): Once we have the prices, the vectors of consumption, output, and land use shares are determined uniquely.

**Proposition B.2.** *A trade equilibrium exists for any vector of depths  $\mathbf{D}$ .*

*Proof.* We just need to check conditions 1-5. We'll do so in order.

1. Continuity is self-evident.
2. Homogeneity of degree zero is also self-evident (multiply every price by the same factor  $\lambda > 0$  and confirm that all the multipliers cancel).
3. Let's look at the demand components first. In  $z_{ik}$  the dot product gives us  $\sum_j p_i^k \delta_{ij}^k C_{ij}^k$ . In  $z_o$  we get  $\sum_i (Y_i - p^o \zeta_i)$ . Now the supply terms: in  $z_{ik}$  we get  $p_i^k Q_i^k$  and in  $z_o$  we get  $p^o Q_i^o$ . So

$$\begin{aligned} \tilde{\mathbf{p}} \cdot \mathbf{z} &= \sum_{i,k,j} p_i^k \delta_{ij}^k C_{ij}^k + \sum_i (Y_i - p^o \zeta_i) - \sum_{i,k} p_i^k Q_i^k - \sum_i p^o Q_i^o \\ &= \sum_{i,k,j} p_i^k \delta_{ij}^k C_{ij}^k - \sum_i p^o \zeta_i \\ &= \sum_{i,k,j} p_i^k \delta_{ij}^k C_{ij}^k - \sum_i P_i C_i \\ &= 0. \end{aligned}$$

4. The demand terms are always non-negative, so set them to zero. For each element of the supply terms, take the maximum value permissible (so  $\max_f h^f$  and  $\max_{fk} A^{fk}$  and so on). Note that the max permissible share is always 1. Since each maximum element is finite, one can construct a finite  $\bar{z}$  using these maximums.

5. Note that, defining  $\Lambda^{fk} \equiv h^f A^{fk} M(\phi^k, D_{q(f)})$  that is independent of prices for fixed  $D$ ,

$$\begin{aligned} \max_{ik} z_{ik}(\tilde{\mathbf{p}}) &\geq \max_{ik} \sum_j \delta_{ij}^k C_{ij}^k - \max_{ik} \sum_{f \in \mathcal{F}_i} \Lambda^{fk} (\pi^{fk})^{(\theta-1)/\theta} \\ &\geq \max_{ik,j} \delta_{ij}^k C_{ij}^k - \max_{ik} \sum_{f \in \mathcal{F}_i} \Lambda^{fk} (\pi^{fk})^{(\theta-1)/\theta} \\ &\geq \max_{ik,j} \delta_{ij}^k C_{ij}^k - \max_{ik} \sum_{f \in \mathcal{F}_i} \Lambda^{fk} \end{aligned}$$

where we get each inequality because, in order,

- (i) we can show  $\max_k (A_k - B_k) \geq \max_k A_k - \max_k B_k$  as follows:
  - suppose  $k^\delta = \arg \max_k (A_k - B_k)$  and  $k^A = \arg \max_k A_k$
  - let  $\delta \equiv A_{k^A} - A_{k^\delta}$
  - consider the difference  $A_{k^\delta} - B_{k^\delta} = A_{k^\delta} + \delta - (B_{k^\delta} + \delta) = A_{k^A} - (B_{k^\delta} + \delta)$
  - now  $B_{k^\delta} + \delta \leq B_{k^A} \leq \max_k B_k$ , else  $k^A$  would be the arg max of  $A_k - B_k$ , not  $k^\delta$ ;
- (ii) a sum of positive terms is greater than its maximum term;
- (iii)  $\pi^{fk} \leq 1$  for all  $fk$ .

So the task reduces to showing that  $\max_{ik,j} C_{ij}^k(\tilde{\mathbf{p}}) \rightarrow \infty$  for the given price sequence, where we overload notation by considering  $k \in \{\mathcal{K}, o\}$ . Consider the definition of  $C_{ij}^k$  (for  $k \in \mathcal{K}$ ) term-by-term:

- the leftmost is  $p^o \zeta_i$ , which is obviously finite whenever  $p^o$  is finite
- the middle is bounded between zero and one
- the rightmost is also bounded between zero and one when pre-multiplied by  $\delta_{ij}^k p_i^k$ , so the rightmost on its own tends to infinity as  $p_i^k \rightarrow 0$ .

And if  $p^o \rightarrow 0$ , it's obvious from the definition of  $C_i^o$  that it will tend to infinity.

□

**Proposition B.3.** *The trade equilibrium is unique for any vector of depths  $\mathbf{D}$ .*

*Proof.* We just need to check the gross substitutes condition.<sup>68</sup> This is easy to verify for the outside good with respect to any agricultural commodity price: in the expression for  $z_o(\tilde{\mathbf{p}})$ , agricultural prices only show up in the denominator of the term being subtracted. Now consider the excess demand for an agricultural

---

<sup>68</sup>The expressions for the relevant partial derivatives are easy to derive but repetitive to show, so we omit them here in favor of a verbal argument.

commodity,  $z_{ik}(\tilde{\mathbf{p}})$ . The gross substitutes condition is satisfied with respect to the outside good: if  $p^o$  increased, demand for any agricultural commodity would increase (the first term), but supply of every agricultural commodity would decrease (the second term), so excess demand for  $ik$  would surely increase. With respect to any agricultural commodity from another country  $i' \neq i$ , an increase in its price implies a direct increase in demand for  $ik$  but no change in its supply, so  $z_{ik}(\tilde{\mathbf{p}})$  increases. Finally, consider the direct effect of an increase in price for a commodity from the same country,  $ik'$  with  $k' \neq k$ . By the same logic as before, demand for  $ik$  increases as consumers substitute away from the higher price (first term) and supply of  $ik$  decreases as domestic producers substitute toward the higher priced  $ik'$  (second term). Thus, excess demand for  $ik$  increases.  $\square$

### B.2.2 ... of the steady-state equilibrium

A *steady state* is a path along which the depth of each aquifer is constant over time. Since depths were the only variables evolving with any fundamental persistence, one can define a steady state as a trade equilibrium in which the inflows to each aquifer offset the outflows.

**Definition B.2.** A *steady-state equilibrium* is a vector of consumption,  $\{C_{ji}^k\}$ , output,  $\{Q_i^k\}$ , prices,  $\{p_i^k\}$ , shares,  $\{\pi^{fk}\}$ , water table depths,  $\{D_q\}$ , and water extractions,  $\{X_q\}$ , such that

$$(1 - \psi)X_q = R_q, \quad \forall q \in \mathcal{Q}$$

and Equations (11), (13), (14), (15), and (16) hold.

**Proposition B.4.** *A unique steady-state equilibrium exists.*

*Proof.* Propositions B.2–B.3 established that for any vector of depths there exists a unique vector of crop prices, which uniquely determines the rest of the trade allocation. Accordingly, we can define the function

$$X_q(D_q) = \sum_{f \in \mathcal{F}_q} \sum_{k \in \mathcal{K}} x^{fk} h^f \frac{(p_{i(f)}^k A^{fk} M(\phi^k, D_q))^{\theta}}{(A_{i(f)}^o)^{\theta} + \sum_{\ell \in \mathcal{K}} (p_{i(f)}^{\ell} A^{f\ell} M(\phi^{\ell}, D_q))^{\theta}},$$

where the prices  $p_{i(f)}^k$  are those from the corresponding trade equilibrium, so that a steady-state equilibrium is  $\bar{\mathbf{D}} = \{\bar{D}_q\}$  such that

$$(1 - \psi)X_q(\bar{D}_q) = R_q, \quad \forall q \in \mathcal{Q}.$$

Equivalently, we can define the operator  $T : \mathbb{R}^{|\mathcal{Q}|} \mapsto \mathbb{R}^{|\mathcal{Q}|}$  by

$$[T(\mathbf{D})]_q = D_q + \rho_q[(1 - \psi)X_q(D_q) - R_q]$$

so that a steady-state equilibrium is  $\bar{\mathbf{D}} = \{\bar{D}_q\}$  such that

$$\bar{\mathbf{D}} = T(\bar{\mathbf{D}}).$$

If  $T$  is a contraction mapping, then the contraction mapping theorem implies that it has a unique fixed point that can be computed by iteration. We conjecture, but as of this draft have not shown, that  $T$  satisfies Blackwell's sufficient conditions for a contraction, which would in turn be sufficient to finish proving the claim.  $\square$

### B.2.3 ... of the full dynamic competitive equilibrium

Notice an important feature of the proof of Proposition B.4: the operator  $T$  is the law of motion for depth in Equation (10). We have shown that, by iterating this operator forward and solving for the unique trade equilibrium at each step, we are sure to converge to a unique steady state. The main result is then simply a corollary of the three preceding propositions.

**Corollary B.1.** *Given any initial vector of water table depths,  $\{D_{q0}\}$ , a unique competitive equilibrium exists.*

### B.2.4 The outside sector as residual claimant

The aim of this section is to demonstrate that we demoted the outside sector from the equilibrium definition only out of convenience; no bugaboos are hiding there.

We've done some of the work already in previous appendices. As we showed in Appendix B.1.1, because the utility function in Equation (2) is quasilinear, the representative consumer in country  $i$  spends her first  $\zeta_i$  of income on agricultural output. All residual income is either (i) spent on the outside good or (ii) taxed away lump-sum.

In the main text we assumed conditions such that the outside good is always consumed and produced in every country. Moreover, we assumed that it is homogeneous and freely traded, so the law of one price holds (and we normalized that price to one). Accordingly, bilateral flows of the outside good are indeterminate; countries are simply net importers or net exporters from a unified global market for the outside good. In Appendix B.2.1, we stated the condition for that market to clear when there are no taxes or subsidies (namely,  $z_o(\tilde{\mathbf{p}}) = 0$ ). That condition is guaranteed to be satisfied in equilibrium by Walras' law.

It just remains to check that reintroducing the distortions does no harm. The market clearing condition becomes

$$\sum_i (Y_{it} - T_{it} - \zeta_i) = \sum_i \sum_{f \in \mathcal{F}_i} h^f A_i^o \left( \pi_t^{fo} \right)^{\frac{\theta-1}{\theta}}$$

where  $Y_{it} = Q_{it}^o + \sum_k \tau_{it}^k p_{it}^k Q_{it}^k$  is total income and  $T_{it}$  is the lump-sum tax. But notice that budget balance would require

$$\begin{aligned} T_{it} &= \sum_k (\tau_{it}^k - 1) p_{it}^k Q_{it}^k \\ &= \sum_k \tau_{it}^k p_{it}^k Q_{it}^k - \sum_k p_{it}^k Q_{it}^k, \end{aligned}$$

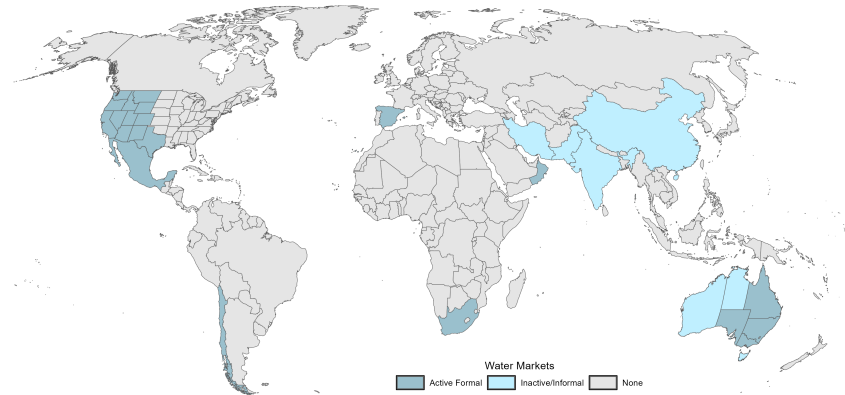
so market clearing with government budgets balanced is just

$$\sum_i \left( Q_{it}^o + \sum_k p_{it}^k Q_{it}^k - \zeta_i \right) = \sum_i \sum_{f \in \mathcal{F}_i} h^f A_i^o \left( \pi_t^{fo} \right)^{\frac{\theta-1}{\theta}}$$

which takes the exact same form as it did before we reintroduced taxes and is therefore satisfied by Walras' law.

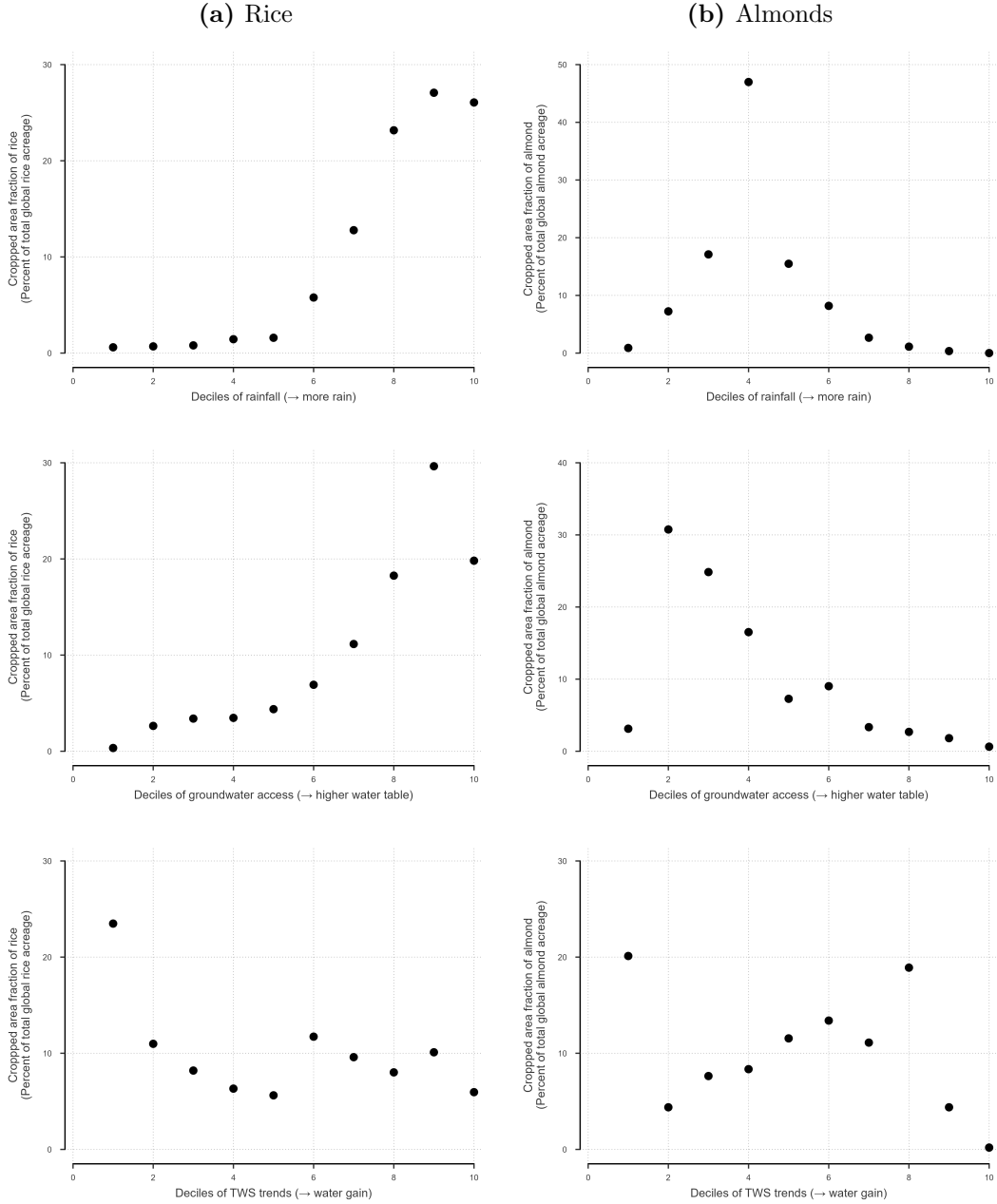
## C Additional figures

**Figure C.1:** Global distribution of water markets



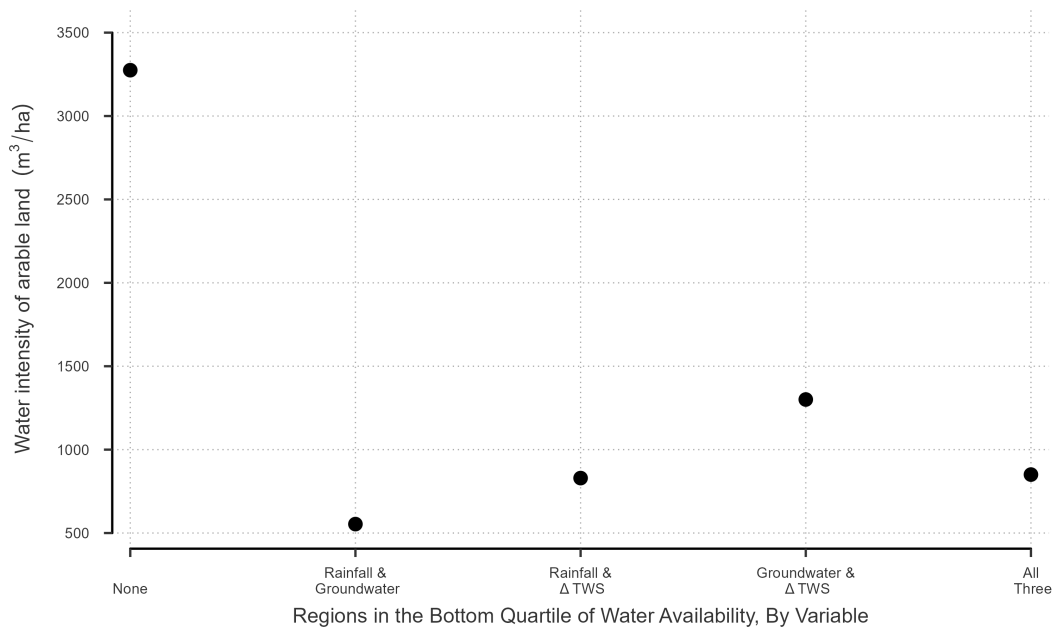
**Notes:** This map shows the global distribution of water markets, as uncovered through an extensive literature review. Subnational regions and countries shaded in dark blue have established formal water markets in which extraction rights can be traded. Regions and countries in light blue indicate locations where informal or inactive water markets are present. Grey areas indicate no formal or informal water markets exist. Water markets rarely extend across the entire regions shaded, but precise extents of these markets are impossible to determine with available data.

**Figure C.2:** Cropped area fraction by decile of water variables



**Notes:** The three graphs in Panel (a) show the cropped area fraction of rice as a percent of total global rice acreage by decile of precipitation, water table depth, and change in total water storage. Similarly, the cropped area fractions of almonds by decile of water variables are shown in the three graphs of Panel (b). [Monfreda, Ramankutty, and Foley \(2008\)](#) compiled the crop-level agricultural use measure; the sources of the water variable data are discussed in Appendix A.

**Figure C.3:** Water intensity of arable land use in water stressed regions



**Notes:** This graph shows the water intensity of arable land use in regions that fall in the bottom quartile of none, two, or all three of selected water variables: precipitation, water table depth, and change in total water storage. Arable land is defined as land that is cropped or pastured. The water intensity measures are calculated using data from [Mekonnen and Hoekstra \(2011\)](#), and the sources of the water variable data are discussed in Appendix A.